

**“የጥበብ ሁሉ መጀመሪያ እግዚአብሔርን መፍራት ነው።”**

**መዝሙር 111፤10**



**University of Alberta**

**Control of Electroosmotic Flow and Separation Selectivity in Nonaqueous  
Capillary Electrophoresis**

By

**Abebaw Gedefaw Diress**



A thesis submitted to the Faculty of Graduate Studies and Research in partial fulfillment  
of the requirements for the degree of Doctor of Philosophy

Department of Chemistry

Edmonton, Alberta

Spring 2006



Library and  
Archives Canada

Bibliothèque et  
Archives Canada

Published Heritage  
Branch

Direction du  
Patrimoine de l'édition

395 Wellington Street  
Ottawa ON K1A 0N4  
Canada

395, rue Wellington  
Ottawa ON K1A 0N4  
Canada

*Your file* *Votre référence*  
*ISBN: 0-494-13963-3*  
*Our file* *Notre référence*  
*ISBN: 0-494-13963-3*

#### NOTICE:

The author has granted a non-exclusive license allowing Library and Archives Canada to reproduce, publish, archive, preserve, conserve, communicate to the public by telecommunication or on the Internet, loan, distribute and sell theses worldwide, for commercial or non-commercial purposes, in microform, paper, electronic and/or any other formats.

The author retains copyright ownership and moral rights in this thesis. Neither the thesis nor substantial extracts from it may be printed or otherwise reproduced without the author's permission.

#### AVIS:

L'auteur a accordé une licence non exclusive permettant à la Bibliothèque et Archives Canada de reproduire, publier, archiver, sauvegarder, conserver, transmettre au public par télécommunication ou par l'Internet, prêter, distribuer et vendre des thèses partout dans le monde, à des fins commerciales ou autres, sur support microforme, papier, électronique et/ou autres formats.

L'auteur conserve la propriété du droit d'auteur et des droits moraux qui protègent cette thèse. Ni la thèse ni des extraits substantiels de celle-ci ne doivent être imprimés ou autrement reproduits sans son autorisation.

---

In compliance with the Canadian Privacy Act some supporting forms may have been removed from this thesis.

Conformément à la loi canadienne sur la protection de la vie privée, quelques formulaires secondaires ont été enlevés de cette thèse.

While these forms may be included in the document page count, their removal does not represent any loss of content from the thesis.

Bien que ces formulaires aient inclus dans la pagination, il n'y aura aucun contenu manquant.

  
**Canada**

*~ Dedicated to My Parents ~*

## ABSTRACT

Capillary electrophoresis (CE) is a powerful and versatile technique for separation of substances ranging from small ions to large biological molecules. In CE, control of the electroosmotic flow (EOF) and charge on the capillary surface are essential for optimizing separations. Capillary wall coatings have been devised to manipulate the EOF and eliminate analyte adsorptions onto the silica capillary. However, most of these wall coatings are not compatible with many organic solvents. This thesis demonstrates systematic control of EOF using surfactant-based coatings in mixed organic-water and pure organic solvents for the analysis of anionic and basic analytes. Cationic surfactants, such as cetyltrimethylammonium bromide ( $C_{16}TAB$ ) and didodecyldimethylammonium bromide ( $2C_{12}DAB$ ), adsorb onto the capillary wall, altering the charge on the capillary surface. The resulting reversed EOF depends on the concentration of the surfactant and the organic solvent in the electrophoretic buffer. The impact of the organic solvent on the EOF is predominantly a function of the diminished zeta potential of the silica surface, and to a lesser extent on the critical micelle concentration of the surfactant. However,  $C_{16}TAB$  or  $2C_{12}DAB$  must be present in the buffer to maintain the coating stability.

Alternatively, long and double chain cationic surfactants such as dihexadecyldimethylammonium bromide ( $2C_{16}DAB$ ) and dioctadecyldimethylammonium bromide ( $2C_{18}DAB$ ) form semi-permanent bilayer coatings in mixed organic-aqueous buffers. This allows performing separations without the need to regenerate the coating or keep the EOF modifiers in the run buffer. These bilayer coatings are pH independent and show high degree of stability for over 150 capillary volumes in aqueous buffers that contain up to 60% (v/v) of various organic solvents (methanol, acetonitrile,

ethanol, 2-propanol, 1-butanol). Rapid separations of anions and basic drugs (< 2.5 min) with migration time reproducibility less than 0.5% RSD and efficiencies in the ranges of 0.4 – 0.6 million plates/m are obtained. Dramatic selectivity changes for small inorganic anions and cationic drugs are also observed when the organic solvent content is adjusted. The bilayer capillary coatings are also successfully employed to achieve EOF modification in buffers prepared from pure formamide solvent. Chemical and physical factors affecting the coatings stability and their influence on separation speed and efficiency of cationic drugs in formamide are investigated. Compared to other types of capillary modifications, these surfactant coatings are effective, versatile and inexpensive.

## ACKNOWLEDGMENTS

First and foremost, I would like to thank my supervisor, Prof. Charles A. Lucy, for his consistent guidance, insight and encouragement during this work and for giving me the opportunity to carry out this research in his lab. I am very thankful for his patience in reading the draft thesis and for his valuable comments and suggestions.

Current and past members of the Lucy group are gratefully acknowledged for their helpful ideas, discussions and comments. In particular, I would like to thank my colleague, Mahmoud Yassine with whom I enjoyed countless discussions on a diversity of research topics and problems. I also thank Dr. Panos Hatsis for his help with the Agilent CE System. I would also like to express my gratitude to members of my candidacy and thesis defense committee: Drs. John-Bruce Green, John Klassen, Chris Le, Hasan Uludag, and Christopher Palmer. My appreciation also goes to the technical support staff in the Department of Chemistry especially those at the IT group, electronics and machine shops.

I should also express my deepest gratitude to my parents, sisters and brothers for their continued love, encouragement and support. I am grateful to all my friends for their friendship and encouragements in last few years of my life in Edmonton. Special thanks also go to my wife, Meseret Admassu, and my lovely son, Abel. Mesi, you are special and without your unconditional love and encouragement, this work would not have been successful. Last but not least, I thank God for giving me the courage and patience to persevere during the course of my research.

The University of Alberta and the Natural Sciences and Engineering Research Council of Canada (NSERC) provided financial support for this research.



## TABLE OF CONTENTS

### CHAPTER ONE: Introduction

1.1 Short History of Electrophoresis.....	1
1.2 Fundamentals of Capillary Electrophoresis .....	3
1.2.1 Instrumentation .....	3
1.2.2 Migration Phenomena in Capillary Electrophoresis .....	5
1.2.2.1 Electrophoretic Mobility .....	5
1.2.2.2 Electroosmotic Flow (EOF).....	6
1.2.2.3 Electroosmotic Mobility .....	10
1.2.2.4 Measurement of Mobility .....	12
1.2.3 Detection Methods .....	13
1.2.3.1 UV Absorbance Detection .....	14
1.2.3.2 Indirect UV Detection.....	15
1.3 Modes of Capillary Electrophoresis.....	18
1.3.1 Capillary Zone Electrophoresis (CZE) .....	18
1.3.2 Micellar Electrokinetic Chromatography (MEKC) .....	20
1.4 EOF and Selectivity Control in CE.....	22
1.4.1 Buffer pH .....	24
1.4.2 Buffer Ionic Strength .....	25
1.4.3 Capillary Coatings .....	28
1.4.3.1 Permanent Wall Coating .....	30
1.4.3.2 Dynamic Wall Coatings.....	32
1.4.3.3 Surfactant Based Coatings .....	34
1.4.4 Organic Solvents.....	43
1.5 Efficiency and Band Broadening in Capillary Electrophoresis .....	46
1.5.1 Longitudinal Diffusion.....	48
1.5.2 Joule Heating .....	49
1.5.3 Electromigration Dispersion .....	51
1.5.4 Extracolumn Broadening .....	53
1.6 Thesis Overview .....	55
1.7 References.....	57

### CHAPTER TWO: Electroosmotic Flow Control in Capillary Electrophoresis for the Determination of Inorganic Anions in Methanol-Water Buffers

2.1 Introduction.....	64
-----------------------	----

2.2	Experimental .....	67
2.2.1	Apparatus .....	67
2.2.2	Chemicals.....	67
2.2.3	EOF Measurements.....	68
2.2.4	Critical Micelle Concentration Determination.....	71
2.2.5	Anion Separations.....	72
2.3	Results and Discussion .....	73
2.3.1	EOF Reversal using CTAB in Aqueous Buffers .....	73
2.3.2	EOF Reversal using CTAB in Methanol-Aqueous Buffers.....	76
2.3.2.1	EOF in MeOH-Water Solutions in the Absence of Surfactant .....	77
2.3.2.2	Magnitude of the Fully Reversed EOF .....	80
2.3.2.3	On-Set of EOF Reversal .....	80
2.3.3	Effect of Surface Ionization of Silica.....	82
2.3.4	EOF Reversal using DDAB in Mixed MeOH-Water Buffers .....	85
2.3.5	Anion Separations in MeOH-Water Buffers.....	86
2.4	Concluding Remarks.....	90
2.5	Reference .....	92

### **CHAPTER THREE: Study of the Selectivity of Inorganic Anions in Hydro-organic Mixtures using Indirect Capillary Electrophoresis**

3.1	Introduction.....	95
3.2	Experimental .....	98
3.2.1	Apparatus .....	98
3.2.2	Chemicals.....	100
3.2.3	EOF Measurements.....	101
3.2.4	Separation and Quantification of Anions.....	101
3.3	Results and Discussion .....	103
3.3.1	Mobility Match in Hydro-Organic Buffers.....	103
3.3.2	Selectivity Changes in Mixed Organic-Water Buffers .....	109
3.3.3	Effect of Type of the Background Barrier Electrolyte.....	114
3.3.4	Influence of Concentration of Background Electrolyte .....	116
3.3.5	Ion Association with the Surfactant in MeOH/Water Buffers.....	119
3.3.6	Quantification and Applications .....	122
3.4	Concluding Remarks.....	125
3.5	References.....	126

## **CHAPTER FOUR: Semi-Permanent Capillary Coatings in Organic-Water Solvents for Capillary Electrophoresis**

4.1 Introduction.....	129
4.2 Experimental .....	132
4.2.1 Apparatus .....	132
4.2.2 Chemical and Reagents.....	133
4.2.3 Capillary Coating Protocol and EOF Measurements.....	134
4.2.4 Coating Stability Studies.....	135
4.2.5 Preparation and Separation of Inorganic Anions .....	135
4.2.6 Separation of Basic Drugs .....	136
4.3 Results and Discussion .....	137
4.3.1 Stability of the Capillary Coatings.....	137
4.3.2 DDAB Coating Stability in MeOH-Water Buffers.....	139
4.3.3 2C <sub>n</sub> DAB Coating Stability in MeOH-Water Buffers.....	142
4.3.4 Effect of pH on the 2C <sub>18</sub> DAB Coating Stability.....	146
4.3.5 Coating Stability in Different Solvents.....	149
4.3.6 Reproducibility and Regeneration of the Coatings.....	152
4.3.7 Separation of Anions and Basic Drugs .....	155
4.4 Concluding Remarks.....	160
4.5 References.....	161

## **CHAPTER FIVE: Non-Covalent Coating for Modification of the Electroosmotic Flow in Nonaqueous Capillary Electrophoresis**

5.1 Introduction.....	164
5.2 Experimental .....	167
5.2.1 Apparatus .....	167
5.2.2 Chemical and Reagents.....	167
5.2.3 EOF Measurements.....	168
5.2.4 Coating Stability Studies.....	169
5.2.5 Separation of Basic Drugs .....	170
5.2.6 Determination of Relative Viscosity.....	170
5.3 Results and Discussion .....	171
5.3.1 Bilayer Stability in Formamide-Water Media .....	173
5.3.2 Effect of Surfactant Concentration on EOF.....	176
5.3.3 Effect of Capillary Diameter.....	179
5.3.4 Effect of Buffer .....	181
5.3.5 Separations of Basic Drugs in Nonaqueous Buffers.....	183

5.4 Concluding Remarks.....	186
5.5 References.....	187
<b>CHAPTER SIX: Summary and Suggestions for Future Work</b>	
6.1 Summary.....	190
6.2 Suggestions for Future Works .....	194
6.2.1 Separation and Identification of Peptides .....	194
6.2.2 Enantiomeric Separation of Pharmaceutical Drugs .....	196
6.3 References.....	198

## LIST OF TABLES

<b>Table 1.1</b>	Physicochemical properties of commonly used organic solvents in CE .....	45
<b>Table 2.1</b>	CMC values for CTAB in MeOH-water mixtures .....	76
<b>Table 3.1</b>	Structure and pKa values of commonly used visualization agents (probes) for indirect detection of small anions.....	99
<b>Table 3.2</b>	Comparison of theoretical plate numbers obtained in 5 mM chromate and 3 mM iodide carrier electrolytes .....	115
<b>Table 3.3</b>	Limits of detection and migration time and peak area reproducibilities.....	123
<b>Table 4.1</b>	Physicochemical properties of some of the double chain surfactants.....	143
<b>Table 4.2</b>	The value and reproducibility of EOF generated using 2C <sub>18</sub> DAB coating in different organic-aqueous solvent mixtures.....	150
<b>Table 5.1</b>	Physicochemical properties of formamide and some selected solvents.....	166
<b>Table 5.2</b>	Effect of buffer organic solvent content on solvent parameters at 25 °C....	175
<b>Table 5.3</b>	Effect of buffer type and surfactant concentration on the value of EOF in formamide.....	182
<b>Table 5.4</b>	Migration time and peak area reproducibilities of four basic drugs in a sodium phosphate buffer prepared with formamide .....	186

## LIST OF FIGURES

<b>Figure 1.1</b>	A schematic setup for capillary electrophoresis instrument.....	4
<b>Figure 1.2</b>	Schematic diagram of electrical double layer and variation of the electric potential with distance from the capillary surface .....	8
<b>Figure 1.3</b>	Flow profile in capillary electrophoresis.....	9
<b>Figure 1.4</b>	Illustration of A) separation process in CZE inside a capillary B) the resulting peaks in the electropherograms.....	19
<b>Figure 1.5</b>	Structure of commonly used additives for dynamic capillary coatings.....	33
<b>Figure 1.6</b>	Aggregations of single chain and double chain cationic surfactants to form micelles and bilayers respectively.....	37
<b>Figure 2.1</b>	Scheme diagram of EOF measurement by sequential injection technique .	70
<b>Figure 2.2</b>	Determination of CMC of cetyltrimethylammonium bromide (CTAB) in distilled water at 25 °C.....	72
<b>Figure 2.3</b>	Effect of CTAB concentrations on the EOF in 10 mM aqueous phosphate buffer at pH 8.0.....	75
<b>Figure 2.4</b>	Effect of CTAB concentration and methanol on the EOF.....	78
<b>Figure 2.5</b>	Variation of ratio of dielectric constant to viscosity with percent of methanol composition at 25 °C .....	79
<b>Figure 2.6</b>	Effect of pH on the magnitude of the EOF in a 10 mM phosphate buffer containing 0% and 40% (v/v) MeOH .....	84
<b>Figure 2.7</b>	Influence of DDAB concentration on EOF in different methanol containing buffers .....	86
<b>Figure 2.8</b>	Separation of five inorganic anions by co-EOF using mixed organic-aqueous buffers .....	88
<b>Figure 2.9</b>	Effect of CTAC concentration on the selectivity of inorganic anion separations.....	89
<b>Figure 3.1</b>	Electrophoretic mobility of common indirect detection probes for anions detection in mixed methanol/water buffers.....	105
<b>Figure 3.2</b>	Effect of pH on the effective mobilities of the probes at constant ionic strength.....	106

<b>Figure 3.3</b>	Comparison of mobility of selected anions with chromate at different percent methanol.....	108
<b>Figure 3.4</b>	Anion selectivity changes with percent methanol in indirect detection ....	111
<b>Figure 3.5</b>	Co-electroosmotic separation of six anions with buffer containing 0.25 mM CTAC and 30% (v/v) MeOH .....	112
<b>Figure 3.6</b>	Effect of concentration of chromate on mobility of inorganic anions in aqueous solutions.....	118
<b>Figure 3.7</b>	Dependence of the reciprocal of the effective mobility of bromide and iodide on the concentration of CTAC.....	121
<b>Figure 3.8</b>	Analysis of common inorganic anions in tap and river waters.....	124
<b>Figure 4.1</b>	Structure of basic drugs ( $\beta$ -blockers) analyzed .....	137
<b>Figure 4.2</b>	Effect of hydrodynamic rinsing on the stability of 2C <sub>12</sub> DAB coating in MeOH-water buffers.....	141
<b>Figure 4.3</b>	EOF stability of 2C <sub>18</sub> DAB coatings in MeOH-water buffer .....	144
<b>Figure 4.4</b>	Effects of surfactant chain length on stability of 2C <sub>n</sub> DAB surfactants .....	145
<b>Figure 4.5</b>	Effect of pH on the stability of 2C <sub>n</sub> DAB coatings in MeOH-water buffers .....	147
<b>Figure 4.6</b>	Electropherograms of separation of five anions in the presence of 1-butanol.....	151
<b>Figure 4.7</b>	Reproducibilities of the EOF and anion separations .....	154
<b>Figure 4.8</b>	Co-electroosmotic separation of five anions using 0.1 mM 2C <sub>18</sub> DAB surfactant and 20% (v/v) MeOH.....	157
<b>Figure 4.9</b>	Effect of methanol on the separation selectivity of basic drugs.....	159
<b>Figure 5.1</b>	Coating stability of 2C <sub>18</sub> DAB in formamide-aqueous phosphate buffers.	174
<b>Figure 5.2</b>	Effect of 2C <sub>18</sub> DAB concentration on the EOF mobility in pure nonaqueous solvent.....	177
<b>Figure 5.3</b>	Effect of capillary inner diameter on stability of double chain surfactant in nonaqueous solvent.....	181
<b>Figure 5.4</b>	Electropherogram of cationic drugs in formamide using a) in bare silica b) 2C <sub>18</sub> DAB coated capillary .....	185

## LIST OF ABBREVIATIONS

ACN	Acetonitrile
AFM	Atomic force spectroscopy
BGE	Background electrolyte
1-BuOH	1-Butanol
CE	Capillary electrophoresis
CGE	Capillary gel electrophoresis
CIEF	Capillary isoelectric focusing
CITP	Capillary isotachopheresis
CMC	Critical Micelle Concentration
cP	Centipoise
CSAC	Critical surface aggregation concentration
CTAB (C <sub>16</sub> DAB)	Cetyltrimethylammonium bromide
CTAC	Cetyltrimethylammonium chloride
CVC	Critical vesicle concentration
CZE	Capillary zone electrophoresis
DDAB (2C <sub>12</sub> DAB)	Didodecyldimethylammonium bromide
DFT	Density Functional Theory
DMF	<i>N,N</i> -Dimethylformamide
DMSO	Dimethyl sulfoxide
DHDAB (2C <sub>16</sub> DAB)	Dimethyldihexadecylammonium bromide
DODAB (2C <sub>18</sub> DAB)	Dimethyldioctadecylammonium bromide
DTDAB (2C <sub>14</sub> DAB)	Dimethylditetradecylammonium bromide
EDL	Electrical double layer
EMD	Electromigration dispersion
EOF	Electroosmotic flow
EPA	Environmental Protection Agency (U.S.)
ESI	Electrospray ionization
EtOH	Ethanol
FA	Formamide



HO	Hubbard-Onsager model
HPLC	High pressure liquid chromatography
I.D.	Inner diameter
IC	Ion Chromatography
IHP	Inner Helmoz plane
kPa	killo Pascal
LOD	Limit of detection
MEKC	Micellar electrokinetic chromatography
MeOH	Methanol
µm	Micrometer
mm	Millimeter
MS	Mass spectroscopy
NMF	<i>N</i> -Methylformamide
O.D.	Outer diameter
OHP	Outer Helmoz plane
PEO	Poly(ethyl)glycol
2-PrOH	2-Propanol
PVC	Poly (vinyl) chloride
RSD	Relative standard deviation
SDS	Sodium dodecylsulfate
SP	System peak
TR	Transfer ratio
TTAB	Tetradecyltrimethylammonium bromide
TTAC	Tetradecyltrimethylammonium chrolide
UV	Ultraviolet
% v/v	Percent volume per volume

## LIST OF SYMBOLS

$A$	Absorbance (absorbance units, AU)
$A_l$	Fitting parameter ( $\text{cm}^2/\text{Vs}$ )
$A_\infty$	Asymptotic value ( $\text{cm}^2/\text{Vs}$ )
$b$	Optical path length (cm)
$C$	Molar concentration (mol/L)
$C_p$	Probe concentration (mol/L)
$D$	Diffusion coefficient ( $\text{cm}^2/\text{s}$ )
$D_r$	Dynamic reserve
$e$	Elementary charge ( $1.602 \times 10^{-19}$ C)
$E$	Electric field strength (V/cm)
$f$	Frictional coefficient ( $\text{CVs}/\text{cm}^2$ )
$F$	Faraday's constant ( $9.65 \times 10^4$ C/mol)
$F_d$	Frictional retarding force (CV/cm)
$F_E$	Electrical force (CV/cm)
$H$	Plate height (m)
$H_D$	Plate height due to diffusion (m)
$H_{det}$	Plate height due to detector volume (m)
$H_{EMD}$	Plate height due to electromigration (m)
$H_{EXR}$	Plate height due to extra column dispersion (m)
$H_{inj}$	Plate height due to injection plug (m)
$H_J$	Plate height due to joule heating (m)
$I$	Ionic strength (mol/L)
$K_a$	Acid dissociation constant
$K_{ass}$	Ion-association constant
$K_b$	Base dissociation constant
$k_b$	Boltzmann constant ( $1.381 \times 10^{-23}$ J/K)
$k_d$	EOF decay rate ( $\text{min}^{-1}$ )
$\kappa$	Electrical conductivity (S/m)
$\tilde{k}'$	Retention factor

$l_c$	Length of the surfactant chain (m)
$L_d$	Capillary length to the detector (cm)
$l_{inj}$	Injection plug length (L)
$L_t$	Total capillary length (cm)
$N$	Theoretical plate number (per meter)
$N_{BL}$	Baseline noise (AU)
$P$	Packing parameter
$P_i$	Incident radiation power (W)
$P_o$	Radiation power after having passed through sample (W)
$q$	Net charge (C)
$r$	Radius of ion (m)
$R$	Universal gas constant (0.08206 L atm K <sup>-1</sup> mol <sup>-1</sup> )
$R_S$	Resolution
$T$	Absolute temperature (K)
$t_{eo}$	Migration time of EOF (neutral) marker (s)
$t_{inj}$	Injection time (s)
$t_m$	Analyte migration time (s)
$t_R$	Retention time (s)
$T_R$	Transfer ratio
$T_r$	Transmittance
$t_{ramp-down}$	Ramp-down time (time for the voltage to change from V to zero, s)
$t_{ramp-up}$	Ramp-up time (time for the voltage to change from zero to V, s)
$\tau$	Solvent relaxation time (s)
$v$	Velocity (cm/s)
$V$	Applied voltage (V)
$V_c$	Volume of the surfactant chain (m <sup>3</sup> )
$W_{1/2}$	Peak width at half-maximum height (s)
$W_b$	Baseline peak width (s)
$z$	Charge number of an ion
$\alpha$	Degree of dissociation
$\varepsilon$	Dielectric constant (dimensionless)

$\epsilon_\lambda$	Molar absorptivity ( $\text{Lmol}^{-1}\text{cm}^{-1}$ )
$\epsilon_0$	Permittivity of vacuum ( $8.85 \times 10^{-12} \text{ C}^2 \text{ N}^{-1} \text{ m}^{-2}$ )
$\zeta$	Zeta potential (potential at the plane of shear, V)
$\eta$	Viscosity of the medium (P)
$\kappa^{-1}$	Electrical double layer thickness (m)
$\Lambda$	Molar conductivity ( $\text{cm}^2 \Omega^{-1} \text{ mol}^{-1}$ )
$\lambda$	Wavelength (m)
$\bar{\mu}_{app}$	Average apparent mobility ( $\text{cm}^2/\text{Vs}$ )
$\mu_0$	Absolute mobility ( $\text{cm}^2/\text{Vs}$ )
$\mu_a$	Apparent mobility ( $\text{cm}^2/\text{Vs}$ )
$\mu_{A^-}$	Electrophoretic mobility of acidic anion ( $\text{cm}^2/\text{Vs}$ )
$\mu_{B^+}$	Electrophoretic mobility of free base cation ( $\text{cm}^2/\text{Vs}$ )
$\mu_e$	Electrophoretic mobility ( $\text{cm}^2/\text{Vs}$ )
$\mu_{eff}$	Effective electrophoretic mobility ( $\text{cm}^2/\text{Vs}$ )
$\mu_{eo}$	Electroosmotic mobility ( $\text{cm}^2/\text{Vs}$ )
$v_{eo}$	Velocity of the electroosmotic flow (cm/s)
$\sigma$	Standard deviation
$\sigma^2$	Variance
$\psi$	Potential function

## **CHAPTER ONE: Introduction**

Capillary electrophoresis (CE) has become a powerful analytical technique in separation science in recent years due to its many advantages over other separations methods. CE requires only small sample volumes; it requires little or no sample preparation; it provides high separation efficiencies; and it offers rapid separation times with easy automation. One major challenge in CE, however, is optimization of the many physiochemical factors that affect the electrophoretic mobility and separation of analytes. In this section, I will first recount a short history on the development of CE, followed by a discussion of the basic principles and instrumentation in CE. Finally, discussion on optimization and control of separation in CE will be presented.

### **1.1 Short History of Electrophoresis**

Separation in electrophoresis is achieved by the differential migration of charged analyte species under the influence of an electric field. The basic concepts of electrophoresis have been known for a long time in electrochemistry. However, the first application of electrophoresis for separation was demonstrated in 1937 when Tiselius [1] developed the moving boundary method to separate proteins in free solution. Since that time electrophoresis has attracted the attention of many researchers for the separation of biological molecules. Most of these studies were performed in the presence of a supportive media such as agarose or polyacrylamide gels to avoid convective mixing in the free solutions [2]. Polyacrylamide gel electrophoresis (PAGE) was first introduced by Raymond and Weintraub [3], and has in particular become widely used for the separation of biological macromolecules. However, gel electrophoresis suffers from long

analysis times and low efficiencies because of the viscous nature of the media and the low applied electric fields.

An alternative approach to replace the non-convective gels and papers was the use of tubes with small inner diameters. Hjerten [2] provided the first demonstration of the use of capillaries for free zone electrophoretic separation in 1967. He employed 3 mm diameter capillary tubes to separate small anions and macromolecules. However, electrophoresis became a more viable analytical technique only after the introduction of narrower diameter capillaries [4]. These narrow capillaries (25-100  $\mu\text{m}$ ) facilitate the dissipation of heat generated by the electrical resistance of the electrolyte within the capillaries. Consequently, the efficient heat transfer from the small diameter capillaries allows the use of much high electric field strengths, resulting in short analysis times and high separation efficiencies.

Despite the early significant contributions of others, Jorgenson and Luckas are considered as pioneers of modern capillary zone electrophoresis (CZE) [5, 6]. In 1981, they demonstrated the possibility of high separation efficiencies using high field strength in narrow capillaries (75  $\mu\text{m}$  I.D.). The invention of micellar electrokinetic chromatography (MEKC) which involves the use of micelles to separate neutral substances by Terabe et al. [7] also represents another significant step in the development of CE. Since the early 1980s, capillary electrophoresis has grown rapidly and is steadily gaining popularity as a useful technique for the separation of molecules ranging from small ions to complex biological molecules. During same period, considerable experimental works have been done to understand and control the various physico-

chemical factors involved in CE separations. Numerous theoretical models have also been developed to simulate electrophoretic separations [8-10].

## **1.2 Fundamentals of Capillary Electrophoresis**

### **1.2.1 Instrumentation**

The general setup of a capillary electrophoresis instrument is basically that introduced by Jorgenson and Lukacs [6] in 1981. The first CE instruments were laboratory-constructed models but commercial automated instruments have been available since 1987 [11]. Figure 1.1 shows a schematic diagram of a CE instrument. The basic components include a capillary, the high voltage supply, inlet and outlet vessels for the buffer solutions, a detector, and the data acquisition and recording systems (personal computer). The capillary is typically made of fused silica, the outside of which is coated with polyimide for flexibility and strength [12]. In addition capillaries made from glass [6], quartz [2], Teflon [13], and polymers such as PTFE [14, 15] have also been employed, but have not shown any specific advantages, so fused silica capillaries are used herein. The capillary inner diameters are usually 10-100  $\mu\text{m}$  while the outer diameter ranges from 130-385  $\mu\text{m}$ . Typically, capillary lengths range between 20 and 100 cm. Both ends of the capillary are immersed into vessels or vials containing the background electrolyte (BGE) solution.

To perform a CE separation, the inlet buffer vial is replaced with a vial containing the sample solution. Then a small plug of sample (1-10 nL) is injected into the capillary either electrokinetically or hydrodynamically. With hydrodynamic injection, a pressure

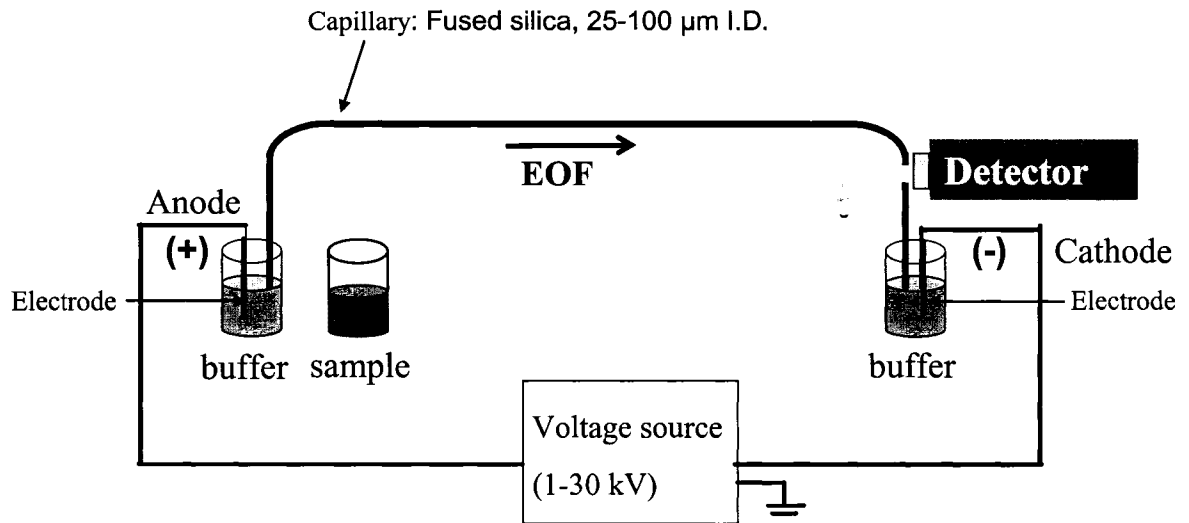


**Figure 1.1** A schematic setup for capillary electrophoresis instrument.

difference is generated between the inlet and outlet ends of the capillary causing the sample solution to flow into the capillary. In electrokinetic injection, the sample is driven into the capillary under an applied electric field by the combined effects of electrophoretic migration and electroosmotic flow. After the sample has been injected a buffer vial is re-introduced to the capillary inlet and separation is initiated by applying a voltage. The voltage required to drive the CE separations is provided by a high voltage power supply (1-30 kV) connected to two electrodes, usually made of platinum or other chemically inert metal, which are positioned along with the capillary ends into the vials. Under the applied electric field, the analyte molecules migrate according to their charge-to-size ratios. Analytes can be detected either on-column (as in Figure 1.1) or post-column. For on-column detection, a small section of the polyimide coating of the fused silica capillary is removed by burning to create the detection window. The output from



the detector is then sent to a personal computer for processing where the height or area of the peak is used as a measure of the concentration of the analyte in the sample solution. Since many parameters in CE are temperature dependent, active temperature control systems are essential to obtain good reproducibility [16]. Another consequence of inefficient temperature control is Joule heating which may lead to peak broadening or drift in the migration times. Most instruments rely on built-in air flow cooling systems but others also employ more efficient cooling methods such as using liquids [16, 17]. The HP<sup>3D</sup> CE instrument used for all the works in this thesis was cooled with a built-in air system.

## 1.2.2 Migration Phenomena in Capillary Electrophoresis

### 1.2.2.1 Electrophoretic Mobility

In the presence of a uniform electric field,  $E$ , an ion experiences a moving force,  $F_E$ , which is equal to the product of its net charge,  $q$  and the electrical field strength,  $E$ ,

$$F_E = qE \quad (1.1)$$

When the ion begins to move through the solvent, it also experiences a frictional retarding force,  $F_d$  which is proportional to its velocity,  $v$ :

$$F_d = -vf \quad (1.2)$$

where  $f$  is the frictional coefficient. For a spherical ion, this frictional coefficient is given by Stokes' law as

$$f = 6\pi\eta r \quad (1.3)$$

where  $\eta$  is the viscosity of the medium, and  $r$  is the hydrodynamic radius of the ion.

With no other significant force acting on the ion (such as electrostatic interaction), the accelerating and retarding forces counter balance quickly resulting in a steady state ion

velocity. Hence, a combination of eqn 1.1, 1.2, and 1.3, gives the steady-state velocity of the ion as:

$$v = \frac{qE}{6\pi\eta r} \quad (1.4)$$

As can be seen from eqn 1.4, the velocity of the ion is proportional to the electric field strength. This proportionality constant of ion velocity per unit field strength is called electrophoretic mobility,  $\mu$  and is given by:

$$\mu = \frac{v}{E} = \frac{q}{6\pi\eta r} \quad (1.5)$$

Eqn 1.5 is known as the Huckel equation. The Huckel equation predicts that the electrophoretic separation of charged analytes is governed by the differences in their charge-to-size ratios. It is the simplest equation used in CE and works well for spherical and large ions [18]. However, there are a number of important limitations to the Huckel equation. Firstly, the equation refers to infinite dilution where the ionic strength and ion-pairing are negligible or absent. As a result, the electrophoretic mobility computed using eqn 1.5 is referred to as the *absolute* or *intrinsic mobility* ( $\mu_o$ ) at infinite dilution. Secondly the Huckel equation fails to predict selectivity changes among analyte ions in various solvents [19, 20]. Finally, the Huckel equation is also unable to describe successfully the electrophoretic mobilities of small inorganic anions [21]. The influence of different factors on ion mobility will be discussed in Section 1.4.

#### 1.2.2.2 Electroosmotic Flow (EOF)

Another important phenomenon in CE is the flow of the bulk liquid inside the capillary upon application of the electric field. This bulk flow of liquid is called electroosmotic flow (EOF) and it results from the effect of the electric field on

counterions adjacent to the charged capillary wall. Under most pH conditions, the inner walls of the fused silica capillaries carry a negative charge due to the presence of weakly acidic silanol (SiOH) groups (pKa ~ 5.3) [24]. To maintain electroneutrality there is an accumulation of positive counterions in the solution adjacent to the capillary wall. Such distribution of counterions in the vicinity of the charged capillary surface lead to the formation of the electrical double layer (EDL) as shown in Figure 1.2.

A fraction of the counterions (cations) along with solvent molecules is adsorbed onto the negatively charged surface to form an immobilized compact layer of solvent molecules and unsolvated ions. The distance from the capillary wall to the center of these specifically adsorbed ions constitutes the inner Helmholtz plane (IHP) [22, 23]. Slightly further from the plane lies the outer Helmholtz plane (OHP) which includes adsorbed solvated ions. The compact layer between the OHP and the capillary wall of the electrical double layer is also referred to as the Stern layer. The diffuse layer extends from the OHP to rest of the bulk solution. At slightly beyond the OHP lies a plane of shear where ions inside this plane remain immobile and ions outside the plane move with the bulk solution. The electric potential at the capillary surface is negative ( $\Psi_0$ ) due the dissociation of the silanol groups. This potential decreases linearly across the Stern layer due to the presence of immobile positive counterions. However, beyond the OHP the potential decreases exponentially within the diffuse layer until it reaches a value close to zero in the bulk solution. The potential at the plane of shear is termed as the zeta potential ( $\zeta$ ). The thickness of the diffuse layer ( $\kappa^{-1}$  in m) in the double layer region is given by [23]:

$$\kappa^{-1} = \sqrt{\frac{\epsilon k_B T}{2e^2 C_i z_i^2}} \quad (1.6)$$

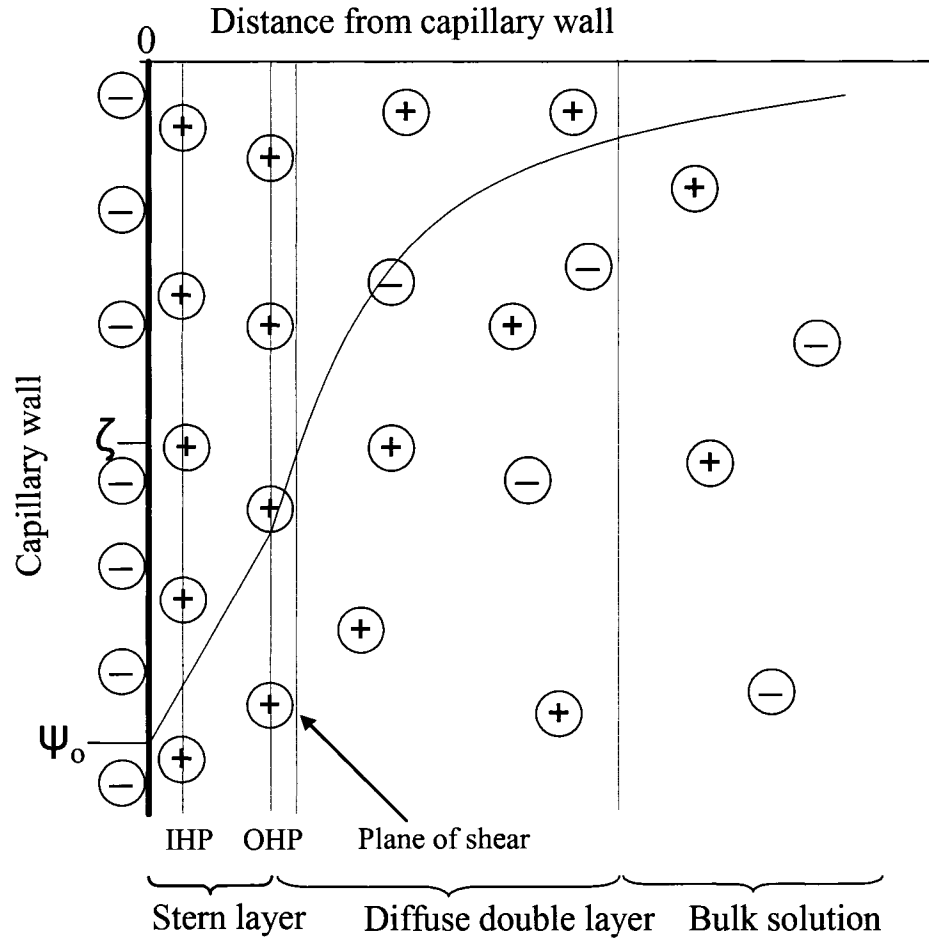
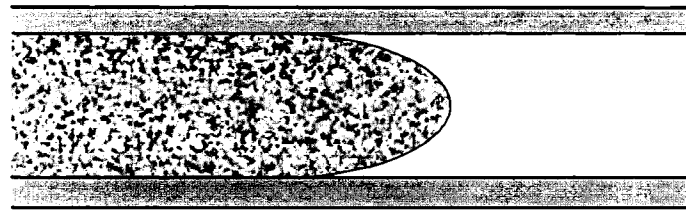
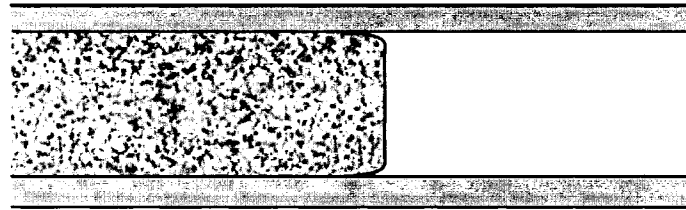


**Figure 1.2** Schematic diagram of electrical double layer (EDL) and variation of the electric potential with distance from the capillary, according to the Gouy-Chapman model refined by Stern and Grahame [22, 23].

where  $\epsilon$  is the dielectric constant,  $k_B$  is the Boltzmann constant,  $T$  is the absolute temperature,  $e$  is the elementary charge,  $z_i$  is charge of the electrolyte ions, and  $C_i$  is concentration of the electrolyte ions. For typical aqueous buffer concentrations used in CE at room temperature, this double layer thickness ranges from 1-20 nm.



A) Hydrodynamic flow



B) Electroosmotic flow

**Figure 1.3** Flow profiles in capillary electrophoresis. A) Hydrodynamic flow B) Electroosmotic flow.

When an electric field is applied, a layer of cations in the diffuse layer (just outside of the plane of shear) is drawn towards the negative electrode (cathode). Since the cations are solvated (hydrated), their migration drags the solvent along with them, resulting in a bulk flow of liquid (EOF) towards the negative electrode. The velocity of the EOF increases radially from zero at the Stern layer to its full magnitude just outside of the diffuse double layer. The double layer thickness is in the range 1-20 nm, and so is essentially negligible compared to the inner diameter of the capillary. In addition, the driving force for the EOF is uniformly distributed along the length of the capillary. Consequently, the flow is nearly uniform throughout the capillary. Hence, unlike the

pressure driven flow, which has a parabolic velocity profile, the EOF has essentially a flat profile (except in the thin EDL near the wall) as shown in Figure 1.3. As shown in the next section, the sign and value of the zeta potential also plays an important role in determining the both the magnitude and direction of the EOF.

### 1.2.2.3 Electroosmotic Mobility

The velocity of the electroosmotic flow ( $v_{eo}$ ) is proportional to the applied electric field ( $E$ ). This proportionality constant is referred to as the electroosmotic mobility ( $\mu_{eo}$ ).

$$v_{eo} = \mu_{eo} E \quad \text{or} \quad \mu_{eo} = \frac{v_{eo}}{E} \quad (1.7)$$

As indicated in the previous section 1.2.3.2, the electroosmotic mobility is a function of the zeta potential ( $\zeta$ ) and this relationship is given by the Smoluchowski equation,

$$\mu_{eo} = -\frac{\varepsilon_0 \varepsilon_r \zeta}{\eta} \quad (1.8)$$

where  $\eta$  is the viscosity of the medium,  $\varepsilon_r$  is the dielectric constant of the medium, and  $\varepsilon_0$  is the permittivity of vacuum ( $8.85 \times 10^{-12} \text{ C}^2 \text{ N}^{-1} \text{ m}^{-2}$ ). The negative sign in eqn 1.8 indicates the negative value of the zeta potential on the capillary surface such that the EOF towards the cathode is represented as normal or positive EOF. As shown in eqn 1.8 the value of zeta potential, dielectric constant and viscosity of the medium determine the magnitude of the EOF. The EOF can be increased by lowering the viscosity of the medium. This can be achieved by using a low viscosity solvent or by increasing the temperature of the solution.

The zeta potential ( $\zeta$ ) is a function of the surface charge density on the fused silica capillary that results from the ionization of the silanol groups (Section 1.2.2.2). Hence, the EOF observed in fused silica capillary depends on the degree of the surface

ionization, *i.e.* the EOF depends strongly on the pH of the electrolyte buffer. The average  $pK_a$  of the surface silanol groups is  $\sim 5.3$  [24]. The  $\mu_{eo}$  increases gradually from pH 2.5 to 4 as only a fraction of the silanol groups are ionized. The EOF then rises significantly with the pH where it reaches a maximum at pH 8-9 as the silanols deprotonate completely. Therefore, control of the pH of the separation electrolyte is essential to maintain a constant EOF and hence reproducible migration times in CE.

The concentration of the electrophoretic buffer (or the ionic strength) and the type of buffer cation also affect the magnitude of the EOF [21, 25]. An increase of the ionic strength compresses the diffuse layer at the plane of shear and lowers the zeta potential (Section 1.2.2.2). This results in a decrease in the electroosmotic mobility as shown in eqn 1.8. The role of buffer ionic strength, pH, type of solvent and buffer ions to control the magnitude of the EOF will be discussed in Section 1.4.

The EOF is responsible for the nonselective transport of ions as well as neutral molecules in CE separations. Often the magnitude of the EOF is so large that it carries both the negative and positive ions to the negative electrode (cathode) providing the possibility of detecting both types of ions simultaneously. Hence, sometimes the EOF is referred to as the “EOF pump” as equivalent to the “pressure pump” in liquid chromatography. However, the presence of a strong cathodic EOF may not be desirable to achieve fast separation and good resolution in certain types of analytes. In addition, it is difficult to obtain repeatable EOF using bare fused silica capillaries [26]. As a result, modification and control of the silica surface is essential to achieve optimized EOF and separations.

### 1.2.2.4 Measurement of Mobility

In the presence of electroosmotic flow, the observed mobility of an analyte ion is the sum of the analyte's intrinsic electrophoretic mobility ( $\mu_e$ ) and the electroosmotic mobility ( $\mu_{eo}$ ). This measurable mobility is referred to as the apparent mobility ( $\mu_a$ ):

$$\mu_a = \mu_e + \mu_{eo} \quad (1.9)$$

Experimentally,  $\mu_a$  is calculated from the observed time the analyte ion takes to migrate from the inlet to the detector ( $t_m$ , in seconds)

$$\mu_a = \frac{L_d L_t}{t_m V} \quad (1.10)$$

where  $L_d$  is the length of the capillary from the inlet to the detector (in cm),  $L_t$  is the total length of the capillary (in cm), and  $V$  is applied voltage (in volts). Similarly, the EOF mobility can be calculated using eqn 1.10 by experimentally measuring the migration time of a neutral solute that does not possess any effective mobility and thus moves with the EOF ( $\mu_{eo}$ ). Common neutral solutes (i.e. markers) used in CE include mesityl oxide, benzyl alcohol, acetone, and methanol [27]. Both the apparent and EOF mobilities are commonly expressed in units of  $\text{cm}^2/\text{Vs}$  although they can also be expressed in SI units as  $\text{m}^2/\text{Vs}$ .

The experimentally measured electrophoretic mobility of an ion is referred as the effective mobility ( $\mu_{eff}$ ). It can be calculated using the following equation:

$$\mu_{eff} = \frac{L_d L_t}{V} \left( \frac{1}{t_m} - \frac{1}{t_{eo}} \right) \quad (1.11)$$

where  $t_m$  and  $t_{eo}$  are the migration times of the analyte ion and the neutral EOF marker respectively measured under same condition. All other terms are as defined for eqn 1.10.

The effective mobility of an ion depends on number of experimental factors such as the



buffer pH, ionic strength, and type of solvents. The effect of these factors on mobility will be discussed in more detail in Section 1.4.

### **1.2.3 Detection Methods**

The diversity of molecules analyzed in CE demands the use of a variety of detection schemes. The detectors for CE should meet the same performance criteria as for other separation techniques such as liquid chromatography. These include good sensitivity, selectivity, linear dynamic range, fast response and low detector noise. Ideally, the detectors should not also respond to the buffer, should not contribute to extra column broadening, and should be reliable and convenient to use. However, no single detector provides all these properties; therefore, an appropriate detector must be chosen based on the particular application.

A number of detection modes have been explored including absorbance, fluorescence, refractive index, chemiluminescence, electrochemical (conductivity, amperometry, potentiometry) and mass spectrometry [28]. Detection can be accomplished either on-column while the analyte zones are migrating through the capillary (UV absorbance, fluorescence, conductivity, refractive index, etc) or off-column as the analytes elute from the capillary (post-column derivatization, electrochemistry, mass spectrometry). For the on-column detection, the detection cell is part of the electrophoresis capillary; thus, zone broadening due to joints, fittings and connectors is eliminated. In off-column detection, however, the detector region usually contributes to band broadening and needs to be evaluated utilizing specific off-column detection techniques. In addition, in post column detection, coupling of the CE system with the detector is technically challenging.

By far the most commonly used detection scheme in CE is on-column measurement of absorption in the ultraviolet (UV) range. This is mainly because of its ease of operation and ability to detect a wide range of molecules. The fused silica capillaries normally used for CE have an absorbance cut-off around 170 nm and thus are suitable for UV detection. The layer of the polyimide coating on the outside of the capillary can be easily be removed by burning off a small section to form a detection window. Hence, almost all commercially available CE instruments employ an ultraviolet-visible (UV-VIS) absorbance detector. In this thesis, the detection used is based on absorbance so a discussion of direct and indirect UV detection in CE is given below.

### 1.2.3.1 UV Absorbance Detection

Absorbance ( $A$ ) of light is defined as:

$$A = -\log_{10}T_r = \log \frac{P_o}{P_i} \quad (1.12)$$

where  $T_r$  is the transmittance,  $P_o$  is power of the incident light and  $P_i$  is the power after having passed through the sample. According to the Lambert-Beer law, the absorbance of light by an analyte is linearly proportional to its concentration ( $C$ ) as:

$$A = \varepsilon_{\lambda}bC \quad (1.13)$$

where  $b$  is optical path length, and  $\varepsilon_{\lambda}$  is the molar absorptivity of the sample. As eqn 1.13 shows the sensitivity in UV detection depends on the path length of the detection cell. With on-column UV detection in CE, the path length is dictated by the inner diameter of the capillary. As a result, detection limits in CE tend to be higher especially when small inner diameter capillaries are used. Typical detection limits obtained with direct absorbance ranges from  $10^{-5}$  to  $10^{-6}$  M.

Different techniques have been explored to overcome low sensitivity of detection in small capillary dimensions. The primary approach has been to increase the optical path length. These include the use of axial illumination [29, 30], a Z-shaped flow cell [31], a multi-reflection cell [30] and the use of a rectangular capillary [32]. The use of egg-shaped or bubble-shaped cell [33] fabricated directly into the fused silica capillary at the site of detection is also used to extend the path length. These modifications enhance the sensitivity and detection limits in the order of  $10^{-8}$  M are achieved. Alternatively, detection sensitivity in CE can also be enhanced using sample stacking and other on-capillary preconcentration techniques [28].

### **1.2.3.2 Indirect UV Detection**

Not all molecules possess a chromophore and hence some can not be detected with direct UV absorbance. Alternative approach for these types of analytes is indirect UV detection which allows detection of non-UV absorbing analytes. The possibility of indirect UV detection in CE was first demonstrated by Hjerten et al. [34] who employed the technique for detection of organic ions. Foret et al. [35] described an indirect UV photometric detection method, which was based on the use of an absorbing co-ion as the principal component of the background electrolyte. Yeung has also published an early comprehensive account of the indirect detection methods in CE [36]. The main advantage of indirect UV detection is the ability to detect a large number of analytes that are undetectable by direct UV methods. Hence, this detection technique is sometimes referred to as “universal detection” as it can be applied to the detection of wide range of non-UV absorbing molecules. Moreover, the instrumentation required is the same as for the direct photometric detection, which is simple and commercially available.

Indirect detection technique utilizes a UV absorbing species in the background electrolyte having the same charge as the analytes. This absorbing co-ion is referred to as the “probe ion” or “visualization agent”. During separations, the migrating analytes (non-absorbing) displace the probe ion providing a quantifiable decrease in the background absorbance and hence allow indirect detection of the analytes. The theoretical limit of detection in indirect detection ( $C_{LOD}$ ) is given by [37]:

$$C_{LOD} = \frac{C_P}{T_R \times D_r} = \frac{N_{BL}}{T_R \times \varepsilon \times b} \quad (1.14)$$

where  $C_P$  is the concentration of the visualization probe,  $T_R$  is the transfer ratio (the number of probe molecules displaced by one analyte molecule),  $D_r$  is the dynamic reserve (ratio of the background absorbance to the noise),  $N_{BL}$  is the baseline noise,  $\varepsilon$  is the molar absorptivity of the probe, and  $b$  is effective path length of the detection window. There are a number of factors, which influence detection sensitivity in the indirect detection mode. The first one involves matching the mobilities of the probe ion and the analytes as closely as possible. Analytes with faster mobilities than the probe generally have a fronted peak profile, while analytes with slower mobility exhibit a tailed peak profile. Hence, the optimum peak shapes and highest sensitivity for a given BGE are achieved for sample ions having effective mobility close to the mobility of the absorbing probe ion.

Second, according to eqn 1.14  $C_{LOD}$  can be optimized by reducing the concentration of the probe,  $C_P$  or by increasing the dynamic reserve,  $D_r$ . However, for indirect absorption detection  $D_r$  is also related  $C_P$ . So decreasing the probe concentration

will not necessarily improve the detection limit as  $D_r$  is simultaneously reduced. Hence, a low-concentration background electrolyte with a high molar absorptivity at the wavelength of detection is required to obtain the best possible detection sensitivity. Detection limits in the ranges of  $10^{-5}$  to  $10^{-6}$  M are commonly achieved for indirect absorbance detections.

Indirect detection is plagued by the frequent occurrence of system peaks. The system peaks may have several different causes (e.g. pH, ionic strength, solvents effects) but are mainly caused by the presence of more than one co-ion in the BGE. Hence most indirect detection have been performed with BGE that consist of only two components, the probe and its counter-cation, under which conditions the displacement process is simple and the possibility of more than one system peak is avoided. Some practical rules for predicting the existence of system peaks have been reported by Macka et al. [38] who proposed a descriptive model based on transient isotachopheresis of the sample species and of the co-anion. Mathematical simulations have also been developed to describe the behavior in multi component electrophoretic system in terms of eigenvalues [10]. It is desirable to know the mobility or position of the system peak to avoid possible interference with the analyte of interest. In summary choice of the appropriate probe and background electrolyte is crucial for the success of separation and detection in CE using indirect UV absorbance.

### 1.3 Modes of Capillary Electrophoresis

Over the years, different modes of capillary electrophoretic separations have been developed. These include capillary zone electrophoresis (CZE), capillary gel electrophoresis (CGE), micellar electrokinetic chromatography (MEKC), capillary electrochromatography (CEC), capillary isoelectric focusing (CIEF), and capillary isotachopheresis (CITP) [39]. In all these modes, separations are carried out in small dimension capillaries in the presence of an electric field, but the modes differ in the nature and composition of the background electrolytes employed. In this thesis, only CZE and MEKC are used. Therefore, the descriptions below are limited to these two techniques.

#### 1.3.1 Capillary Zone Electrophoresis (CZE)

Capillary zone electrophoresis (CZE) is the most widely used form of CE because of its simplicity and versatility. In this mode, the sample is applied as a narrow zone (band), which is surrounded by the separation buffer. When an electric field is applied, each component in the sample zone migrates according to its apparent mobility (Section 1.2.2.1). This apparent mobility ( $\mu_a$ ) determines the overall migration time of an analyte and is therefore related to both the electrophoretic mobility of the analyte ( $\mu_e$ ) and the EOF as:

$$\mu_a = \mu_e + \mu_{eo} \quad (1.9)$$

Under the influence of an applied electric field sample ions will move towards their appropriate electrode. The speed of the ions movement towards the electrodes is governed by their size and number of appropriate charges. Smaller molecules with a

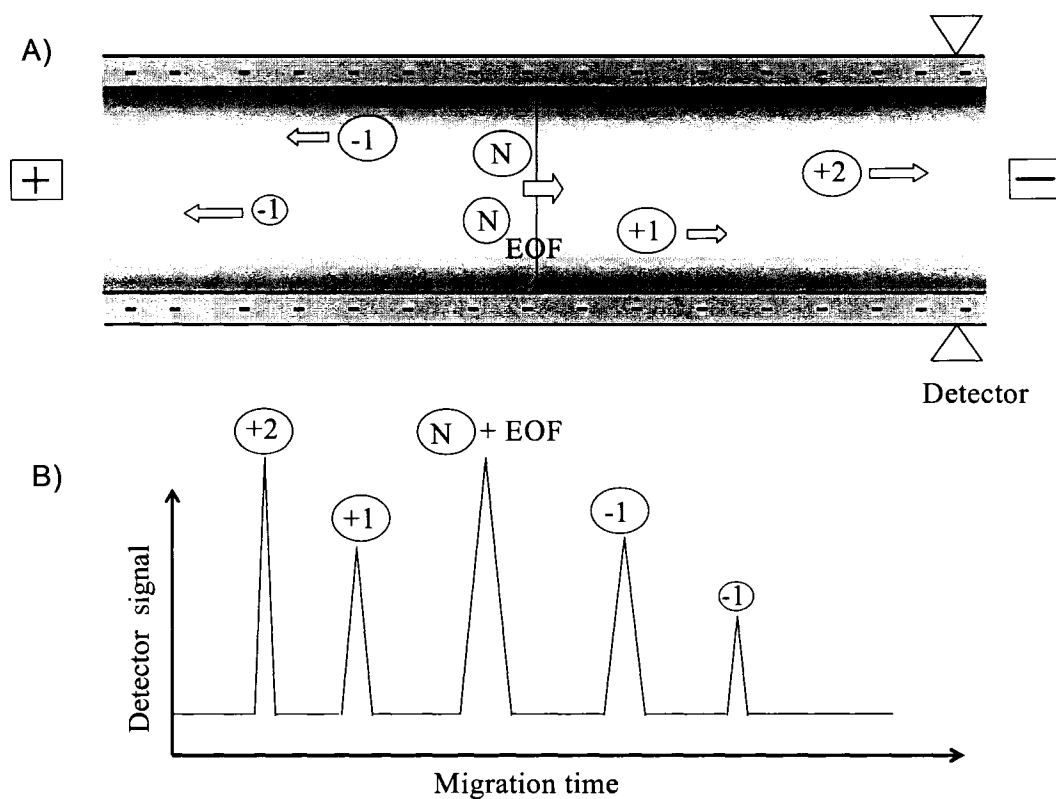


**Figure 1.4** Illustration of A) separation process in CZE inside a capillary B) the resulting peaks in the electropherograms.

large number of charges will move more quickly than larger or less charged compounds as shown in Figure 1.4.

However, the presence of EOF allows the separation and detection of both cations and anions within a single analysis in CZE. This is because at moderate pH values ( $> 4$ ) the magnitude of the EOF mobility is greater than the electrophoretic mobilities of most analytes, such that both cations and anions are swept past the detector placed near the

cathode. Under this condition, cations, which move in the same direction as the EOF, are detected first and the anions migrating counter to the EOF are detected last. All the neutral molecules migrate with the EOF, unresolved, and are detected as a single band between the cations and anions (Figure 1.4). Therefore, pH is the major operating parameter in CZE as it affects the separation of ionic species by controlling both the analyte charge (Section 1.4.1) and the magnitude of the EOF (Section 1.2.2.3). Other variables that can be used in the optimization of CZE separations include the electrolyte type and concentration, temperature and additives to the buffer such as organic solvents and chiral selectors [26, 40]. As shown in subsequent Chapters, one of the objectives of this thesis is to develop separation methods in the presence of various organic solvents or nonaqueous solvents.

### **1.3.2 Micellar Electrokinetic Chromatography (MEKC)**

Micellar electrokinetic chromatography (MEKC) was initially developed for the resolution of uncharged compounds, which cannot be separated using free solution CE [7, 41]. The separation conditions involve use of buffer containing relatively concentrated surfactant solutions. Surfactants are amphiphilic species comprising both hydrophobic tail and hydrophilic head regions. They can be anions, cations, zwitterions or neutral molecules. The most commonly used surfactants for MEKC include sodium dodecylsulfate (SDS), cetyltrimethylammonium bromide (CTAB), bile salts (e.g. sodium cholate) or a mixture of different surfactants [42]. Above a specific concentration, known as the critical micelle concentration (CMC), the surfactant molecules self-aggregate to form micelles. The micelles are composed of the hydrophilic head groups on the outer shell and the hydrophobic tail groups (non-polar) in the inner core.



In MEKC, the micelles serve as a pseudo-stationary phase that resembles the stationary phase in reverse-phase high-pressure liquid chromatography (RP-HPLC). However, the micelles are not stationary but rather move along the capillary against the EOF. The separation is a result of the combined effect of the differential partitioning of neutral sample molecules between the aqueous buffer and the micellar (pseudo stationary) phase as well as any differential migration of the ionic species. Various types of interactions can occur between the analytes and micelles, including hydrophobic, electrostatic and hydrogen-bonding interactions.

The retention factor ( $\tilde{k}'$ ) for a neutral species in MEKC can be calculated using the equation [7]:

$$\tilde{k}' = \frac{t_R - t_{eo}}{t_{eo} (1 - t_R / t_{mc})} \quad (1.15)$$

where  $t_R$ ,  $t_{eo}$  and  $t_{mc}$  are the migration (or retention) times of the neutral analyte, the EOF and micelle respectively. The retention factor is the ratio of the total solute in the micelles to those in the bulk solution. Strongly interacting solutes migrate with the micelle and would have  $\tilde{k}'$  value approaching infinity. Solutes that do not interact with the micelle migrate with the EOF and would have  $\tilde{k}' = 0$ . A solute spending equal time in the buffer and in the micelle would have a  $\tilde{k}'$  value of 1. Thus, the migration time of neutral analytes ( $t_R$ ) should lie between that of the EOF ( $t_{eo}$ ) and that of the micelle ( $t_{mc}$ ). This range is often referred to as the migration window in MEKC. Highly hydrophobic molecules such as Sudan III [7] are totally included into the micelle so they are widely used to mark the migration time of the micelle ( $t_{mc}$ ).

Although originally developed for the separation of neutral molecules, MEKC has increasingly been used to separate charged analytes using both ionic and neutral (zwitterionic) surfactants [43-45]. Separations of analytes can be obtained due to differences in electrophoretic mobilities as well as differences in degree of interactions with the surfactant. For separations involving anionic micelles, cationic analytes undergo ion-exchange type of interactions with the surface of the micelle. Depending on the degree of the interactions (charge), the cationic analytes could migrate before or with the micelle. In contrast, minimal interaction is expected between the anionic analytes and the micelles owing to electrostatic repulsion by the negatively charged surface of the micelle. The separation mechanism for anionic analytes using cationic surfactants is similar except just the opposite.

Different techniques are used to control the partitioning of analytes between the micelles and the aqueous buffer. These include the type and concentration of the surfactant [46] and presence of other additives to the buffer, such as organic solvents [47, 48], ion-pairing [49] and complexing agents [49]. The degree of interaction can also be manipulated by changes in temperature [50], pH, and ionic strength [46]. The role of these factors to alter selectivity in CE in general will be discussed in the next Section.

#### **1.4 EOF and Selectivity Control in CE**

Although often neglected, the electroosmotic flow (EOF) plays a key role in electrophoretic separations. Alteration of the EOF could result in more rapid separation, improved reproducibility or resolution of particularly difficult separation tasks. As shown in eqn 1.9 (Section. 1.2.2.4) the apparent mobility is a function of both the analyte ion's electrophoretic mobility ( $\mu_e$ ) and the electroosmotic flow ( $\mu_{eo}$ ). Thus, rapid

separations can be achieved if the electrophoretic mobility and the EOF are in the same direction. This mode of separation is referred to as *co-EOF*. Using this technique, for instance, very rapid separation of anions have been demonstrated [51]. However, while co-EOF separations are rapid, achieving full resolution can be challenging.

Resolution in CE is governed by the expression [26]:

$$R_s = \frac{\sqrt{N}}{4} \frac{\Delta\mu}{\bar{\mu}_{app}} = \frac{\sqrt{N}}{4} \left( \frac{\Delta\mu}{\mu_{eo} + \mu_e} \right) \quad (1.16)$$

where  $N$  is the average number of theoretical plates,  $\Delta\mu$  is the difference in the electrophoretic mobility of the ions and  $\bar{\mu}_{app}$  is the average apparent mobility of the analytes. If the EOF and ion mobility are equal in magnitude but opposite in direction, the denominator term in the brackets of eqn 1.16 becomes zero, and resolution goes to infinity in theory. This condition is known as *counter-EOF*, where the electrophoretic mobility of the ion is offset by the electroosmotic flow. The resultant separation power is extremely high, and in practice this approach has been used to separate isotopic species [52, 53].

Alternatively, if the EOF and electrophoretic mobility are in the same direction, this denominator term becomes large, and achieving resolution can be challenging. Hence, in co-EOF separations, resolution is fundamentally dependent upon there being a significant difference in the electrophoretic mobilities between the two species ( $\Delta\mu$ ). Thus, control of the EOF enables rapid separation speed or excellent separating power. This section will discuss the performance and characteristics of capillary coatings for the

alteration and control of the EOF. In addition, various buffer conditions and additives that can be used to increase efficiencies and improve separations in CE will be described.

### 1.4.1 Buffer pH

Manipulation of the pH of the buffer is a common method to modify the separation selectivity in CE. By varying the pH, the degree of ionization of the analytes and hence their effective electrophoretic mobilities can be altered. The acid-base equilibrium between the ionized and unionized species so rapid compared to their migrations that the analyte appears as one peak. The influence of the pH on the effective electrophoretic mobility ( $\mu_{eff}$ ) of a monoprotic weak acid and base are given respectively by [54]:

$$\mu_{eff} = \alpha_{A^-} \mu_{A^-} = \frac{K_a}{[H^+] + K_a} \mu_{A^-} \quad \text{and} \quad \mu_{eff} = \alpha_{B^+} \mu_{B^+} = \frac{[H^+]}{[H^+] + K_a} \mu_{B^+} \quad (1.17)$$

where  $\mu_{A^-}$  and  $\mu_{B^+}$  are the effective mobilities of the fully deprotonated weak acid ( $A^-$ ) and weak base ( $B^+$ ) respectively,  $K_a$  is the acid dissociation constant of the analyte,  $\alpha$  is the degree of ionization of the analyte, and  $[H^+]$  is the concentration of hydronium ions in the buffer solution. Accordingly, the effective mobility of the analyte is function of the extent of ionization, which is determined by the pKa of the analyte and pH of the solution. The relationship in eqn 1.17 predicts that the most dramatic changes in the analyte electrophoretic mobility occur when the pH is at or near the pKa of the analyte. Hence variations of the buffer pH have been used as a means to achieve selectivity changes among analytes such as organic acids [54] and anions [55].

For weak acid anions, the effective charge on the anion can be controlled using the pH. Borate (pK<sub>a</sub> = 9.2), carbonate (10.3) and phosphate (7.2) show dramatic

selectivity changes as the electrolyte pH is varied over the 8-13 range [51]. Similarly, use of acidic buffer conditions (pH 2.5) enhances the selectivity ( $\Delta\mu$ ) between nitrate and nitrite ( $\text{pK}_a = 3.15$ ) enabling their rapid separation [56]. However, this approach has limited use for small inorganic species such as chloride, bromide, iodide and fluoride that have unattainable  $\text{pK}_a$  values [26].

In addition to the influence on the ionization of analytes, the buffer pH also affects the ionization of silanol groups at the capillary wall and hence the EOF. The silanol ( $\text{SiOH/SiO}^-$ ) group is a weak acid with an average  $\text{pK}_a$  of about 5.3 (Sections 1.2.2.2 and 1.2.2.3). As the ionization of the silanol increases with the pH, the magnitude of the EOF also increases. In general, the EOF displays a sigmoidal behavior as a function of pH [26]. The use of extreme buffer pH is avoided in CE, because the current would be extremely high due to the high mobility (or conductivity) of the  $\text{H}^+$  and  $\text{OH}^-$  and because the buffer would slowly dissolve the silica at high pH ( $>12$ ).

#### 1.4.2 Buffer Ionic Strength

In order to make a run buffer solution for CE, a defined concentration of ionic electrolytes have to be dissolved, resulting in an ionic strength ( $I$ ) defined as:

$$I = \frac{1}{2} \sum_{i=1}^n c_i z_i^2 \quad (1.18)$$

where  $z_i$  and  $c_i$  are the charge and molar concentration of each ionic species in the background electrolyte. In CE, varying the ionic strength or concentration of the run buffer has been used to affect migration times, selectivity and separation efficiencies. High ionic strength buffers have been used to reduce electrodispersion broadening [57], and extremely high ionic strength buffers (up to 2 M) have been employed to minimize

adsorption of cationic proteins on capillary walls [58]. High buffer ionic strengths have been used to concentrate or "stack" sample analyte on-capillary [59].

However, most commonly CE buffers range between 5 and 50 mM - governed at the low end by the need for buffering capacity and at the high end by the effects of Joule heating. Within this range, dramatic electrophoretic mobility, and thus selectivity, changes among analyte ions have been observed [19, 25]. Different empirical relations and theoretical models have been developed to describe the influence of ionic strength on electrophoretic mobility. One of the first theoretical models is the Debye-Hückel-Onsager (DHO) equation which can be written in general form as [60]:

$$\mu_{eff} = \mu_0 - const\sqrt{I} \quad (1.19)$$

where  $\mu_{eff}$  is the effective electrophoretic mobility,  $\mu_0$  is the mobility of the ion at infinite dilution, and  $I$  is the ionic strength of the buffer. The *constant* is sometimes referred to as the *Onsager slope* and accounts for the effect of the ionic atmosphere surrounding the analyte ion on its mobility. According to this model, the ionic strength, or more specifically the ionic atmosphere affects the mobility of the ion in two ways. First, the ionic atmosphere that surrounds the analyte ion possesses a charge equal in magnitude but opposite in sign to the analyte ion. Under an applied electric field, this ionic atmosphere will migrate in a direction opposite to the analyte mobility. Thus, the ion atmosphere will try to drag along all of its constituent ions, including the analyte ion. This is known as the *electrophoretic effect*. Second, the center of charge of the ionic atmosphere is displaced from the centre of charge of the analyte ion owing to the movement of the analyte ion. Thus, the attractive force existing between the analyte ion and the lagging ionic atmosphere will slow down the motion of the ion. This ion

retarding effect is known as the *relaxation effect*. Hence, according to the Debye-Hückel-Onsager equation for dilute buffers (<1 mM) the electrophoretic mobility of an ion decreases linearly with the square root of the ionic strength. As a result, mobilities observed in CE have been generally plotted against the square root of the buffer ionic strength. However, non-linear relationships have been observed particularly at high ionic strengths and for multi charged analytes.

Li et al. used the Pitts equation to describe the influence of ionic strength on the mobility of singly and multiply charged anions [25]. The DHO theory assumes that the ions are point charges but the Pitts treatment allows for the finite size of the ions. Based on the Pitts treatment [61], the mobility dependence for 1:1 electrolyte system can be expressed in a general form as:

$$\mu_{eff} = \mu_0 - Az \frac{\sqrt{I}}{1 + Ba\sqrt{I}} \quad (1.20)$$

where  $z$  is the charge on the analyte ion,  $A$  and  $Ba$  are constants.  $A$  encompasses terms including the electrophoretic effect and relaxation effect. The authors experimentally determined based on 42 test analytes that the optimal value for  $Ba$  is 2.4 [25]. This equation successfully predicted a linear dependence of mobilities of all anions on the ionic strength up to  $I = 0.1$  M. As a rule of thumb, the ionic strength is most effective in changing the relative migration if the analytes possess different charges or if there is significant difference in the absolute mobilities ( $\mu_0$ ) of the ions [21]. In addition, ionic strength more significantly affects the mobility of multiply charged ions than singly charged ions.

The ionic strength of the buffer electrolyte also affects the magnitude of the electroosmotic mobility. This is because as shown in eqn 1.6, the double layer thickness

( $\kappa^{-1}$ ) is inversely proportional to the buffer concentration [23] and therefore, the EOF is dependent on the ionic strength of the electrolyte buffer. An increase in ionic strength decreases the double layer thickness as a result of which the potential falls off rapidly with distance. This is commonly referred to as the compression of the double layer. In aqueous solution at 25 °C, the value of  $\kappa^{-1}$  ranges from 3 nm at  $I = 10$  mM to 96 nm at  $I = 0.01$  mM. Nonetheless, the effect of ionic strength on the EOF is relatively small compared to the effect of pH.

### 1.4.3 Capillary Coatings

The fused silica capillaries used in CE possess an intrinsic negative charge owing to the presence of weakly acidic silanol (SiOH) groups. In addition to isolated silanol groups, the surface also contains geminal and vicinal silanol groups at the silica wall with slightly different acidic strength. Because of this heterogeneous nature of the surface, the pKa of the silanol groups ranges from 4 to 6 with an average value of 5.3. This gives rise to irreproducible electromigration of ions in bare fused silica capillaries. Surface modifications (covalent or adsorption) can dramatically change the properties of capillary surfaces and allow silica capillaries to solve various separation problems in CE. By choosing appropriate chemical modification of the inner surface of the capillary, the EOF and the hydrophilicity of the capillary column can be manipulated. Enormous effort has been made to find a coating procedure that is simple, reproducible and that yields stable coatings under conditions required for separations preferably over a broad range of buffer pH. With the introduction of high-throughput capillary array electrophoresis separations, the importance of a reproducible coating process has dramatically increased. While altering the EOF the coating should also not affect the analyte mobility but



suppress any interactions between the surface and the analytes. Consequently, there are strong driving forces for chemical modification of the surface charge on the capillary wall.

The first reason for surface modification is reduction or elimination of interactions of analytes with the capillary wall. Since the capillary surface is negatively charged at most pH values, the wall interactions are severe for positively charged analytes. Adsorption of the analytes onto the bare capillary wall arises primarily from electrostatic attraction although nonspecific interactions may be present. Secondary interactions due to hydrophobic and hydrogen-bonding between the adsorbed and the free analytes could also occur [62]. Such analyte adsorptions lead to significant band-broadening, poor migration time reproducibility, and low sample recovery [62, 63].

The second reason for the need to modify the surface is alteration of the EOF to effect more rapid separation, improved reproducibility and resolution. In general, the magnitude of the EOF mobility ( $\mu_{eo}$ ) in bare silica capillaries is greater than the electrophoretic mobility ( $\mu_e$ ) of most analytes. At neutral pH, the  $\mu_{eo}$  typically ranges from  $5.0 \times 10^{-4}$  to  $8.0 \times 10^{-4} \text{ cm}^2/\text{Vs}$ . This allows for simultaneous determination of both positively and negatively charged species when the detector is placed at the cathodic (negative) end of the capillary. However, in the case of high mobility analytes such as small anions, the  $\mu_e$  values are comparable to or even greater than that of  $\mu_{eo}$ . For instance, the electrophoretic mobilities of inorganic anions, chloride and bromide are 7.92 and  $8.09 \times 10^{-4} \text{ cm}^2/\text{Vs}$  respectively. Hence, some of these anions migrate faster than the EOF but in the opposite direction. Consequently, separation of these anions using counter-EOF mode would not only take a long time but would fail to detect some of the

faster migrating ones. Furthermore, bare silica capillaries generate irreproducible EOF from run to run and the EOF can vary even more drastically from capillary to capillary.

Thus, coating or modification of the capillary surface is performed to suppress analyte adsorption and more importantly to alter or fine-tune the EOF. By choosing the appropriate chemical modification for the inner surface of the capillary, the charge state of the capillary and hence the EOF can be manipulated. Different approaches have been reported in the literature for surface modification of CE capillaries. Generally, these coating techniques are classified as permanent or dynamic based on the nature of the attachment of the coating to the capillary wall.

#### **1.4.3.1 Permanent Wall Coating**

A static or a permanent wall coating is generally used to eliminate EOF and interactions of analyte with the inner walls of the capillary. The coating procedure involves chemical derivatization of the capillary surface with a modifier, such that the permanent coating deactivates or shields the anionic charge on the silanols. The modifiers can be covalently bonded onto the capillary wall via siloxane bonds [64], silane bond [65] or silicon-carbon bonds [66] which results in a surface layer that cannot be removed or regenerated easily during normal capillary rinsing. These bonds serve to either attach the coating materials directly onto the surface or linkers/anchor groups for subsequent derivatization such as polymerization or immobilization step. Examples of such anchor groups include glycidiosilanes for poly(ethylene glycol) (PEG) coatings [67], aminosilanes for maltopolysaccharides [68], methacryloyltrimethoxysilane for polyacrylamide [69], vinylsilanes for polymerization of acrylamide [70], and vinyl acetate to prepare poly(vinyl alcohol) (PVA) coatings [71, 72]. Noncovalent

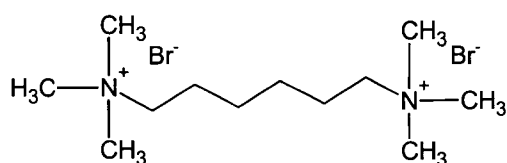
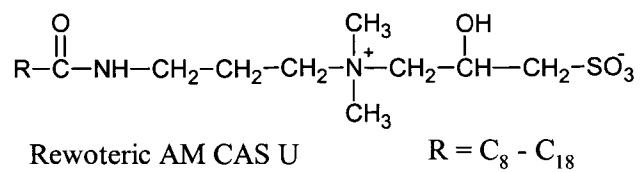
immobilization of polymers such as PVA and PEG have also been used as permanent coatings [71, 72]. The research on permanent capillary modification in CE is still an ongoing area of interest but a number of reviews are also available in the literature [73, 74].

Permanent wall coatings are generally more effective at eliminating analyte interaction with the silica wall of the capillary. However, permanent coatings also result in alteration of the EOF such that the direction and magnitude of the EOF is determined by the electrostatic properties of the coating. Most of the existing derivatized capillaries consist of neutral coatings that are applied to deactivate the charged silanol surface. Thus, the value of the EOF from a given coating is constant and usually the EOF obtained is generally suppressed near to zero. Since the migration of the analytes is completely based on their electrophoretic mobilities under such condition, analytes with a low electrophoretic mobility show long separation times. Moreover, the coating procedures can be complex and time consuming. The derivitization process involves a sequence of steps such as capillary pretreatment, coating, washing and drying. The whole procedure could take up to several hours [70, 75]. Furthermore, homogeneity and reproducible application of the coating are also areas of particular concern in the use of permanent coatings. Consequently, most research in CE capillary permanent coatings are directed towards specific applications such as preventing analyte-wall interactions, rather than for the more general purpose of EOF modification. Permanently modified capillaries are commercially available particularly for biomolecule analysis but these capillaries are expensive and show poor stability at high pH values [76].

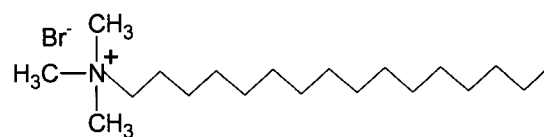
### 1.4.3.2 Dynamic Wall Coatings

An alternative to permanent capillary wall coatings is the use of dynamic coatings. Dynamic wall coatings are attractive because they overcome the difficulties in conducting reproducible, homogeneous chemical derivatization reactions on the capillary surface. Dynamic coatings are typically prepared by rinsing the capillary with a buffer containing a suitable coating agent such as polyamines, polymers or surfactants. Figure 1.5 shows examples of some commonly used polyamines and surfactants for dynamic coating. The term “dynamic” refers to the behavior where there is dynamic equilibrium between the additive molecules in the buffer and on the capillary wall. As a result, dynamic coated capillaries require occasional regeneration and/or addition of a small concentration of the coating agent into the separation buffer. The effectiveness and stability of such coatings depends mainly on the degree of interaction between the modifying molecule and the surface, and on the concentration of the modifying additive in the buffer. The types of interactions involved between the capillary surface and modifying molecules include electrostatic [52], hydrophobic [71], hydrogen bonding [71] or simple physical adsorption [76].

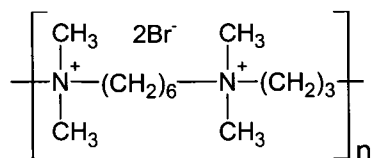
Dynamic modification of the surface against adsorption of cationic or acidic analytes and the simultaneous suppression or variation of the EOF lead to significant improvements in efficiency and peak symmetry, and consequently much higher resolution [76, 77]. These types of coatings have been used for the separation of various types of large biomolecules such as peptides [71], proteins [71, 78] and carbohydrates [79], and for acid and basic pharmaceuticals [80]. Dynamic coatings have also been successfully applied in the fast separation of inorganic and small organic anions for



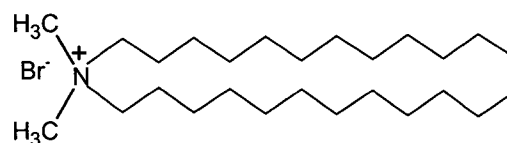
Hexamethonium bromide (HMB)



Cetyltrimethylammonium bromide (CTAB)



Hexadimethrine bromide (HDB)



Didodecyldimethylammonium bromide (DDAB)

**Figure 1.5** Structure of commonly used additives for dynamic capillary coatings.

which polyamines, surfactants or polymeric materials are added to the buffer to reverse the EOF [51, 55]. This enables which polyamines, surfactants or polymeric materials are added to the buffer to reverse separation in the co-EOF mode where both the EOF and anions are migrating in the same direction (Section 1.4). Variation of the EOF in such a manner increases the apparent mobility of the anions and shortens the migration times, which leads to an increase of efficiency but decreases in resolution (eqn 1.16).

One of the main objectives of this thesis is the development an EOF modification procedure, which satisfies the above features. Our dynamic coatings are based on single and double chain cationic surfactants of varying hydrocarbon lengths. These surfactant-based coatings are simple to apply, versatile, robust, and inexpensive. Furthermore, these coatings provide an effective means to control and alter the EOF for fast anion analysis. A discussion on the properties, aggregation and adsorption mechanisms of cationic surfactants is given below.

### **1.4.3.3 Surfactant Based Coatings**

The first use of long chain cationic surfactants for EOF modification in CE was reported by Reijenga et al. [81] in 1983. Tsuda also employed the surfactant cetyltrimethylammonium bromide ( $C_{16}TAB$  or CTAB) for EOF reversal in anion analysis [82]. Similarly, Zare and co-workers [83] had also used cationic surfactants for EOF reversal in the separation of small carboxylic acids. Since then cationic surfactants have been widely used in CE mainly to control the EOF and optimize separation times and efficiencies in the separation of small inorganic anions [51, 55, 78]. Although widely used to modify the EOF, the mechanism by which cationic surfactants alter the EOF was not well understood. Most cationic surfactants reverse the EOF when they are used

above a certain concentration that is characteristic of the surfactant and buffer. However, what are the characteristics of surfactants? Why do they assembly together to form aggregates and what are the factors affecting their aggregation formations? The next discussion will focus on these points, which are necessary to successfully utilize surfactants for CE separations.

The term “surfactant” is a contraction of the term “surface-active agent”.

Surfactants are amphiphilic molecules with a characteristic molecular structure consisting of a functional group that has very little attraction for the solvent, known as a lyophobic group, together with a group that has strong attraction for the solvent, called the lyophilic group [84]. In the case of a surfactant dissolved in aqueous medium, the lyophobic and lyophilic groups are known as the hydrophobic (water disliking) and hydrophilic (water liking) groups, respectively. The hydrophobic group usually consists of one or more long-chain hydrocarbon residues, and less often of halogenated, oxygenated hydrocarbon or siloxane chains. The hydrophilic head group, on the other hand, is either an ionic or a polar functionality. Depending on the nature of the hydrophilic group, surfactants are classified as anionic, cationic, zwitterionic, and non-ionic if the head group bears a negative, positive, both or no apparent charges, respectively.

When a surfactant is dissolved in water, the hydrocarbon chain (hydrophobic group) distorts the structure of the water, and therefore increases the free energy of the system. This distortion occurs via breakage of the hydrogen bonds between the water molecules and structuring the water in the vicinity of the hydrophobic group. The solution responds so as to minimize the contact between the hydrophobic group of the surfactant and the solvent molecules. As a result, the surfactant molecules will be

concentrated at the surface of the water, with their hydrophobic groups oriented predominantly away from the water and the hydrophilic groups suspended in the aqueous solution.

However, as the concentration of surfactant increases, there is a point at which the interface is completely covered and there is no more space for extra surfactant molecules. At this point the surfactant molecules start to aggregate into clusters within the solution with their hydrophobic groups directed toward the interior of a cluster and their hydrophilic groups directed toward the solvent. For single chained surfactants, these aggregated structures are known as micelles, and the concentration at which the free surfactants start to form micelles is called the critical micelle concentration (CMC). Micellization is therefore a means for removing the hydrophobic groups from contact with the water, thereby decreasing the distortion of the solvent's structure and reducing the free energy of the system. Consequently the hydrophobic tails of the surfactants associate in the core of the micelle to maximize their interactions with one another (van der Waals interactions) and minimize their interactions with water. However, as the surfactant molecules aggregate there is interaction (repulsive) between the hydrophilic head groups. For ionic surfactants, the electrostatic repulsion between the head groups inhibits aggregation. Hence, the hydrophobic tails of the surfactants cause the surfactants to aggregate, while the electrostatic repulsion between the head groups disfavors the micelle formation. When there is little distortion of the structure of the solvent by the hydrophobic group (e.g., in water, when the hydrophobic group of the surfactant is short), or the head group repulsion is strong, then there is little tendency for micellization to



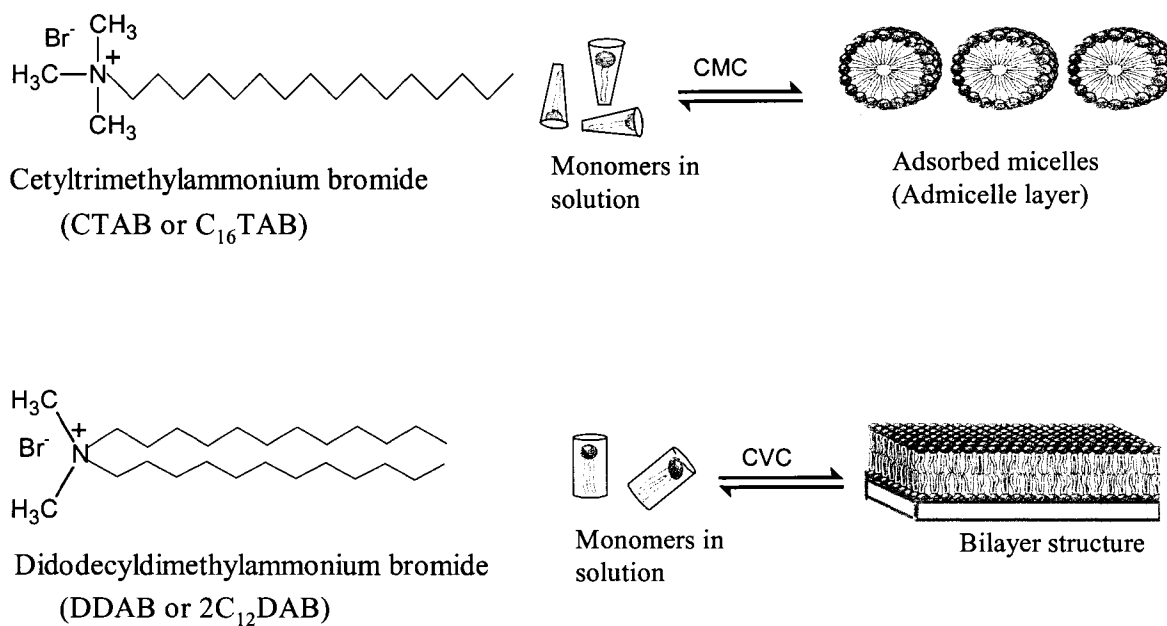


**Figure 1.6** Aggregations of single chain and double chain cationic surfactants to form micelles and bilayers respectively

occur. This is often the case in nonaqueous solvents, and therefore micelles of size comparable to those formed in aqueous media are seldom found in other solvents.

The aggregation of surfactant molecules into various assemblies has been studied extensively. Israelachvili et al. [85] introduced a simple but important molecular packing parameter model that allows prediction of the shapes and sizes of surfactant aggregates.

They used packing parameter ( $P$ ) which is defined as:

$$P = \frac{V_c}{l_c a_h} \quad (1.21)$$

where  $V_c$  and  $l_c$  are the volume and the length of the surfactant tail and  $a_h$  is electrostatic cross-sectional area of the head group expressed per surfactant molecule constituting the aggregate. The values of  $V_c$  and  $l_c$  can be obtained according to Tanford's model using the equations [86]:

$$l_c \approx 0.154 + 0.126n \text{ (nm)} \quad (1.22a)$$

$$V_c \approx (27.4 + 26.9n) (\times 10^{-3} \text{ nm}^3) \quad (1.22b)$$

where  $n$  is the number of carbon atoms on the hydrocarbon tail. The value of  $a_h$  can be determined from the aggregation number of single-chain surfactants. The length of the alkyl chain has less effect on the aggregation structure, as both  $V_c$  and the  $l_c$  of the hydrocarbon chain increase proportionally, and thus the packing parameters remains constant.

Accordingly, if the value of the packing parameter is such that  $0 \leq P \leq 1/3$ , the surfactant molecules aggregate to form spherical micelles [85]. Similarly, if the  $P$  value such that  $1/3 \leq P \leq 1/2$  and  $1/2 \leq P \leq 1$ , respectively cylindrical and bilayer shapes are formed. In general, single chained cationic surfactants are classified in the first range ( $P < 1/3$ ) whereas the double chained surfactants are in the last category ( $P$  is in the range 0.5 – 1). For instance, the single chained surfactant,  $C_{16}$ TAB has a packing parameter of 0.33 in aqueous solution consistent with spherical micelle formation [87]. On the other hand, the double-chained surfactant, didodecyldimethylammonium bromide ( $2C_{12}$ DAB) has a  $P$  value of 0.62 in water and forms a bilayer (vesicle) structure at concentrations higher than the critical vesicle concentration (CVC, referred hereafter as CMC for

simplicity) [87]. This difference in aggregate structures is attributed to the increased tail group cross-sectional area of the double hydrocarbon chain compared to the single chain. Single chained surfactants possess a conical shape owing to the large cross sectional area of the head group while the double-chained surfactants are cylindrical in shape. The packing factor can be changed by decreasing the electrostatic repulsion between the adjacent head groups.

However, the exact mechanism of surfactant adsorption onto the silica capillary surfaces has been subject of debate. This has been mainly due to absence of techniques to directly observe the aggregates on a surface. Most of the studies in the literature were based on indirect evidence using adsorption isotherms [88]. For instance the adsorption of cationic single-chained surfactants onto silica surfaces has been described as a bilayer structure as shown in Figure 1.6. In recent years, Atomic Force Microscopy (AFM) has been used to directly image surfaces coated with different surfactants to more directly determine their coating morphology [89, 90]. AFM studies by Liu et al. have shown that single chain surfactants such as  $C_{16}TAB$  form spherical aggregates on silica surfaces [90]. The AFM images obtained on the silica in the presence of 1.8 mM  $C_{16}TAB$  in aqueous solution showed aggregates with a diameter of about 4.4 nm roughly double the extended length of one  $C_{16}TAB$  molecule. Similar AFM imaging results have also been observed for other quaternary ammonium surfactants adsorbed on silica surfaces [89]. Baryla et al. [77] had also observed  $C_{16}TAB$  micelles adsorbed to the silica surface using AFM imaging.

Formation of a surface micelle structure as depicted in Figure 1.6 seems reasonable in light of the packing factor for single chained surfactants such as  $C_{16}TAB$ .

The surface spherical structures could result from direct adsorption of the micelles or could be formed through aggregation of the surfactant monomers on the surface. Double-chained surfactants with alkyl chains longer than eight carbon atoms form bilayers (vesicles) in solution, and the same bilayer structure is expected at the surfaces such as silica. The packing parameter also suggests bilayer aggregations for double chain surfactants as discussed above. AFM studies of 2C<sub>12</sub>DAB on mica [89] and silica [77] revealed a uniform and featureless image indicative of a flat bilayer, which was consistent with theoretical predications.

The CMC and the aggregation structures can be altered by varying the hydrophobicity of the surfactant tail (*i.e.*, increasing the length or number of the hydrocarbon chains in the surfactant) or modifying the buffer conditions. In general, the CMC in aqueous medium decreases as the hydrophobic character of the surfactant increases. A general rule for ionic surfactants is that the CMC is halved by the addition of one methylene group to a straight-chain hydrophobic group attached to a single terminal hydrophilic head group [91]. For nonionic and zwitterionic surfactants the decrease with length of the hydrophobic group is larger, an increase by one methylene unit reducing the CMC to about one-fifth from its previous value [85, 91]. For double chained surfactants the CMC [92] can be estimated by:

$$\log (\text{CMC in M}) = 3.495 - 0.6625 n \quad (1.23)$$

where  $n$  is the number of carbon atoms in each alkyl chain. Thus, the CMC decreases by about 21-fold for every two methylene groups added to each hydrocarbon chain of the surfactant monomer.

The ionic repulsion between head groups at the micelle surface is weakened by the addition of salts (electrolytes) to the surfactant solution. The buffer ions shield electrostatic repulsions between adjacent head groups. With decreasing ionic repulsion between the head groups, the CMC decreases and the average aggregation number of the micelle increases. For instance, the CMC of  $C_{16}TAB$  in distilled water is 0.9 mM [91] whereas in 10 mM phosphate (pH 7.2) buffer, the CMC is reduced to 0.2 mM [77]. The addition of salts also could increase the packing factor due to a lower electrostatic head group area,  $a_h$ . For instance for CTAB, the packing factor increases from 0.33 in water to 0.50 in 50 mM NaBr, resulting in the formation of cylindrical (rod-like) micelles [90]. Addition of a small amount of negatively charged surfactant such as SDS to CTAB also reduces the electrostatic repulsion between adjacent surfactant molecules strongly such that CTAB-SDS mixture generates a bilayer structure [93]. The buffer counterion also binds to the ionic head group through ion-pair interactions thereby altering the CMC. The stronger the counterion binds to the head group, the smaller the CMC of the surfactant. For instance, the CMC of cetyltrimethylammonium bromide ( $C_{16}TAB$ ) and chloride ( $C_{16}TAC$ ) in aqueous solution are 0.9 and 1.3 mM [77] respectively owing to the stronger degree of binding of the bromide than the chloride.

The presence of organic (nonaqueous) additives produce marked changes in the CMC of surfactants in aqueous media. To understand the effects, these additives are classified as: class I, materials that affect the CMC by being incorporated into the micelle; and class II, materials that change the CMC by modifying solvent–micelle or solvent–surfactant interactions [84]. Materials in class I are generally polar organic compounds such as amides and long chain alcohols ( $\geq 4$  carbons). They affect the CMC

at much lower concentrations than those in the second class. The longer-chain members mainly partition between the surfactant molecules into the micelle. The hydrophobic group of the additive would interact with the hydrophobic groups of the surfactant. Inclusion of the additives in this fashion can screen the electrostatic repulsion between surfactant head groups, thereby decreasing the surfactant CMC.

The members of the class II additives change the CMC by modifying the interaction of water with the surfactant molecule or with the micelle. This is done by modifying the structure of the water, its dielectric constant, or its solubility parameter. Members of this class include urea, water-soluble esters, dioxane, ethylene glycol, and short-chain alcohols such as methanol, ethanol and 2-propanol. For instance, urea is believed to increase the CMC of surfactants in aqueous solution by disrupting the structure of water [94]. Dioxane, ethylene glycol and short-chain alcohols increase the CMC by decreasing the cohesive energy density, or solubility parameter of the water and thus increasing the solubility of the monomeric form of the surfactant [84]. An alternative explanation for the action of these compounds is based on the reduction of the dielectric constant of the aqueous solution because the force between two charge species is inversely proportional to the dielectric constant of the medium. Consequently, this would cause increased mutual repulsion of the ionic heads in the micelle, thus opposing micellization and increasing the CMC. Nonetheless, there are only few studies on the influence of organic solvents particularly short chain alcohols on the CMC and aggregations of surfactants when they are employed to alter the EOF in CE. Part of Chapter 2 focuses on how to systematically fine-tune the EOF in a capillary dynamically coated with cationic surfactants in methanolic electrolytes.

The properties of the solutions containing surfactants change markedly when the monomer surfactants aggregate to form micelles. Hence, the determination of the value of the CMC is usually made from the sharp changes in the physical properties of the solution that occur upon micelle formation. These properties include the specific conductivity, surface tension, light scattering, and fluorescence intensity. Observation of one of these properties against successive surfactant concentrations enables one to establish a curve with a sudden break point at the CMC. An excellent evaluation of the methods for determination and comprehensive compilation of CMC's in aqueous solution is given by Mukerjee and Mysels [91]. In this thesis, the CMC's of the cationic surfactants in different buffer solutions were determined from surface tension measurement using a Fisher surface tensiometer. A discussion of the technique is given in Section 2.2.4.

#### **1.4.4 Organic Solvents**

The use of organic solvents in CE as either organic modifiers or as pure nonaqueous media offers many advantages compared to purely aqueous media. Organic solvents and their mixtures provide different physio-chemical properties than aqueous solutions allowing alteration of the analyte solubility, electroosmotic mobility, and separation efficiency. Furthermore, varying the type and content of the organic solvent in the buffer can also have tremendous impact on alterations in the separation selectivity [21, 95, 96]. Other attractive features of organic-water mixtures or pure nonaqueous solvents include lower Joule heating, reduced interaction of hydrophobic analytes with the capillary wall and suitability for detection by mass spectroscopy (MS) [40].

The use of organic solvents to prepare electrophoretic buffers goes back to the early 1970's when Everaerts et al. [97] performed isotachopheresis in methanol. It was

Wahlbroehl and Jorgenson [98] in 1984, however, who performed the first application of pure nonaqueous media in CZE. Since then non-aqueous capillary electrophoresis (NACE) has undergone a rapid development for variety of applications including pharmaceuticals [96], enantiomers [80], surfactants [95], peptides [95], as well as organic and inorganic anions [21, 55, 99].

The change of solvent properties has significant influence on both the electrophoretic and electroosmotic mobilities as shown in eqn 1.18. In particular, the magnitude of the mobility is affected by the zeta potential at the capillary wall, dielectric constant and viscosity of the medium. In media with a low dielectric constant/viscosity ratio, ions will migrate slower than in water. Hence, nonaqueous solvents with high dielectric constant and low viscosity are preferred in CE to enhance the EOF. However, there a number of other parameters to consider when selecting solvent or solvent mixtures for a given electrophoretic separation. These include the volatility of the solvent (boiling point), the solvating power of the solvent, and the UV transparency. The physical and chemical parameters of some commonly used organic solvents are given in Table 1.1. In CE, the detection is often performed by direct UV absorbance at a relatively short wavelength in the range of 200-250 nm. However, some organic solvents have a UV cut off in as high as 275 nm and detection in this region could compromise sensitivity. Solvents with high volatility may be inconvenient for long analysis or repeated runs due to evaporation from the run vials or sample vials.



**Table 1.1** Physicochemical properties of commonly used organic solvents in CE.

Solvent	Abbreviation	Boiling point (°C)	Viscosity ( $\eta$ , cP)	Dielectric constant ( $\epsilon$ )	$pK_{\text{auto}}$	UV-cut off (nm)
Water	H <sub>2</sub> O	100	0.89	78.4	14.0	190
Methanol	MeOH	64	0.55	32.7	16.9	205
Ethanol	EtOH	78	1.08	24.6	19.1	200
2-Propanol	2-PrOH	82	2.04	19.9	21.1	195
1-Butanol	1-BuOH	118	2.57	17.5	20.9	190
Acetonitrile	ACN	82	0.34	35.9	32.2	195
Formamide	FA	210	3.30	109.5	16.8	245
<i>N</i> -Methylformamide	NMF	200	1.65	182.4	10.7	275
<i>N,N</i> -Dimethylformamide	DMF	153	0.80	36.7	23.1	260
Dimethylsulfoxide	DMSO	189	1.99	46.5	31.8	260

The solvents commonly used in CE can also be classified as amphiprotic (water, MeOH, FA, NMF, EtOH, 2-PrOH) or aprotic (ACN, DMSO and DMF) depending on their ability to act as proton donors and acceptors. The amphiprotic solvents possess both acidic and basic properties and have good solvating power towards the electrolytes used in non-aqueous CE. Aprotic solvents, on the other hand, have very weak acidic and basic characteristics (i.e. have extremely small autoprotolysis constants).

The influences of the organic solvents on the separation selectivity are attributed to alterations in the intrinsic mobility of the analyte ions and the EOF. It has been suggested that these changes result from shifts in the acid-base or complexation equilibria, hydrogen bonding, ion-pairing, dielectric friction effects [19, 20] or changes in solvation of the analytes in presence of organic solvents [95, 100]. For instance the analyte  $pK_a$ , which governs the degree of dissociation for weak acids or bases at a

particular pH, changes with the type and compositions of the solvent in the buffer [101-103]. Thus selecting a solvent that can differentiate between analytes based on their degree of ionization may yield separations that are not possible with aqueous systems. Sarmini and Kenndler [100, 104, 105] have made extensive studies on the influence of solvent pH and analyte  $pK_a$  on anion mobility in organic-aqueous media. Theoretical models have also been developed to predict anion mobility in organic-aqueous mixtures as a function of pH and  $pK_a$  [106]. However, these models can only account for some selectivity changes for weak analytes based on pH and  $pK_a$  effects.

Roy and Lucy [19, 20] have shown the importance of charge-induced friction to explain the mobility behavior of multiply charged ions in aqueous-organic and nonaqueous CE. In the case of small inorganic anions whose conjugated acids remain strong in most of the common solvents, the charge-induced friction effects amenable to selectively impact are minimal. Consequently, a general and successful prediction of selectivity of anions in different solvents is not yet achieved. Hence, empirical method optimization to achieve separation selectivity in various solvent systems would be essential.

### **1.5 Efficiency and Band Broadening in Capillary Electrophoresis**

Under typical CE conditions, a narrow sample plug of 1-10 nL is injected. However, the peaks obtained in the electropherograms have larger sizes/width and are sometimes even distorted. This is a result of broadening or dispersion of the sample zone that occurs as the sample migrates through the capillary. These broadening processes include longitudinal diffusion, Joule heating, solute adsorption of the capillary, and electromigration dispersion [107, 108]. As in chromatography, efficiency is an important

parameter used to measure the degree of the peak broadening or dispersion in CE. The number of theoretical plates or efficiency ( $N$ ), is defined as the ratio of the total distance migrated by the peak ( $L$ ) to second statistical moment of the spatial concentration distribution or total variance ( $\sigma_T^2$ ) of the peak as:

$$N = \frac{L^2}{\sigma_T^2} \quad (1.24)$$

The variance is simply the square of the standard deviation ( $\sigma$ ) of the eluted peak. Both  $\sigma_T^2$  and  $L$  are observable parameters, so the value of  $N$  (dimensionless) can be easily calculated. The number of theoretical plates of the peak also can be determined experimentally from the migration time ( $t_m$ ) and from either the peak width at base line ( $W_b$ ) or peak width at half-maximum height ( $W_{1/2}$ ) as:

$$N = 16 \left( \frac{t_m}{W_b} \right)^2 = 5.54 \left( \frac{t_m}{W_{1/2}} \right)^2 \quad (1.25)$$

The value of  $W_b$  is obtained by extrapolating the tangents to the inflection points down to the baseline. For a Gaussian peak, the baseline peak width ( $W_b$ ) is four times the standard deviation, *i.e.*  $W_b = 4\sigma$ . Most commercial instruments use computer software to compute the efficiency automatically. Efficiencies in excess of one million plates per meter can be achieved in CE [109, 110].

Another very useful measure of separation efficiency or zone dispersion in CE is the plate height ( $H$ ) and is defined as:

$$H = \frac{L}{N} = \frac{\sigma_T^2}{L} \quad (1.26)$$

The overall variance ( $\sigma_T^2$ ) is the sum of the variances from all peak broadening or dispersive processes. Hence, the contribution of all the independent band-broadening processes to the total plate height ( $H_T$ ) is additive [39]:

$$H_T = H_D + H_J + H_{EMD} + H_{EXR} + \dots \quad (1.27)$$

where  $H_D$ ,  $H_J$ ,  $H_{EMD}$ ,  $H_{EXR}$  represent plate heights due to longitudinal diffusion, Joule heating, electromigration dispersion, extracolumn band broadening, respectively. As a result,  $H$  is more convenient measure of efficiency than  $N$  because the individual contributions can be easily combined to calculate the overall value of  $H_T$  as shown in eqn 1.27. The task of this section is to describe each of the individual processes and their contribution to the overall plate height.

### 1.5.1 Longitudinal Diffusion

Longitudinal diffusion is the major source of peak dispersion in CE and refers to the axial movement of molecules away from the center of sample zone where the concentration is highest. The plate height due to the longitudinal diffusion,  $H_D$  can be expressed as:

$$H_D = \frac{\sigma^2}{L_d} = \frac{2Dt_m}{L_d} = \frac{2D}{v} \quad (1.28)$$

where  $D$  is the diffusion coefficient,  $L_d$  is the capillary length to the detector,  $t_m$  is the migration time, and  $v$  is the actual velocity of the analyte (*i.e.*, sum of the electrophoretic and electroosmotic velocities). Hence, longitudinal diffusion is high for solutes with large diffusion coefficient and for solutes spending longer time in the capillary.

At infinite dilution, the diffusion coefficient and the electrophoretic mobility,  $\mu_e$  are related through the Nernst-Einstein equation as:

$$\mu_e = \frac{DzF}{RT} \quad (1.29)$$

where  $R$  is the universal gas constant and  $T$  is the temperature. This equation can be further combined with eqn 1.5 to get:

$$D = \frac{k_B T}{6\pi\eta r} \quad (1.30)$$

where  $k_B$  is the Boltzmann constant. As can be seen from eqns 1.28 and 1.29, a decrease in the diffusion coefficient (e.g., by increasing  $\eta$ ) will also proportionally decrease  $\mu_e$ . Therefore, the best way to decrease broadening due to diffusion is to reduce analysis time by increasing the electric field strength and/or increasing the EOF.

### 1.5.2 Joule Heating

The movement of analyte ions and background electrolyte with respect to the solvent causes friction and Joule heat is continuously generated inside the capillary under an applied voltage. This heat is carried to the outer surface of the capillary through the capillary walls by conduction. The use of narrow bore capillaries with high surface area to volume ratios facilitates dissipation of the heat in CE. However, because heat generated near the walls is dissipated faster than that at the capillary center, radial temperature gradients are generated in the capillary. The temperature profile inside the capillary is approximately parabolic with the highest temperature at the center of the capillary. The temperature inside the capillary is of importance because most of the essential parameters in CE are temperature dependent. Particularly the temperature gradient gives rise to viscosity and diffusion coefficient differences within the buffer system and hence leads to peak dispersion [111]. The plate height ( $H_j$ ), due to this radial temperature gradient is given by [107]:

$$H_J = \frac{r^6 E^6 \kappa^2 f_T^2 \mu_e^2 t_m}{1536 \lambda_b^2 D} \quad (1.31)$$

where  $r$  is the radius of the capillary,  $E$  is applied field strength,  $\kappa$  is specific electrical conductivity of the buffer,  $f_T$  is temperature coefficient of electrophoretic mobility,  $\mu_e$  is the effective electrophoretic mobility,  $\lambda_b$  is the thermal conductivity of the electrolyte buffer,  $D$  is the diffusion coefficient and  $t_m$  is the migration time of the analyte ion. Note the strong dependence of  $H_J$  on the radius and electric field strength (both to the power of six). Therefore, use of smaller capillaries or electric field can minimize the band broadening due to Joule heating. The contribution of the radial temperature gradients to the total dispersion can also be minimized by using a low voltage, one which does not cause excessive Joule heating. The maximum value of this voltage for a particular buffer system can be experimentally determined from an Ohm's plot. After filling the capillary with the desired buffer, voltage is applied to the system for short intervals and the current is recorded at each voltage. The current obtained at various applied voltages is plotted to construct the Ohm's plot. Linearity of the plot indicates adequate heat dissipation because the current ( $I$ ) is linearly proportional to the voltage ( $V$ ) according to Ohm's law:

$$I = \frac{V}{R} \quad (1.32)$$

This relation is linear provided the resistance ( $R$ ) is constant. However, a temperature rise within the capillary results in decreases in resistance. The point where the plot deviates positively from linearity indicates a change in temperature of the buffer due to excessive Joule heating. Hence, working with applied voltage less than or equal to this value can minimize any broadening due to heating.

### 1.5.3 Electromigration Dispersion

Electromigration dispersion (EMD) is caused by a difference in the electrophoretic mobility between sample zone and the surrounding buffer electrolyte. This mobility difference causes the local field strength to vary resulting in peak broadening. When the analyte mobility is higher than that of the co-ion in the BGE, the field strength is lower in the sample zone. Therefore, the analyte velocity is lower in this region, but the analyte ion moves faster in the background electrolyte. In other words, the analyte ions overrun the co-ion and leave the leading boundary of the sample zone into the buffer zone. On the other hand, the buffer co-ion with lower mobility lags beyond the sample zone. The result is a triangular analyte concentration profile with a diffuse leading edge and sharp trailing edge. The peak in the electropherogram would appear fronted [112]. The situation is just the opposite for analytes with mobilities lower than that of the buffer co-ion. In that case, the sample ions with a lower mobility would not cross the leading sample boundary into the fast moving buffer co-ion zone. The resulting peak profile is a sharp leading edge and diffused trailing edge. Hence, the electropherogram would have tailed peak [112].

The plate height due to EMD ( $H_{EMD}$ ) is expressed as [107]:

$$H_{EMD} = \frac{2El_{inj}C_s k_{EDM}}{9C_b v} \quad (1.33)$$

where  $E$  is the electric field strength,  $l_{inj}$  is the length of the injection plug,  $C_s$  and  $C_b$  are the concentrations of the analyte and BGE respectively,  $v$  is the actual velocity of the analyte and  $k_{EDM}$  is the electromigration dispersion factor which depends on the effective mobilities of the constituent ions in the buffer and the sample. The concentration profile of the analyte zone is strongly affected by the relations of the mobilities of analyte and

BGE ions. The electromigration dispersion also depends on the relative concentrations of the sample zone and BGE and therefore it is sometimes referred to as *concentration overload* [113]. In CE, the concentration of the sample is kept low relative to the surrounding buffer in order to keep the conductivity difference between the two regions as small as possible. This ensures that the field strength across the capillary is constant and that each sample ion migrates independently at rate governed by its electrophoretic mobility. The conductivity difference ( $\Delta\kappa$ ) is expressed as [107]:

$$\Delta\kappa = \frac{C_s}{\mu_s} (\mu_c - \mu_s) (\mu_{ct} - \mu_s) \quad (1.34)$$

where  $C_s$  and  $\mu_s$  are concentration and electrophoretic mobility of the sample ion, and  $\mu_c$  and  $\mu_{ct}$  are electrophoretic mobilities of the co-ion and counter ion respectively of the buffer. The asymmetry of the analyte peak increases with increasing value of  $\Delta\kappa$ . Thus, it is important to select a buffer whose ions have effective mobilities close to the mobility of analyte ion to minimize EMD. A reduction in the magnitude of the EDM can also be achieved by decreasing the length of sample zone or by decreasing the  $C_s/C_b$  ratio as shown in eqn 1.33.

Most inorganic ions have very little or no absorbance in the UV-visible region. Therefore, methods for the determination of these analytes have relied upon indirect UV detection. Indirect detection requires dilute buffers because the detection limit also depends on the co-ion concentration (Section 1.2.3.2). In most cases, co-ion concentrations of 2-10 mM are used which are about 5-7 times less than those buffers typically used with direct UV detection. Hence, peak asymmetry due to conductivity difference and mobility mismatch is more pronounced with indirect UV analysis of inorganic ions. Increasing the electrolyte co-ion concentration can decrease the degree of



peak asymmetry and improve the EMD. However, at higher co-ion concentration, the noise level will also increase (dynamic reserve decreases) which leads to poor sensitivity and resolution according to eqn 1.14. In addition, choosing a co-ion that matches mobilities of all analyte ions is also challenging. Because of this compromise between sensitivity and peak symmetry, some degree of EMD exists in most indirect detection.

#### 1.5.4 Extracolumn Broadening

All the broadening phenomena mentioned in the previous sections occur “on-capillary” during the migration process. However, there are other sources of broadening which do not occur during the separation process. These broadening arise primarily from injection and detection processes and are referred to as extracolumn peak broadening or sometimes referred to as extraseparation band broadening [114]. The lengths of the injection plug and detection area could contribute to the broadening of the analyte peaks and therefore could influence the efficiency of the peaks. Under normal CE conditions the contributions from the injection and detector are much lower than that of longitudinal diffusion. Ideally, the extracolumn broadening should not decrease the efficiency by more than 10% [114, 115].

The plate height ( $H_{inj}$ ) resulting from injection plug is expressed as:

$$H_{inj} = \frac{l_{inj}^2}{12L_d} \quad (1.35)$$

where  $l_{inj}$  is the length of the injection plug, and  $L_d$  is capillary length to the detector. All the experiments in this thesis are performed using hydrodynamic injection. Therefore, the sample injection volume is optimized by varying both the duration and magnitude of the applied pressure. The injection plug length ( $l_{inj}$ ) can be calculated using the Hagen-Poiseuille equation [34] :

$$l_{inj} = \frac{\Delta P r^2}{8\eta L_t} t_{inj} \quad (1.36)$$

where  $\Delta P$  is the applied pressure difference in Pascals (1 Pa = 1.01 mbar = 1.45x10<sup>-4</sup> p.s.i),  $r$  is the radius of the capillary in meters,  $t_{inj}$  is the injection time in seconds,  $\eta$  is the viscosity of the buffer (8.91x10<sup>-4</sup> Pa.s for water at 25 °C) and  $L_t$  is the total capillary length in meters. Based on the 10% decrease in efficiency due to injection, the maximum permissible injection length is calculated as [114] :

$$l_{inj,max} = \sqrt{2.4Dt_m} \quad (1.37)$$

where  $D$  is the diffusion coefficient of analyte, and  $t_m$  is the analyte's migration time.

Common sources of detector based broadening are detector rise time, detection window length and data acquisition rate. The detector rise time refers to the time required for the detector to respond to an increase in signal output from 10% to 90% of its final value. The electronics take a finite period to respond to an abrupt change in detector signal. Hence, the detector rise time should be reasonably short to respond quickly to fast moving peaks. Detection rise time of 1.0 s is used for most analytes but for fast moving ions, a smaller rise time (0.1 s or less) is required. The detection window or the slit width can also give rise to detector band broadening. This occurs when the width of the window is significant relative to the width of the sample band migrating along the capillary. The plate height due to the finite detection volume ( $H_{det}$ ) is given by:

$$H_{det} = \frac{l_{det}^2}{12L_d} \quad (1.38)$$

where  $l_{det}$  is the width of the detection window. However, for the CE instrument used in this work (HP<sup>3D</sup> CE, Agilent instruments) the contribution from the detection window (less than 200  $\mu\text{m}$ ) is not significant.

Another source of detector broadening is the data acquisition rate or data-sampling rate. Data acquisition refers to the frequency at which data points are collected by the detector to generate the electropherogram. High efficiency CE separations, in which the peak widths range between 0.1 to 5 second require high data acquisition rates (15 to 20 points per second). For wider peaks, lower acquisition rates can be used. The drawback of using extremely high data acquisition rate is the generation of detector noise. Thus, a reasonably high acquisition rate should be used to collect enough data points so all the details of the peak are well defined. Unless otherwise stated, the data acquisition rate used to generate the electropherograms in this thesis is 20 Hz (i.e. 20 data points per second).

## 1.6 Thesis Overview

As explained above, attaining high resolution in CE requires precise and accurate control of the EOF. Hence, a large portion of this thesis focuses on the modification and optimization of the EOF particularly for anion analysis. Systematic studies on how to control the EOF in the presence of single chain and double chain surfactants in methanolic electrolytes to improve resolution, analysis time and selectivity of anions will be presented in Chapters 2 and 3. Results from the experimental studies in both direct (Chapter 2) and indirect UV detection (Chapter 3) modes help for a better understanding of the selectivity alterations observed for some common inorganic anions (chloride, bromide, iodide, nitrate, nitrate, sulphate, perchlorate, fluoride, thiocyanate) on varying

the solvent composition (water–methanol mixtures) of the background electrolyte. The suitability of a coating technology in nonaqueous media consisting of various mixtures of organic solvents (methanol, acetonitrile, ethanol, 2-propanol, 1-butanol) and water is investigated in Chapter 4. Finally, Chapter 5 explores the application of the double chain surfactant-based coatings for modification of the charge on the capillary and the EOF for separation of basic analytes in formamide solvent, pure nonaqueous buffer systems.

## 1.7 References

- [1] Tiselius, A., *Trans. Faraday Soc.* 1937, 33, 524.
- [2] Hjerten, S., *Chromatogr. Rev.* 1967, 9, 122-219.
- [3] Raymond, S., Weintraub, L., *Science* 1959, 130, 711.
- [4] Jorgenson, J. W., Lukacs, K. D., *J. Chromatogr.* 1981, 218, 209-216.
- [5] Jorgenson, J. W., Lukacs, K. D., *Clin. Chem.* 1981, 27, 1551-1553.
- [6] Jorgenson, J. W., Lukacs, K. D., *Anal. Chem.* 1981, 53, 1298-1302.
- [7] Terabe, S., Otsuka, K., Ichikawa, K., Tsuchiya, A., Ando, T., *Anal. Chem.* 1984, 56, 111-113.
- [8] Biswas, R., Bagchi, B., *J. Chem. Phys.* 1997, 106, 5587-5598.
- [9] Jaros, M., Vcelakova, K., Zuskova, I., Gas, B., *Electrophoresis* 2002, 23, 2667-2677.
- [10] Stedry, M., Jaros, M., Vcelakova, K., Gas, B., *Electrophoresis* 2003, 24, 536-547.
- [11] Brownlee, R. G., Compton, S. W., *Am. Lab.* 1988, 20, 66-76.
- [12] Green, J. S., Jorgenson, J. W., *J. High Resolut. Chromatogr. Chromatogr. Comm.* 1984, 7, 529-531.
- [13] Caslavaska, J., Gebrauer, P., Thormann, W., *Electrophoresis* 1994, 15, 1167-1175.
- [14] Everaerts, F. M., Hoving-Keulemans, W. L., *Sci. Tools* 1970, 17, 25-28.
- [15] Tsuda, T., Nomura, K., Nakagawa, G., *J. Chromatogr.* 1983, 264, 385-392.
- [16] Veraart, J. R., Gooijer, C., Lingerman, H., *Chromatographia* 1997, 44, 129-134.
- [17] Cifuentes, A., Kok, W. T., Poppe, H., *J. Microcol. Sep.* 1995, 7, 365-374.
- [18] Fu, S. L., Lucy, C. A., *Anal. Chem.* 1998, 70, 173-181.
- [19] Roy, K. I., Lucy, C. A., *Anal. Chem.* 2001, 73, 3854-3861.

- [20] Roy, K. I., Lucy, C. A., *J. Chromatogr. A* 2002, 964, 213-225.
- [21] Lucy, C. A., *J. Chromatogr. A* 1999, 850, 319-337.
- [22] Hiemenz, P. C. *Principles of Colloid and Surface Chemistry*; Marcel Dekker, Inc.: New York, 1986.
- [23] Hunter, R. J. *Zeta Potential in Colloid Science: Principles and Applications*; Academic Press: New York, 1981.
- [24] Schwer, C., Kenndler, E., *Anal. Chem.* 1991, 63, 1801-1807.
- [25] Li, D. M., Fu, S. L., Lucy, C. A., *Anal. Chem.* 1999, 71, 687-699.
- [26] Jandik, P., Bonn, G. *Capillary Electrophoresis of Small Molecules and Ions*; VCH Publishers, Inc.: New York, 1993.
- [27] Beckers, J. L., Everaert, F. M., Ackermans, M. T., *J. Chromatogr.* 1991, 537, 407-428.
- [28] Swinney, K., Bornhop, D., *Critical Rev. Anal. Chem.* 2000, 30, 1-30.
- [29] Grant, I. H., Steuer, W., *J. Microcol. Sep.* 1990, 74-79.
- [30] Taylor, J. A., Yeung, E. S., *J. Chromatogr.* 1991, 550, 831-837.
- [31] Chevret, J. P., Van Soest, R. E. J., Ursem, M., *J. Chromatogr.* 1991, 543, 439-449.
- [32] Tsuda, T., Sweedler, J. V., Zare, R. N., *Anal. Chem.* 1990, 62, 2149-2152.
- [33] Gordon, G. B., Tella, R. P., Martins, H. A. S., *Hewlett-Packard J* 1995, 46, 62-70.
- [34] Hjerten, S., Elenbring, K., Kilar, F., Liao, J., Chen, A. J., Siebert, C. J., Zhu, M., *J. Chromatogr.* 1987, 403, 47-61.
- [35] Foret, F., Fanali, S., Ossicini, L., Bocek, P., *J. Chromatogr.* 1989, 470, 299-308.
- [36] Yeung, E. S., *Acc. Chem. Res.* 1989, 22, 125-130.
- [37] Johns, C., Macka, M., Haddad, P. R., *Electrophoresis* 2003, 24, 2150 - 2167.

- [38] Macka, M., Haddad, P. R., Gebauer, P., Bocek, P., *Electrophoresis* 1997, 18, 1998-2007.
- [39] Grossman, P. D., Colbrun, J. C., Eds. *Capillary electrophoresis: theory and practice*; Academic Press, Inc.: San Diego, CA, 1992.
- [40] Landers, J. P., Ed. *Hand book of Capillary Electrophoresis*, 2nd ed.; CRC Press, Inc.: Boca Raton, FL, 1996.
- [41] Lukacs, K. D., Jorgenson, J. W., *J. High Resolut. Chromatogr. Chromatogr. Comm.* 1985, 8, 407-411.
- [42] Muijselaar, P. G., Otsuka, K., Terabe, S., *J. Chromatogr. A* 1997, 780, 41-61.
- [43] Chen, N., Terabe, S., Nakagawa, T., *Electrophoresis* 1995, 16, 1457-1462.
- [44] Watanabe, T., Nishiyama, R., Yamamoto, A., Nagai, S., Terabe, S., *Anal. Sci.* 1998, 14, 435-438.
- [45] Otsuka, K., Higashimori, M., Koike, R., Karuhaka, K., Okada, Y., .., Terabe, S., *Electrophoresis* 1994, 15, 1280-1283.
- [46] Khaledi, M. G., *J. Chromatogr. A* 1997, 780, 3-40.
- [47] Lukkari, P., Vuorela, H., Riekkola, M. L., *J. Chromatogr. A* 1993, 655, 317-324.
- [48] Bretnall, A. E., Clarke, G. S., *J. Chromatogr. A* 1995, 716, 49-55.
- [49] Terabe, S., *J. Pharm. Biomed. Anal.* 1992, 10, 705-715.
- [50] Nishi, H., Fukuyama, T., Terabe, S., *J. Chromatogr.* 1991, 553, 503-516.
- [51] Jones, W. R., Jandik, P., *J. Chromatogr.* 1991, 546, 445-458.
- [52] Lucy, C. A., Mcdonald, T. L., *Anal. Chem.* 1995, 67, 1074-1078.
- [53] Yeung, K. K. C., Lucy, C. A., *Anal Chem* 1998, 70, 3286-3290.
- [54] Smith, S. C., Khaledi, M. G., *Anal. Chem.* 1993, 65, 193-198.

- [55] Harakuwe, A. H., Haddad, P. R., *J. Chromatogr. A* 1996, 734, 416-421.
- [56] Melanson, J. E., Lucy, C. A., *J. Chromatogr. A* 2000, 884, 311-316.
- [57] Sustáček, V., Bocek, P., Foret, F., *J. Chromatogr.* 1991, 545, 239-248.
- [58] Green, J. S., Jorgenson, J. W., *J. Chromatogr.* 1989, 478, 63-70.
- [59] Burgi, D. S., Chien, R. L., *Anal. Chem.* 1991, 63, 2042-2047.
- [60] Bockris, J. O. M., Reddy, A. K. N. *Modern Electrochemistry*; Plenum Press: New York, 1970.
- [61] Pitts, E., Tabor, B. E., Daly, J., *Trans. Faraday Soc.* 1970, 66, 693-707.
- [62] Ermakov, S. V., Zhukov, M. Y., Capelli, L., Righetti, P. G., *J. Chromatogr. A* 1995, 699, 297-313.
- [63] Towns, J. K., Regnier, F. E., *Anal. Chem.* 1991, 63, 1126-1132.
- [64] Lux, J. A., Yin, H., Schomberg, G., *J. High Res. Chromatogr.* 1990, 13, 145-152.
- [65] Balchunas, A. T., Sepaniak, G., *Anal. Chem.* 1987, 59.
- [66] Liu, J. P., Cobb, K. A., Novotny, M., *J. Chromatogra.* 1990, 519, 189-197.
- [67] Bruin, G. J. M., Chang, J. P., Kuhlman, R. H., Zegers, K., Kraak, J. C., Poppe, H., *J Chromatogr A* 1989, 471, 429-436.
- [68] Bruin, G. J. M., Huisden, R., Kraak, J. C., Poppe, H., *J. Chromatogr. A* 1989, 480, 339-349.
- [69] Hjerten, S., *J. Chromatogr.* 1985, 347, 191-197.
- [70] Engelhardt, H., Walter, M. C., *J. Chromatogr. A* 1995, 716, 27-33.
- [71] Gilges, M., Kleemiss, M. H., Schomburg, G., *Anal. Chem.* 1994, 66, 2038-2046.
- [72] Belder, D., Elke, K., Husmann, H., *J. Chromatogr. A* 2000, 63-71.
- [73] Dolník, V., Hutterer, K. M., *Electrophoresis* 2001, 22, 4163-4178.



- [74] Doherty, E. A. S., Meagher, R. J., Albarghouthi, M. N., Barron, A. E.,  
*Electrophoresis* 2003, 24, 34-54.
- [75] Figeys, D., Aebersold, R., *J. Chromatogr. B* 1997, 695, 163-168.
- [76] Horvath, J., Dolnik, V., *Electrophoresis* 2001, 22, 644-655.
- [77] Baryla, N. E., Melanson, J. E., McDermott, M. T., Lucy, C. A., *Anal. Chem.* 2001,  
73, 4558-4565.
- [78] Córdova, E., Gao, J., Whitesides, G. M., *Anal. Chem.* 1997, 69, 1370-1379.
- [79] Mechref, Y., Ostrander, G. K., El Rassi, Z., *J. Chromatogr. A* 1997, 792, 75-82.
- [80] Wang, F., Khaledi., M. G., *J. Chromatogr. A* 2000, 875, 277-293.
- [81] Reijenga, J. C., Aben, G. A., Verheggen, T. P. E. M., Everaert, F. M., *J.*  
*Chromatogr.* 1983, 260, 241-254.
- [82] Tsuda, T., *J. High Res. Chromatogr. Chromatogr. Commun.* 1987, 10, 622-624.
- [83] Huang, X., Luckey, J. A., Gordon, M. J., Zare, R. N., *Anal. Chem.* 1989, 61, 766-  
770.
- [84] Rosen, M. *Surfactants and Interfacial Phenomena*; John Wiley & Sons: New York,  
1989.
- [85] Israelachvili, J. N., Mitchell, D. J., Ninham, B. W., *J. Chem. Soc., Faraday Trans.*  
1976, 2, 1525-1568.
- [86] Tanford, C., *J. Phys. Chem.* 1974, 78, 2469-2479.
- [87] Warr, G. G., Sen, R., Evans, D. F., Trend, J. E., *J. Phys. Chem.* 1988, 92, 774-783.
- [88] Yeskie, M. A., Harwell, J. H., *J. Phys. Chem.* 1988, 92, 2346-2352.
- [89] Manne, S., Gaub, H. E., *Science* 1995, 270, 1480-1482.
- [90] Liu, J.-F., Ducker, W. A., *J. Phys. Chem. B* 1999, 103, 8558-8567.

- [91] Mukerjee, P., Mysels, K. *Critical micelle Concentrations of Aqueous Surfactant Systems*; National Bureau of Standards: Washington, 1971.
- [92] Svitova, T. F., Smirnova, Y. P., Pisarev, S. A., Berezina, N. A., *Colloids Surf. A* 1995, 98, 107-115.
- [93] Wang, C. Z., Lucy, C. A., *Electrophoresis* 2004, 25, 825-832.
- [94] Baglioni, P., Ferroni, E., Kevan, L., *J. Phys. Chem.* 1990, 94, 4296-4298.
- [95] SalimiMoosavi, H., Cassidy, R. M., *Anal. Chem.* 1996, 68, 293-299.
- [96] Bjornsdottir, I., Tjornelund, J., Hansen, S. H., *Electrophoresis* 1998, 19, 2179-2156.
- [97] Beckers, J. L., Everaert, F. M., *J Chromatogr* 1970, 51, 339-342.
- [98] Wahlbroehl, Y., Jorgenson, J. W., *J. Chromatogr.* 1984, 315, 135-143.
- [99] Roy, K. I., Lucy, C. A., *Electrophoresis* 2003, 24, 370-379.
- [100] Sarmini, K., Kenndler, E., *J. Chromatogr. A* 1998, 806, 325-335.
- [101] Sarmini, K., Kenndler, E., *J. Chromatogr. A* 1997, 792, 3-11.
- [102] Porras, S. P., Riekkola, M. L., Kenndler, E., *J Chromatogr A* 2001, 905, 259-268.
- [103] Roses, M., *J. Chromatogr. A* 2004, 1037, 283-298.
- [104] Sarmini, K., Kenndler, E., *J. Chromatogr. A* 1998, 818, 209-215.
- [105] Sarmini, K., Kenndler, E., *J. Chromatogr. A* 1998, 811, 201-209.
- [106] Barrón, D., Jiménez-Lozano, E., Irlles, A., Barbosa, J., *J. Chromatogr. A* 2000, 871, 381-389.
- [107] Hjerten, S., *Electrophoresis* 1990, 11, 665-690.
- [108] Kenndler, E., Schwer, C., *J. Chromatogr.* 1992, 595, 313-318.
- [109] Gilges, M., Kleemiss, K., Schomburg, G., *Anal. Chem.* 1994, 66, 2038-2045.

- [110] Cunliffe, J. M., Baryla, N. E., Lucy, C. A., *Anal. Chem.* 2002, 74, 776-783.
- [111] Knox, J. H., McCormack, K. A., *Chromatographia* 1994, 38, 207-214.
- [112] Jorgenson, J. W., Lukacs, K. D., *Science* 1983, 222, 266-272.
- [113] Xu, X., Kok, W. T., Poppe, H., *J. Chromatogr. A* 1996, 742, 211-227.
- [114] Lucy, C. A., Yeung, K. K. C., Pang, X. J., Chen, D. D. Y., *LC.GC* 1998, 16, 26-31.
- [115] Grushka, E., McCormick, R. M., *J. Chromatogr.* 1989, 471, 421-428.

## CHAPTER TWO: Electroosmotic Flow Control in Capillary Electrophoresis for the Determination of Inorganic Anions in Methanol-Water Buffers<sup>†</sup>

### 2.1 Introduction

Capillary electrophoresis (CE) is often described as a complementary technique to ion chromatography (IC) for the determination of small organic and inorganic ions [1, 2]. This is because the separation selectivity observed in CE is distinctly different from that of IC. In IC, the separation selectivity is based on the ion-exchange equilibrium where ions are separated based on their interaction with the stationary phase. In contrast, in CE the separation results from differences in the electrophoretic mobility of the ions, which is a function of charge to size (mass) ratio of the ions. For instance, the separation of acetate and fluoride is challenging in ion chromatography, but straightforward in CE.

In normal CE using bare silica capillary, the electrophoretic mobilities of many small inorganic anions are opposite and comparable in magnitude or even greater than the EOF. As a result, separations of these small anions using such a counter-EOF mode would not only take a long time, but would fail to detect some of the faster migrating anions. Jones and Jandik used the cationic surfactant, tetradecyltrimethylammonium bromide (TTAB or C<sub>14</sub>TAB) as a buffer additive to reverse the EOF [3]. In this manner, the reversed EOF augments the anions. Using this co-EOF approach, they separated 30 anions in just over 3 minutes [3]. Melanson and Lucy [4] had also achieved separation of nitrate and nitrite ions in 12 seconds in the co-EOF mode [4].

---

<sup>†</sup> A version of this chapter has been published as **Diress, A; Lucy, C.A.** *Journal of Chromatography A*, **2004**, 1027, 85-91.

However, as shown in eqn 1.16 (Section 1.4) the resolution between two peaks in CE is given by:

$$R_s = \frac{\sqrt{N}}{4} \frac{\Delta\mu}{\bar{\mu}_{app}} = \frac{\sqrt{N}}{4} \left( \frac{\Delta\mu}{\mu_{eo} + \mu_e} \right) \quad (1.15)$$

In co-EOF mode, the EOF and the anion migrations are additive, making the term in denominator (of eqn 1.16) large. The EOF sweeps the analytes towards the detector as the anions migrate along with the EOF in the same direction. Hence, while co-EOF separations are rapid, achieving full resolution under this mode can be challenging. Thus, there must be a significant difference in the electrophoretic mobilities of the two species to achieve separation (i.e.  $\Delta\mu$  should be large in eqn 1.16). Resolution is fundamentally dependent upon there being a significant difference in the electrophoretic mobilities of the two species ( $\Delta\mu$ ). For cations such as alkaline earth and transition metals, the cation mobility can be altered by complexation [5, 6]. For anions, complexation has seen only limited use [7, 8]. For weak acid anions, the effective charge on the anion can be controlled by varying the pH, as was discussed in Section 1.4.1. Borate ( $pK_a = 9.2$ ), carbonate (10.3) and phosphate (7.2) show dramatic selectivity changes as the electrolyte pH is varied over the 8-13 range [3]. However, this approach has limited use for inorganic anions as many of these ions have no  $pK_a$  values in the pH range that is attainable in most CE applications [9].

Another important approach to modifying selectivity in CE is the addition of organic solvents to the buffer. The use of organic solvents in CE either as organic modifiers or as pure nonaqueous media offers many advantages compared to purely aqueous media (Section 1.4.4). However, most important with respect to inorganic

anions is that dramatic alterations in selectivity can be achieved by varying the type and content of the organic solvent in the buffer. There are only a few specific examples of selectivity changes upon addition of organic solvents in the literature. Buchberger and Haddad investigated the effect of up to 30% (v/v) of methanol, acetonitrile, tetrahydrofuran, acetone or ethylene glycol on anion mobilities in a chromate electrolyte containing TTAB [10]. With all of the organic solvents used: the mobility of sulfate decreased relative to all monoanions; the resolution between thiosulfate, bromide and chloride tended to degrade as organic modifier was added; and the migration order of nitrite and nitrate was reversed.

In addition to altering the selectivity of ions, the presence of organic solvents in the run buffer also influences the EOF (Section 1.4.3.3). Hence, control of EOF is essential to achieving rapid separations and resolutions in buffers containing the organic additives. For inorganic anion separations, it would be desirable to combine the selectivity alterations offered by organic solvents, with the quick analysis times offered by reversal of the EOF (eqn 1.16). In this chapter, I will present systematic studies of the EOF in CE capillaries dynamically coated with cetyltrimethylammonium bromide (CTAB or  $C_{16}TAB$ ) and didodecyldimethylammonium bromide (DDAB or  $2C_{12}DAB$ ) in mixed water-methanol electrolytes. Although these surfactants have been used extensively to reverse the EOF in aqueous CE (Section 1.4.4.3), there have been no studies on EOF optimization with cationic surfactants in the presence of organic solvents. Methanol was chosen because it is a common solvent miscible with water and is capable of solvating surfactants to a greater extent than other organic solvents [11]. Changes in

EOF, micellar properties of the surfactant and the separation selectivity for inorganic anions upon addition of various percent of methanol are investigated.

## **2.2 Experimental**

### **2.2.1 Apparatus**

All experiments were performed on a HP<sup>3D</sup> CE (Hewlett-Packard, Palo Alto, CA, USA) capillary electrophoresis instrument equipped with an on-column diode array UV absorbance detector. Data acquisition and control was performed using ChemStation software (HP<sup>3D</sup>, Hewlett Packard). Untreated fused silica capillaries (Polymicro Technologies, Phoenix, AZ, USA) with an inner diameter of 50  $\mu\text{m}$ , an outer diameter of 365  $\mu\text{m}$ , and a total length of 37 cm (28.5 cm to the detector) were used unless otherwise specified. In all experiments, the capillary was thermostatted at  $25.0 \pm 0.1$  °C.

### **2.2.2 Chemicals**

All solutions were prepared with Nanopure 18 M $\Omega$  water (Barnstead, Chicago, IL, USA). All of the chemicals used were reagent grade or better, and were used without further purification. Buffers were prepared from hydrated sodium salts of dihydrogen orthophosphate and hydrogen orthophosphate (BDH, Toronto, Canada), HPLC grade methanol (MeOH; Fisher, Fair Lawn, NJ, USA), and a surfactant: either cetyltrimethylammonium bromide (CTAB; Sigma, St. Louis, MO, USA), or didodecyldimethylammonium bromide (DDAB; Aldrich, Milwaukee, WI, USA). The pH values were measured using a Model 445 digital pH meter (Corning, Acton, USA) calibrated with aqueous standards immediately prior to use. The pH was adjusted using 0.1 M NaOH (BDH) before the required amount of methanol or surfactant (0.0 – 2.5 mM) was added. All the methanol contents in the buffers are expressed in volume per

volume (v/v) units unless otherwise specified. A 1 mM aqueous solution of mesityl oxide (Aldrich) was used as the neutral EOF marker. Previous studies have shown that mesityl oxide is an effective EOF marker in dilute micellar solutions [12, 13]. Anion samples were prepared from reagent grade sodium nitrite (BDH), potassium nitrate (BDH), potassium bromide (Fisher), potassium iodide (BDH), and potassium thiocyanate (BDH).

### 2.2.3 EOF Measurements

New capillaries were used for each new coating study or buffer condition. Each new capillary was pretreated at high pressure (93.8 kPa) with sequentially 1.0 M NaOH for 10 min, 0.1 M NaOH for 10 min and H<sub>2</sub>O for 8 min. Prior to each run, the capillary was rinsed at high pressure with 0.1 M NaOH for 2 min, H<sub>2</sub>O for 2 min, and running buffer for 3 min. A 0.5-s hydrodynamic injection (5.0 kPa) was used for aqueous buffers while a 2.0-s injection (5.0 kPa) was used for all methanol-water electrolytes. EOF measurements were performed under an applied voltage of –15 kV unless otherwise indicated. All voltages used herein were experimentally verified to be within the linear region of the Ohm's plots. Direct UV detection at 214 nm or 254 nm was used with a data acquisition rate of 20 Hz.

Two different methods were used to measure the electroosmotic mobility ( $\mu_{eo}$ ) in the aqueous and methanol containing buffers. When the  $\mu_{eo}$  was greater than  $2 \times 10^{-4}$  cm<sup>2</sup>/Vs (*i.e.*, in pure aqueous and low methanolic buffers), the EOF was measured by conventional injection of mesityl oxide followed by application of a constant voltage of  $\pm 15$  kV at 25 °C. The EOF was then calculated using the equation:



$$\mu_{eo} = \frac{L_t L_d}{V t_{eo}} \quad (2.1)$$

where  $L_t$  is the total length of the capillary,  $L_d$  is the length to the detector,  $t_{eo}$  is the migration time of the neutral marker, and  $V$  is the voltage applied across the capillary.

When the  $\mu_{eo}$  was less than  $2 \times 10^{-4} \text{ cm}^2/\text{Vs}$ , the EOF generated was so slow that conventional EOF measurements required inconveniently long run times. To overcome this problem the three-peak injection technique developed by Williams and Vigh was employed. The method was found to be effective in previous studies to determine the EOF particularity when the EOF is low or strongly suppressed [14-16]. This method, which consists of two pressure-assisted steps combined with an electrophoretic separation step, was used in the present studies in buffers containing more than 20% (v/v) methanol. The procedure we employed to determine the EOF is described briefly as follows. First mesityl oxide (neutral marker, N1) was injected into the capillary for 0.5 s at 5.0 kPa. This band was then pushed a certain distance through the capillary using low pressure (5.0 kPa) for 1 min. A second mesityl oxide (N2) was introduced as before, and both markers were pushed along the capillary by applying low pressure (5.0 kPa) for 0.5 min. A constant voltage of +15 kV was applied for 1.5 min during which the position of the two bands was altered by the resultant EOF. Finally, a third mesityl oxide (N3) was injected and all the three bands were pushed past the detector by applying 5.0 kPa pressure for 15 min. Direct detection was performed at 254 nm. A summary of the sequential injection steps is given in Figure 2.1. The  $\mu_{eo}$  was calculated using [14]:

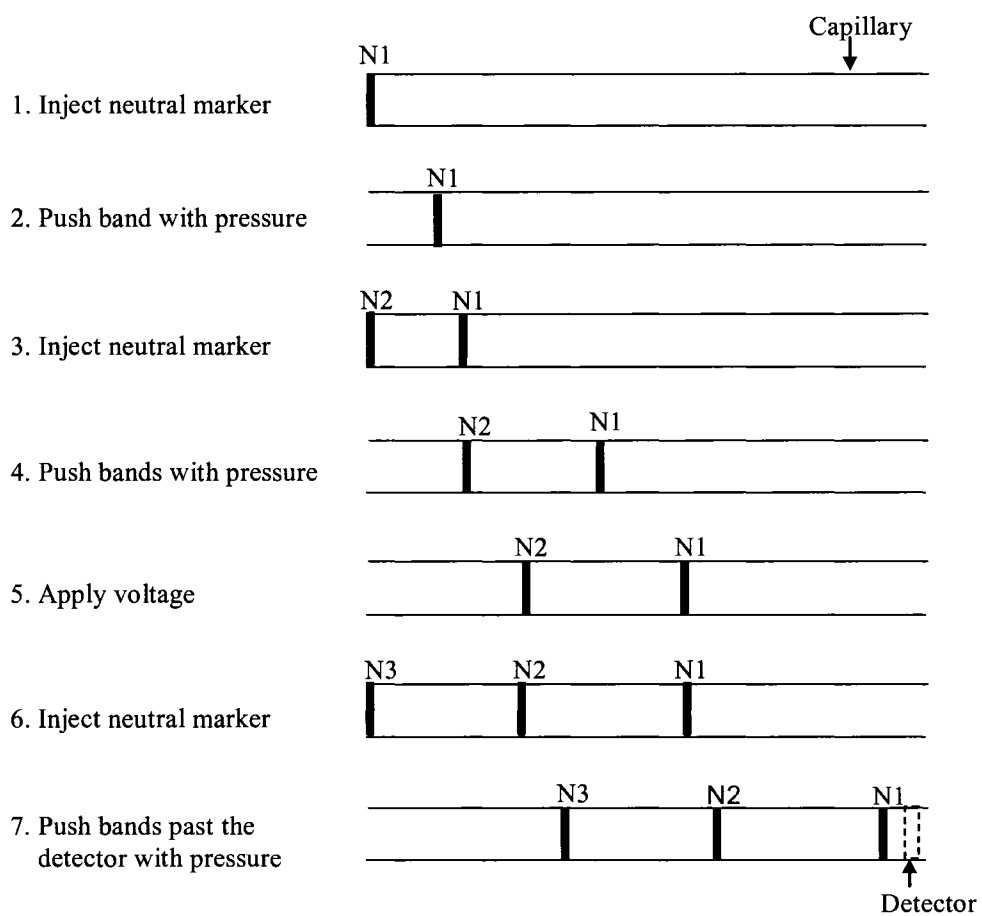


**Figure 2.1** Scheme diagram of EOF measurement by sequential injection technique (see the text in Section 2.2 for details).

$$\mu_{eo} = \frac{[(t_3 - t_2) - (t_2 - t_1)]L_t L_d}{V \left[ \left( t_3 + \frac{t_{inj}}{2} \right) \left( t_m - \frac{t_{ramp-up}}{2} - \frac{t_{ramp-down}}{2} \right) \right]} \quad (2.2)$$

where  $t_1$ ,  $t_2$ , and  $t_3$  are the migration times of the first (N1), second (N2) and third (N3) EOF markers, respectively,  $t_{inj}$  is the injection time,  $t_m$  is the time necessary for which the voltage was applied, and  $t_{ramp-up}$  (3 s) and  $t_{ramp-down}$  (1 s) are voltage ramp-up and ramp-down times. The voltage ramp-up and down times refer to the times necessary for the applied voltage to increase from 0 and  $V$  and decrease from  $V$  to 0, respectively. All other terms are as defined in eqn 2.1.

#### 2.2.4 Critical Micelle Concentration Determination

Critical micelle concentrations (CMC) were determined from surface tension measurements using a Fisher surface tensiometer (Model 20, Fisher Scientific, Pittsburgh, PA, USA). Both the platinum-iridium ring (6.0 cm I.D.) and the glass sample beaker were cleaned with 2-butanone (Fisher) and rinsed with water prior to each measurement. The surface tension was then measured in 10 mM aqueous or methanolic phosphate buffer (pH 8.0) solutions containing increasing concentrations of CTAB (from 0.01 to 2.0 mM). All measurements were made at room temperature ( $\sim 25$  °C) and in duplicate. The CMC was determined based on the inflection point/break point of a plot of surface tension (in dyne/cm) versus the log of the surfactant concentration (in M). To validate the procedure, the CMC of CTAB was determined in distilled water at room temperature and a value of 0.87 mM was obtained. This is comparable with the literature

values of 0.90 mM [17]. A typical graph showing the determination of the CMC of CTAB in distilled water is shown in Figure 2.2.

### 2.2.5 Anion Separations

The effect of methanol content on the selectivity between small inorganic anions was studied over the range of 0 to 60% (v/v) MeOH in a 15 mM phosphate buffer at pH 8.0 containing different concentration of CTAB or DDAB. Mixed anion samples were prepared in the running buffer and contained 0.2 mM of each ion ( $\text{NO}_2^-$ ,  $\text{NO}_3^-$ ,  $\text{Br}^-$ ,  $\text{I}^-$  and  $\text{SCN}^-$ ). These specific ions were chosen because they absorb light in the UV region. Sample was injected hydrodynamically for 2.0 s at 5.0 kPa. The direction of the EOF

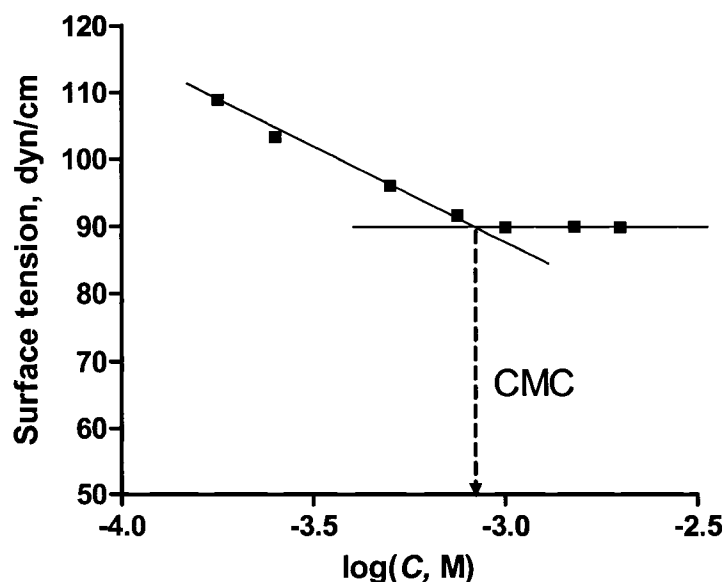


**Figure 2.2** Determination of CMC of cetyltrimethylammonium bromide (CTAB) in distilled water at 25 °C. Regression of the data points before and after the break point fit to straight lines ( $R^2 > 0.998$ ) at the 95% confidence interval.

was reversed when cationic surfactants were used (*i.e.*, from the cathode to the anode) so that the anions were separated in the co-EOF mode and detected using direct UV detection at 214 nm with a data acquisition rate of 18 Hz. An applied potential of  $-15$  kV was used in all anion separations unless otherwise specified. Standard addition of each anion was performed to confirm the identity of the peaks. All mobility measurements were performed in triplicate. The effective mobilities,  $\mu_{eff}$ , of the anions were calculated from the migration times under constant voltage conditions using eqn 1.11 (Section 1.2.2.4).

### 2.2.6 Measurements of relative viscosity

The viscosities of the buffers containing methanol were measured relative to that of the pure aqueous buffer. For each of the buffers, mesityl oxide was injected into the capillary for 1.0 s at 4.0 kPa and then was pushed past the detector hydrodynamically using 5.0 kPa pressure. The relative viscosities were determined from the ratios of the mesityl oxide elution times in the MeOH-containing buffers to the pure aqueous buffers.

## 2.3 Results and Discussion

### 2.3.1 EOF Reversal using CTAB in Aqueous Buffers

The effect of CTAB concentration on EOF in a 10 mM aqueous phosphate buffer at pH 8.0 is shown in Figure 2.3. The normal EOF in a bare silica capillary is towards the negative electrode (cathode), and is denoted with a positive EOF mobility. As can be seen from Figure 2.3, there is a rapid transition from normal (cathodic) to a reversed (anodic) EOF mobility as the CTAB concentration increases from 0 to 0.1 mM. For concentration ranges between 0.01 and 0.025 mM CTAB, the EOF mobility is practically zero. Thereafter, the reversed EOF is constant at about  $-4.45 \times 10^{-4}$  cm<sup>2</sup>/Vs, independent

of the CTAB concentration. This rapid transition in EOF is consistent with the results reported in the literature [12].

The surfactant concentration at which the EOF is reversed is generally referenced versus the CMC of the surfactant in the bulk solution [12, 18, 19]. To examine this relationship in these buffer systems, we determined the CMC of CTAB in aqueous solution using the tensiometer, as discussed in Section 2.2.4. The CMC values along with approximate surfactant concentrations at which the EOF is fully reversed are tabulated in Table 2.1. All the measurements were made at 25 °C. Addition of electrolyte to a solution decreases the CMC of a surfactant by diminishing the electrostatic repulsion between the ionic head groups of the surfactants as indicated in Section 1.4.3.3 of Chapter 1. For instance, the CMC of CTAB decreases from 0.87 mM in distilled water to 0.18 mM in the 10 mM aqueous phosphate (pH 8.0) buffer used herein (Table 2.1). As the behavior of the EOF change in aqueous solution reveals (Figure 2.3), the EOF is reversed at concentration (*ca* 0.1 mM) less than the CMC of the surfactant in the run buffer. Tavares et al. have also reported flow reversal with CTAB at a concentration that is about 10% of the standard (*i.e.* in distilled water) CMC value [20].

Similarly, Lucy and Underhill reported complete EOF reversal by the conditional CMC for CTAB in phosphate buffer (50 mM ionic strength) at pH 9.0 [12]. In contrast, Martin-Jouet et al. [21] observed full reversed EOF at 1/3 of the conditional CMC of CTAB in 20 mM creatinine/4 mM nicotinic acid (pH 5.5) and Baryla et al. observed fully reversed EOF at half the conditional CMC of CTAB in a 10 mM phosphate (pH 7.0) buffer [22]. These latter observations are consistent with the aqueous phase behavior in

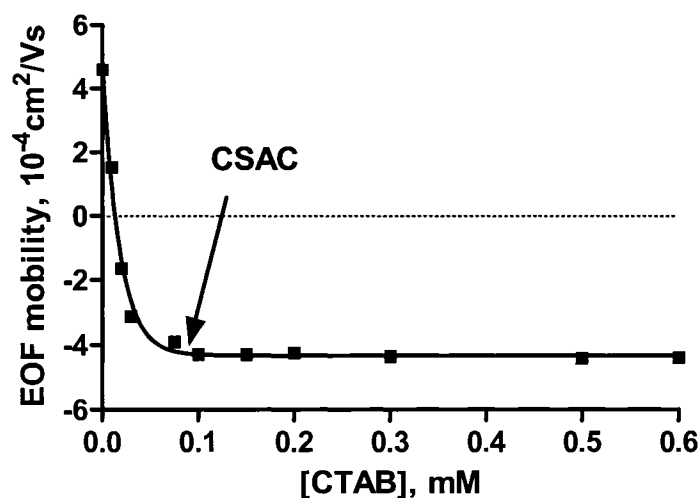


**Figure 2.3** Effect of CTAB concentrations on the EOF in 10 mM aqueous phosphate buffer at pH 8.0. Experimental conditions: applied voltage,  $\pm 15$  kV; capillary length, 37 cm (28.5 cm to the detector); marker: benzyl alcohol at 214 nm.

Figure 2.3, where the EOF is fully reversed by 0.1 mM, which is about half the conditional CMC for CTAB in 10 mM phosphate (0.18 mM, Table 2.1). As discussed in Section 1.4.3.3, recent Atomic Force Microscopy (AFM) studies have shown that single chain cationic surfactants such as CTAB form spherical aggregates at silica surfaces [17, 22]. These AFM studies also corroborate that surfactant aggregation occurs at the silica surface at  $1/3 - 1/2$  of the conditional CMC of the surfactant in the bulk solution. This sub-CMC aggregation is attributed to surfactant being concentrated in the wall region due to electrostatic attraction between the cationic head groups of the surfactant and the negative zeta potential of the surface (*i.e.*, capillary wall).

**Table 2.1** CMC values for CTAB in MeOH/water mixtures (Buffer: 10 mM phosphate at pH 8.0) <sup>a</sup>

MeOH (%v/v)	CMC (mM)	EOF reversal (mM) <sup>b</sup>
0	0.18	0.1
30	0.25	0.3
40	0.31	0.4
60	0.69	1.5

<sup>a</sup> Experimentally measured CMC of CTAB in distilled water is 0.87 mM.

<sup>b</sup> [CTAB] at which full EOF reversal is observed.

The surface excess thus leads to micelle formation at the surface even when the surfactant concentration is below the bulk solution CMC. The concentration at which this surface aggregation starts is referred to as the “*critical surface aggregation concentration, (CSAC)*”. In this study, the CSAC corresponds to the surfactant concentration where a fully reversed EOF is achieved as shown in Figure 2.3. Therefore, aggregation of surfactant molecules at the wall occurs slightly before micelle formation in the bulk solution (Figure 2.3).

### 2.3.2 EOF Reversal using CTAB in Methanol-Aqueous Buffers

The influence of methanol on the behavior of the EOF change was systemically studied at various concentrations of CTAB. Figure 2.4 shows the effect of increasing CTAB concentration on EOF in a 10 mM aqueous phosphate buffer at pH 8.0 containing 0-60% MeOH. A highly unstable baseline was observed for CTAB solutions containing more than 60% MeOH and no further studies were made of these buffers. The EOF reversal observed in the presence of methanol displays a number of changes in behavior



relative to that in the pure aqueous buffer (Figure 2.3). First, in the absence of CTAB, the magnitude of the normal EOF decreases with the content of methanol. Secondly, the fully reversed EOF decreases in magnitude as the amount of methanol increases. Thirdly, the CTAB concentration necessary to reverse the EOF increases with volume of methanol added to the buffer. Each of these behaviors will be discussed in detail in the following Sections.

### 2.3.2.1 EOF in MeOH-Water Solutions in the Absence of Surfactant

As indicated in Section 1.2.2.3 (eqn 1.8), the electroosmotic flow mobility ( $\mu_{eo}$ ) depends on the dielectric constant ( $\varepsilon$ ) and the viscosity ( $\eta$ ) of the medium and on the zeta potential ( $\zeta$ ) of the capillary wall according to:

$$\mu_{eo} = -\frac{\varepsilon\varepsilon_o\zeta}{\eta} \quad (1.8)$$

where  $\varepsilon_o$  is the permittivity of vacuum. Thus, the  $\mu_{eo}$  is proportional to the ratio of  $\varepsilon/\eta$ . Indeed these are the key solvent parameters affecting the electrophoretic and electroosmotic mobilities in mixed solvents (Section 1.4.4 and Table 1.1) although recent studies have also demonstrated the importance of solvent relaxation time ( $\tau$ ) for electrophoretic mobilities [15, 23-25]. The results in Figure 2.4 show that the magnitude of the EOF decreases as the amount of methanol increases in the absence of surfactant. This is partly due to a decrease in the dielectric constant and an increase in the viscosity of the buffer upon addition of methanol. I calculated the  $\varepsilon/\eta$  ratio using literature dielectric constant values [26] and experimentally determined viscosities as described

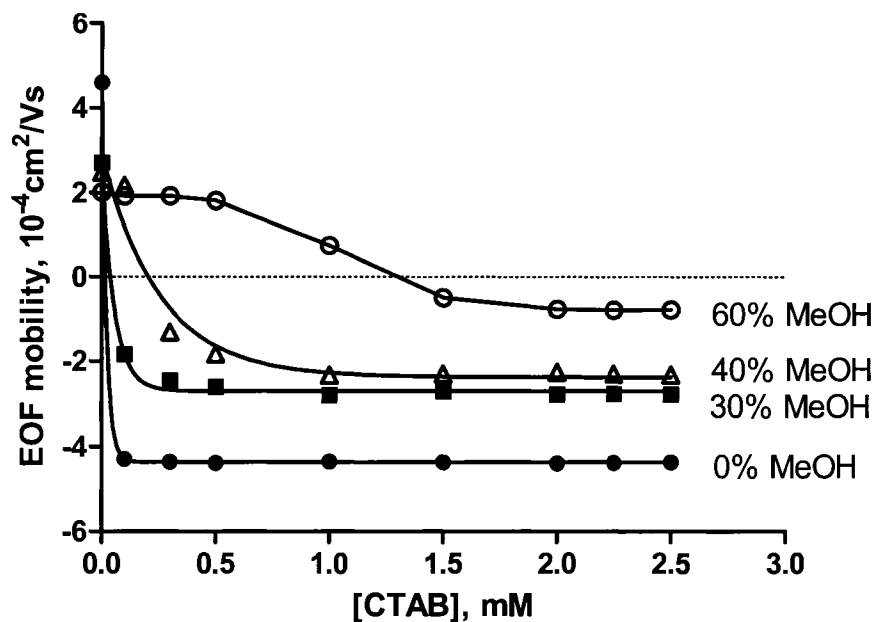


**Figure 2.4.** Effect of CTAB concentration and methanol on the EOF. Experimental conditions:  $V = -15\text{ kV}$ ;  $L = 37.0\text{ cm}$  (28.5 cm to detector); 10 mM phosphate buffer, pH 8; direct UV detection at 254 nm using mesityl oxide as neutral marker. A) 0% MeOH (●) B) 30% MeOH (■) C) 40% MeOH (Δ), and D) 60% MeOH (○).

above in Section 2.3.6. The dielectric constant and viscosity of the aqueous solution are assumed to be equal to those of water.

Figure 2.5 shows the relationship of the value of the  $\varepsilon/\eta$  ratio to percent methanol. For mixture of MeOH ( $\varepsilon = 32.7$ ,  $\eta = 0.55\text{ cP}$ ) and water ( $\varepsilon = 78.5$ ,  $\eta = 0.89\text{ cP}$ ), the dielectric constant decreases almost linearly with increasing volume of methanol. In contrast, the viscosity of the mixtures changes from 0.89 cP in pure aqueous solution to 0.55 cP in 100% MeOH reaching a maximum value of 1.60 cP at about 45% MeOH.

Hence, the value of the  $\varepsilon/\eta$  ratio shows a parabolic relationship with percent MeOH with steady decrease to a minimum at about 65% and thereafter increases slightly.

Schwer and Kenndler had reported that the magnitude of  $\varepsilon/\eta$  in 60% MeOH solution is about 45% of that in pure aqueous solution [27]. This change is consistent with the EOF decrease observed in Figure 2.4. However, because the observed EOF changes are rather large, the variation of the EOF cannot be attributed solely to changes in the value of the  $\varepsilon/\eta$  ratio. Some additional decrease in EOF would be expected due to decreases in the zeta potential in buffers containing the organic solvents. However, this latter effect is probably offset by variations in the ionic strength of our buffer upon dilution with the MeOH. Nonetheless, the potential effect of decreases in the zeta potential of the capillary wall on EOF reversal using CTAB will be discussed in Section 2.3.3.

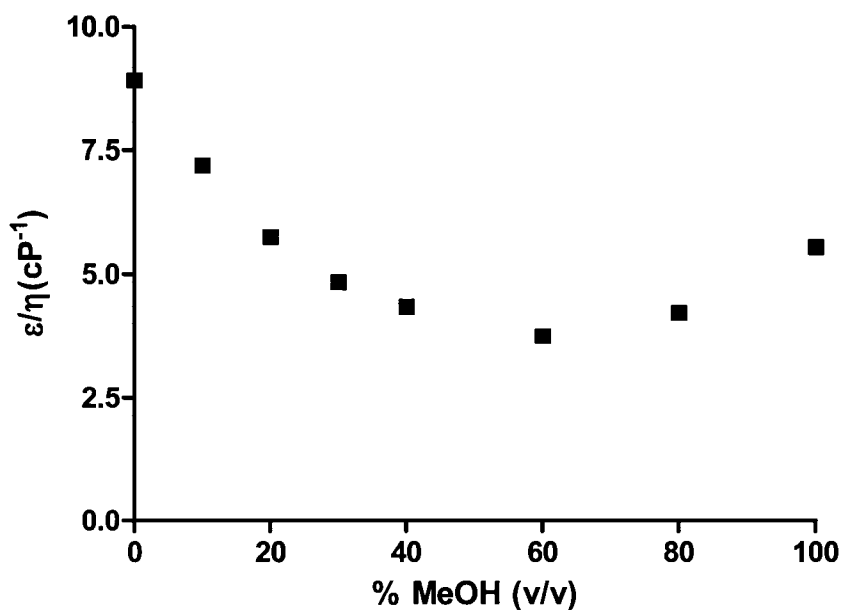


**Figure 2.5** Variation of ratio of dielectric constant to viscosity with percent of methanol composition at 25 °C.

### 2.3.2.2 Magnitude of the Fully Reversed EOF

The magnitude of the fully developed reversed EOF (>2 mM CTAB) decreases upon addition of MeOH as shown in Figure 2.4. The EOF decreases from  $-4.45 \times 10^{-4}$  cm<sup>2</sup>/Vs in pure aqueous buffer to  $-0.78 \times 10^{-4}$  cm<sup>2</sup>/Vs in 60% MeOH. Between 0 and 40% MeOH the change in the reversed EOF is strongly correlated with the change in the normal EOF observed in the absence of CTAB ( $R^2 = 0.985$ ). This suggests that the changes in the magnitude of the fully reversed EOF are directly related to solution conditions ( $\epsilon/\eta$ ), rather than to a disruption of the adsorbed surfactant layer. However, the magnitude of the reversed EOF in 60% MeOH is much smaller than the corresponding normal EOF. This suggests that there is a disruption or alteration in the micellar layer under this condition. This is similar to the observations of Colic and Fuersteanau [28] who observed an order of magnitude decrease in the maximum surface coverage of SDS on alumina (pH 3) upon switching from pure aqueous buffer to 50% ethanol (EtOH).

### 2.3.2.3 On-Set of EOF Reversal

In aqueous buffers, EOF reversal is complete by a CTAB concentration of about one-half the CMC in the bulk solution, as discussed in Section 2.3.2.1. To determine if a similar relationship exists in MeOH-water electrolytes the CMC of CTAB in the methanol containing buffers was determined. The CMC measured and CTAB concentrations at which a reversed and stable EOF is achieved for various buffers are listed in Table 2.1. The CMC of CTAB increases only gradually with increasing percent methanol. This increase is consistent with MeOH being a class II additive [29] as discussed in Section 1.4.3.3. Short chain alcohols such as methanol and ethanol partition

very little into the micelles and so only affect the CMC by altering the bulk properties and interactions of the solvent [30]. For instance, the CMC of TTAB is only 40% higher in 23% (w/w) ethanol than in pure water (4.46 mM vs. 3.2 mM) [30]. In contrast, longer chained alcohols (> 4 carbon) are referred to Class I additives and affect a surfactant's CMC at much lower concentrations than Class II additives [29]. Long chain alcohols partition into the micelle and can screen the electrostatic repulsion between surfactant head groups, thereby decreasing the surfactant CMC.

As shown in Figure 2.4, the behavior the EOF observed for buffers containing MeOH was different from the aqueous solutions. As the concentration of MeOH in the buffer increases, the transition from normal to reversed EOF becomes more gradual and the concentration of CTAB necessary to reverse the EOF increases. In 30% MeOH reversal of the EOF occurred at approximately the conditional CMC and in 40% MeOH the EOF reversal occurred at a concentration greater than the CMC. In 60% MeOH, however, the EOF reversal did not occur until a CTAB concentration much greater than the CMC was employed. Ye et al. have also reported similar dramatic increases in the concentration of surfactant necessary to reverse the charge of a surface in mixed MeOH-water solutions. They observed a gradual EOF transition between 0.25 mM (strong normal EOF) and 2 mM CTAB (fully reversed) in a 5 mM phosphate buffer (pH 7.5) containing 50% methanol. In studies of lithium perfluorooctane sulfonate (LiOFS) on alumina, Esumi et al. [31] found that the point of zero charge occurred at 0.34 mM LiOFS in water, 0.66 mM in 30% w/w MeOH, and 1.6 mM in 50% w/w MeOH. No reversal in the surface charge of alumina was observed in solutions containing higher concentrations of MeOH. Similarly, in studies of sodium dodecylsulfate (SDS)

adsorbing onto alumina at pH 3, charge reversal was observed at 0.02 mM SDS in pure aqueous (pH 3) buffer, at 0.09 mM SDS in 30% ethanol and no reversal was observed in 50% ethanol, even at SDS concentrations as high as 50 mM [31].

Comparison of the CMC values and the CTAB concentration required to reverse the EOF (Table 2.1) suggests that there is some change in the mechanism or morphology of surfactant aggregation at the capillary wall in the presence of MeOH (Figure 2.4 and Table 2.1). In AFM studies of CTAB aggregation on mica, Wall and Zukoski [32] observed that the morphology of the adsorbed micelles changed from cylinders at low EtOH concentration to short cylinders at about 1 M (~5% w/w) EtOH and then to spheres at about 3 M (14% w/w) EtOH. The concentration of EtOH was not increased above 3 M, and so no disappearance of micelle structure was observed. However, corresponding studies with *n*-butanol demonstrated a transition from short cylinder to sphere at 0.1 M followed by a disappearance of structure at 0.15 M *n*-butanol [32]. Similarly, as discussed above the maximum surface coverage of SDS on alumina (pH 3) was an order of magnitude lower in 50% EtOH than in pure water [28].

### 2.3.3 Effect of Surface Ionization of Silica

The results in Figure 2.4 also demonstrated that changes in the CMC of CTAB upon addition of methanol were not solely responsible for the changes in the EOF. An alternate hypothesis is that a reduction in the zeta potential of the silica surface might cause a decrease in surface aggregation of CTAB. Addition of organic solvents decreases the zeta potential of silica surfaces in two ways. First, the intrinsic lower dielectric constant of the mixed aqueous-organic solvent results in a steeper drop of the potential within the double layer (Section 1.2.2.2). Thus for a fully ionized silica capillary the zeta

potential in 50% MeOH is 40% lower than that in a purely aqueous buffer [27]. Secondly, the  $pK_a$  of the surface silanols shifts to a value of  $\sim 7.5$  in mixed aqueous-organic solvents, compared to a  $pK_a$  of  $\sim 5.3$  in pure water [27]. Thus, in buffers containing organic solvents the zeta potential is further diminished by incomplete ionization of the silanols.

The effect of zeta potential on surface aggregation of CTAB can be conveniently explored by lowering the pH of the buffer. Figure 2.6 shows the dependence of EOF versus CTAB concentration in 10 mM aqueous phosphate buffer at pH 3. The corresponding EOF behavior in aqueous pH 8 buffer is reproduced from Figure 2.4 for reference. With no CTAB in the running buffer, the EOF is much lower at pH 3 than pH 8, as is expected due to the reduced deprotonation of the silanols. At high CTAB concentration ( $>1$  mM) the reversed EOF in Figure 2.6a becomes independent of surfactant concentration and shows only a small dependence on pH.

The most striking difference between the EOF behaviors at pH 3 and 8 in Figure 2.6a is the characteristics of the transition from normal to reversed EOF. The sharp transition in EOF at pH 8 has been discussed in Section 2.3.1. In contrast, at pH 3 the EOF undergoes a much more gradual transition (EOF is not fully reversed until 0.5 mM CTAB), as compared to the transition at pH 8 (EOF is reversed by 0.1 mM CTAB). This change in behavior is reminiscent of that observed in Figure 2.4 as a result of the addition of  $\sim 40\%$  MeOH to the buffer. Addition of 40% MeOH to the pH 3 buffer (Figure 2.6b) shifts the point of EOF reversal to higher CTAB concentrations relative to the purely aqueous pH 3 buffer. Likewise, the EOF transition in 40% MeOH is much more gradual

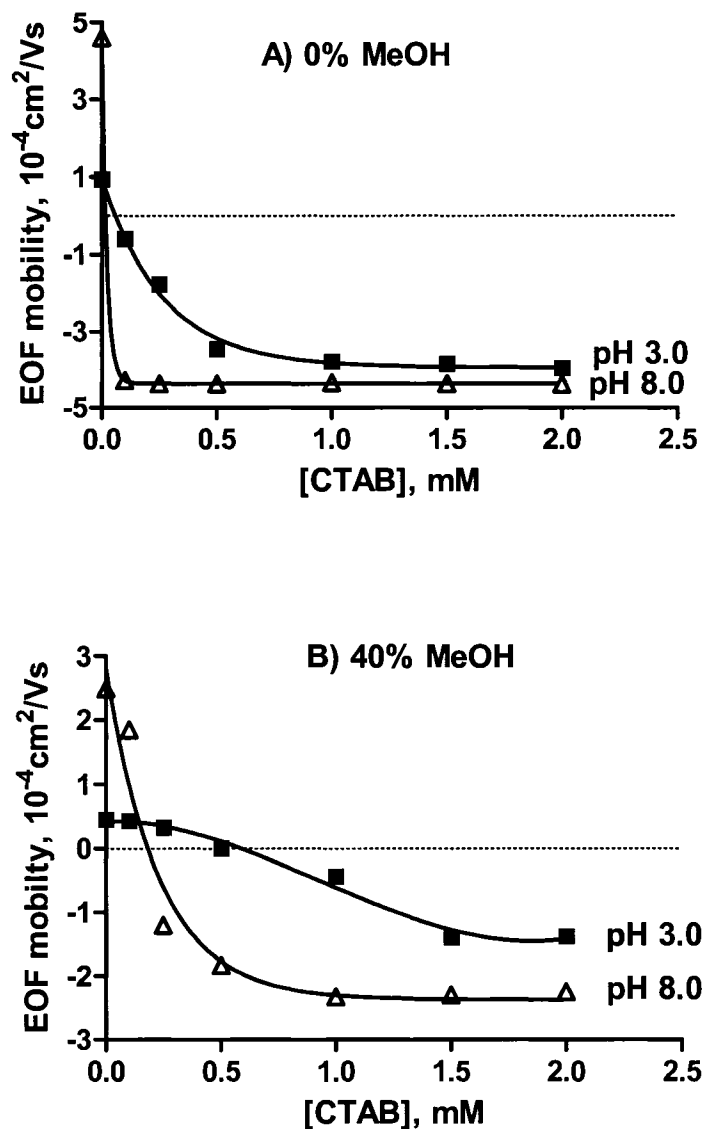


**Figure 2.6** Effect of pH on the magnitude of the EOF in a 10 mM phosphate buffer containing A) 0% MeOH and B) 40% (v/v) MeOH. All other experimental conditions as described in Figure 2.4.



at pH 3 than at pH 8. Thus, the impact of MeOH on CTAB concentration at which EOF reversal occurs is predominantly a function of the diminished zeta potential of the silica, and to a lesser extent on the effect of MeOH on the CMC of the surfactant.

#### **2.3.4 EOF Reversal using DDAB in Mixed MeOH-Water Buffers**

The double-chained surfactant, DDAB, has previously been used for ultra-rapid separations of nitrate and nitrate at low pH [4]. It was also shown that DDAB forms a semi-permanent coating owing to a formation of bilayer structure on the surface as shown in Figure 1.6. This enables removal of the excess surfactant from the buffer prior to separation [4, 22, 33] and thus avoids undesirable interaction between the surfactant monomers and the analyte anions. However, there was no previous report on the use of DDAB for surface modification in mixed nonaqueous-water buffer or in pure nonaqueous CE.

In this work, I also investigated the effect of DDAB on the EOF in aqueous and mixed aqueous-methanol buffers. The results are shown in Figure 2.7. The general trends in EOF observed are similar to those of CTAB (Figure 2.4). The concentration of DDAB required to reverse the EOF in aqueous buffers is less than the CMC in the running buffer, which is approximately 0.05 mM [22]. In addition, a rapid transition from normal to reversed EOF is observed as the DDAB concentration increases from 0.05 to 0.1 mM. However, as the %MeOH increases from 0 – 20% the concentration of DDAB necessary to reverse the EOF rises only slightly. With the DDAB, the EOF is reversed at a much lower surfactant concentration than the CTAB both in aqueous and

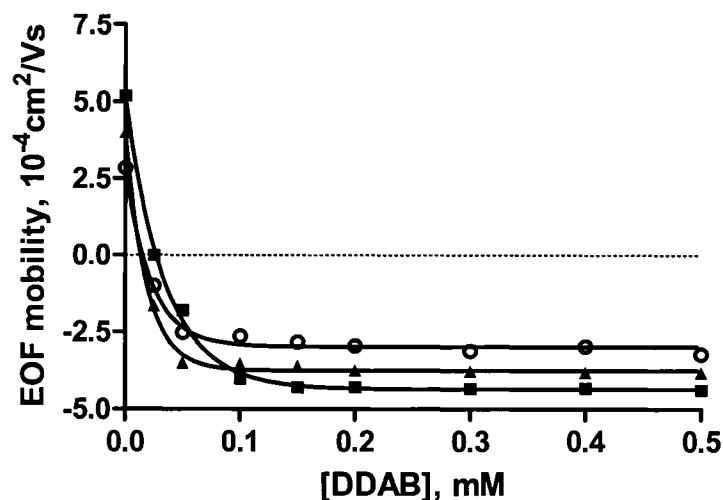


**Figure 2.7** Effect of DDAB concentration on EOF. A) 0% MeOH (■), B) 10% MeOH (▲), C) 20% MeOH (○). Other conditions as in Figure 2.4.

methanol containing buffers. Stable reversed EOF is obtained with up to 20% MeOH in running buffer but above 20% MeOH, the migration times become irreproducible and the baseline showed strong disturbances.

### 2.3.5 Anion Separations in MeOH-Water Buffers

The effect of methanol content on the separation of small inorganic anions was studied over the range of 0 to 60% (v/v) MeOH in a 15 mM phosphate buffer at pH 8.0 containing cetyltrimethylammonium chloride (CTAC). Our attempts to use more than 60% MeOH was unsuccessful due to high background disturbances. The chloride form of the surfactant was used instead of bromide to reduce the UV background. The anions were separated in the co-EOF mode and detected using direct absorbance at 214 nm.

The electropherograms in Figure 2.8 show the influence of increasing concentrations of MeOH on the separation of the five anions. The mobility order in aqueous buffers is  $\text{Br}^- > \text{NO}_2^- \sim \text{NO}_3^- > \text{I}^- > \text{SCN}^-$ . This is the same order as that observed in typical electrostatic ion chromatography [3, 9]. The large but less hydrated anions such as iodide and thiocyanate undergo strong ion-exchange interactions with the surfactants. Thus such polarizable anions are retained in the capillary longer. In addition, the peaks for these anions are broad and tailed. Interactions with the dynamically coated surfactant layers on the capillary wall would cause tailed peaks due to resistance to mass transfer of the anions to and from the surface to the bulk solution [16].

When methanol is used in the electrophoretic buffers significant changes in the separation order and resolution are observed relative to those in pure aqueous systems (Figure 2.8). In all cases, the migration time of the anions increased with increasing MeOH concentration, as would be expected from the lower EOF velocity caused by the lower dielectric constant and higher solvent viscosity.  $\text{NO}_3^-$  and  $\text{NO}_2^-$  are not separated in aqueous solutions whereas these ions are baseline resolved in 20% MeOH. In 60% MeOH the mobility of iodide and thiocyanate have been significantly altered, such that the mobility order is now:  $\text{I}^- > \text{Br}^- > \text{NO}_3^- > \text{NO}_2^- > \text{SCN}^-$ .  $\text{I}^-$  is the second slowest ion in 20% MeOH but the fastest in 60% MeOH. Changes in solvation of ions and ion-association interactions with the surfactant are likely the major factors determining the observed changes in selectivity [34, 35].

In addition to reversing the EOF, cationic surfactants were reported to affect the

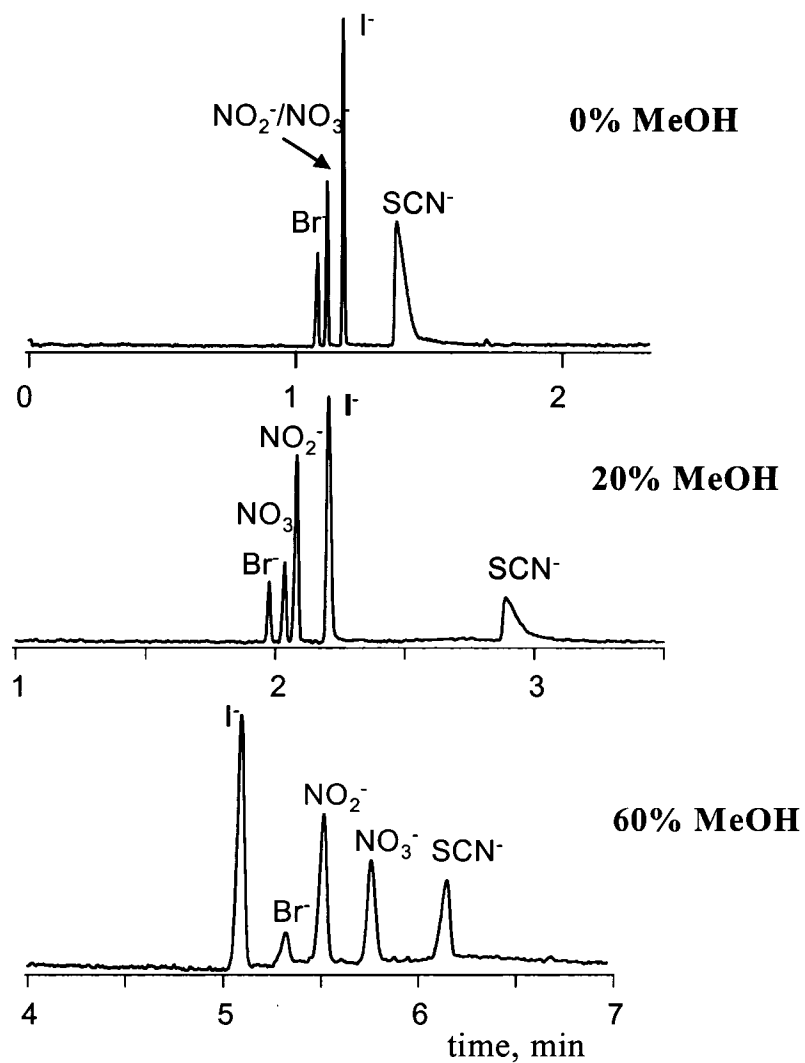


**Figure 2.8** Separation of five inorganic anions by co-EOF using mixed organic-aqueous buffers. Experimental conditions: [CTAC]= 0.5 mM; V= -15 kV; L=37.0 cm (28.5 cm to the detector); 15 mM phosphate buffer (pH 8.0); 0.2 mM sample concentration;

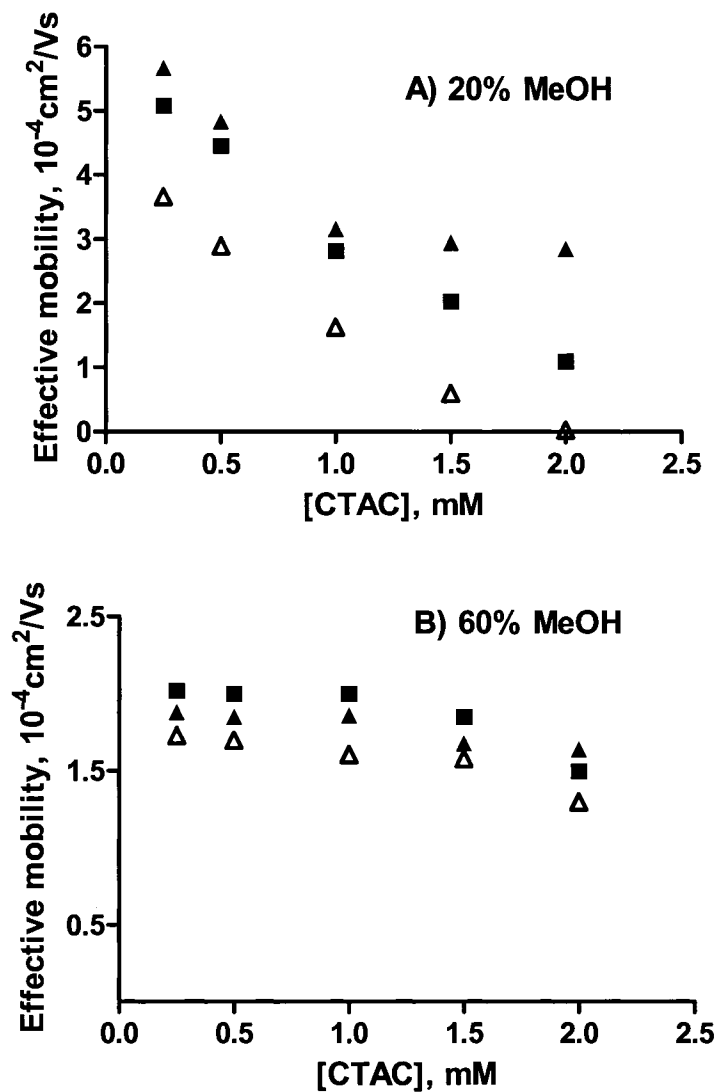


**Figure 2.9** Effect of CTAC concentration on the selectivity of inorganic anion separations. A) 20% MeOH; B) 60% MeOH. NO<sub>3</sub><sup>-</sup> (●); I<sup>-</sup> (■); SCN<sup>-</sup> (Δ). Other experimental conditions as in Figure 2.7.

migration times of anions through ion-pair interactions [3, 36] or hydrophobic interaction [37]. Hence, we investigated whether more drastic selectivity changes could be achieved by using a higher concentration of CTAC. Figure 2.9 shows the effective mobilities (Section 2.2.5) of selected anions at increasing concentrations of the CTAC and different percent volumes of methanol. In pure aqueous solutions, the mobility of the anions, particularly the more polarizable ones such as  $I^-$ , are retarded as the concentration of surfactant increases in the running buffer. However, in methanolic buffers the effect is substantially reduced (Figure 2.9). In 20% MeOH, there is slight change in mobility of the anions but in buffers containing 60% MeOH, the mobility of  $I^-$  and  $SCN^-$  change only by 4% and 6.5% respectively when the concentration of the CTAC is increased from 0.5 to 2.5 mM. The presence of MeOH in the solution suppresses the interactions of polarizable anions with the surfactant, thereby increasing their effective mobility [38]. This reduction in ion-exchange interactions enables anions such as iodide to migrate faster than other anions and the peaks become more symmetrical, a big improvement over the aqueous buffers.

#### 2.4 Concluding Remarks

This work demonstrates that the reversed EOF generated by the cationic surfactants, CTAB and DDAB, can be systematically altered by the addition of methanol to the background electrolyte. For both aqueous and low methanol containing buffers surface aggregation of the surfactants at the capillary wall and EOF reversal occurs at concentration below their CMC in the bulk solution. In aqueous solutions, the resultant critical surface aggregation concentration (CSAC) is in the range of  $1/3$  to  $1/2$  of the CMC in the buffer solutions. Decreasing the zeta potential of the silica surface either by

lowering the pH or adding MeOH results in an increase in the CSAC of the surfactant required to reverse the EOF. Consequently, in 60% MeOH the CSAC is more than the CMC of the surfactant in the running buffer. Dramatic selectivity changes were also observed by adjustment of the methanol content for the separation of five inorganic anions. Changes in solvation of ions and ion-association interactions with the surfactant are likely the major factors responsible for the observed changes in selectivity. Hence modifying the electroosmotic flow using CTAC and methanol helps to obtain baseline separation of anions while retaining the rapid analysis times and high efficiencies associated with co-EOF separations.

## 2.5 References

- [1] Haddad, P. R., *J. Chromatogr. A* 1997, 770, 281-290.
- [2] Lucy, C. A., *J. Chromatogr. A* 1998, 804, 3-15.
- [3] Jones, W. R., Jandik, P., *J. Chromatogr.* 1991, 546, 445-458.
- [4] Melanson, J. E., Lucy, C. A., *J. Chromatogr. A* 2000, 884, 311-316.
- [5] Timerbaev, A. R., *J. Cap. Elec.* 1995, 2, 165-174.
- [6] Timerbaev, A. R., *J. Chromatogr. A* 1997, 792, 495-518.
- [7] Stathakis, C., Cassidy, R. M., *Can. J. Chem.* 1998, 76, 194-198.
- [8] Zakaria, P., Macka, M., Haddad, P. R., *Anal. Chem.* 2002, 74, 1241-1248.
- [9] Jandik, P., Bonn, G. *Capillary Electrophoresis of Small Molecules and Ions*; VCH Publishers, Inc.: New York, 1993.
- [10] Buchberger, W., Haddad, P. R., *J. Chromatogr.* 1992, 608, 59-64.
- [11] Salimi-Moosavi, H., Cassidy, R. M., *Anal. Chem.* 1995, 67, 1067-1073.
- [12] Lucy, C. A., Underhill, R. S., *Anal. Chem.* 1996, 68, 300-305.
- [13] Yeung, K. K.-C., Lucy, C. A., *Anal. Chem.* 1997, 69, 3435-3441.
- [14] Williams, B. A., Vigh, G., *Anal. Chem.* 1996, 68, 1174-1180.
- [15] Roy, K. I., Lucy, C. A., *Anal. Chem.* 2001, 73, 3854-3861.
- [16] Woodland, M. A., Lucy, C. A., *Analyst* 2001, 126, 28-32.
- [17] Liu, J. F., Ducker, W. A., *J. Phys. Chem. B* 1999, 103, 8558-8567.
- [18] Melanson, J. E., Baryla, N., E., Lucy, C. A., *Trends Anal. Chem.* 2001, 20, 365-374.
- [19] Kaneta, T., Tanaka, S., Taga, M., *J. Chromatogr. A* 1993, 653, 313-319.



- [20] Tavares, M. F. M., Colombara, R., Massaro, S., *J. Chromatogr. A* 1997, 772, 171-178.
- [21] Martin-Jouet, M., Hagege, A., Leroy, M. J. F., *J. Chromatogr. A* 2002, 946, 255-263.
- [22] Baryla, N. E., Melanson, J. E., McDermott, M. T., Lucy, C. A., *Anal. Chem.* 2001, 73, 4558-4565.
- [23] Roy, K. I., Lucy, C. A., *Electrophoresis* 2003, 24, 370-379.
- [24] Roy, K. I., Lucy, C. A., *J. Chromatogr. A* 2002, 964, 213-225.
- [25] Roy, K. I., Lucy, C. A., *Electrophoresis* 2002, 23, 383-392.
- [26] Akhadov, Y. Y. *Hand book of Dielectric Properties of Binary Solutions*; Pergamon Press: New York, 1980.
- [27] Schwer, C., Kenndler, E., *Anal. Chem.* 1991, 63, 1801-1807.
- [28] Colic, M., Fuerstenau, D. W., *Langmuir* 1997, 13, 6644-6649.
- [29] Rosen, M. *Surfactants and Interfacial Phenomena*, 2nd ed.; John Wiley & Sons: New York, 1989.
- [30] Zana, R., Yiv, S., Strazielle, C., Lianos, P., *J. Colloid Int. Sci.* 1981, 80, 208-223.
- [31] Esumi, K., Ikemoto, M., Meguro, K., *Colloids Surf.* 1990, 46, 231-237.
- [32] Wall, J. F., Zukoski, C. F., *Langmuir* 1999, 15, 7432-7437.
- [33] Baryla, N. E., Lucy, C. A., *J. Chromatogr. A* 2002, 956, 271-277.
- [34] Carou, M. I. T., Mahia, P. L., Lorenzo, S. M., Fernandez, E. F., Rodriguez, D. P., *J. Chromatogr. A* 2001, 918, 411-421.
- [35] Lucy, C. A., *J. Chromatogr. A* 1999, 850, 319-337.

- [36] Harakuwe, A. H., Haddad, P. R., Buchberger, W., *J. Chromatogr. A* 1994, 685, 161-168.
- [37] Masselter, S. M., Zemmann, A. J., *Anal. Chem.* 1995, 67, 1047-1053.
- [38] Harakuwe, A. H., Haddad, P. R., *J. Chromatogr. A* 1999, 834, 213-232.

## CHAPTER THREE: Study of the Selectivity of Inorganic Anions in Hydro-organic Mixtures using Indirect Capillary Electrophoresis<sup>‡</sup>

### 3.1 Introduction

Ion chromatography (IC) is the most popular method for the analysis of small inorganic anions. However, capillary electrophoresis (CE) represents a valuable alternative to IC due to its complementary separation selectivity. In IC, analyte ions are separated primarily by differences in ion-exchange interactions with a stationary phase, whereas CE separation is based on differences in electrophoretic mobility. Nonetheless, CE separations provide shorter analysis times, higher separation efficiency, and much lower sample and electrolyte volumes than IC [1-3].

Separation selectivity in CE depends on the difference in the effective electrophoretic mobilities of the analytes of interest. Selectivity changes can be achieved by varying the ionic strength, pH, and using additives as discussed in Section 1.4. A number of studies have noted a change in selectivity in CE separations of anions due to the buffer concentration [4, 5]. In particular, Li et al. demonstrated the influence of ionic strength on the mobility of singly and multiply charged carboxylates and sulfonates using the Pitts equation [6]. However, the use of indirect detection in CE of inorganic anions limits the utility of ionic strength for controlling selectivity because it could compromise the sensitivity. Anion selectivity can also be achieved by adjusting the pH of the buffer to maximize the difference in electrophoretic mobility of the ions. Dramatic changes in selectivity have been observed particularly for borate, carbonate, and phosphate whose

---

<sup>‡</sup>A version of this chapter has been published as **Diress, A; Lucy, C.A.** *Journal of Chromatography A*, **2005**, 1085: 155-163.

$pK_a$  lie in the pH range 8-13 [7]. Melanson and Lucy have also used an acidic buffer (pH 2.5) to separate nitrite and nitrate [8]. However, this approach has limited use for inorganic anions as many of these ions have no  $pK_a$  in the pH range that is attainable in most CE applications[3, 9].

In recent years there has been significant interest in the use of organic solvents to modify selectivity in CE, as discussed in Section 1.4.4. However, there has been a limited amount of work on CE separations of inorganic anions in the presence of organic solvents [4, 10]. Salimi-Moosavi and Cassidy investigated the effect of methanol and dimethylformamide for the separation of inorganic anions [10]. They noted some significant changes in separation order relative to aqueous systems, with some instances in reversal of order of migration. Buchberger and Haddad [4] also studied the effect of up to 30% of methanol, acetonitrile, tetrahydrofuran, acetone or ethylene glycol on anion mobilities.

With respect to CE separations of inorganic anions, two unique issues that arise are detection and the control of the electroosmotic flow (EOF). In CE, detection is usually performed by directly monitoring absorption of UV light by the analytes (Section 1.2.3.1). However, only a few inorganic anions absorb in the UV-visible range. As a result, it is necessary to use indirect detection [7, 8, 11]. As discussed in Section 1.2.3.2, the application of indirect UV detection in CE requires that a chromophore ion (a probe) be present in the separation buffer to provide a background absorbance. The analyte ion then displaces the probe as it migrates along the capillary, resulting in a decrease in the background absorbance. To maximize this displacement and the resultant relative change in the absorbance background, it is essential that the concentration of the probe be dilute

and that the mobility of the probe be close to the mobility of the analytes (eqn 1.13). If the mobility of the probe differs significantly from that of the analyte, electrodispersion band broadening will occur [12]. Therefore, selection of a suitable UV absorbing probe must consider not only factors related to optimizing sensitivity, but also the separation efficiency [2]. Choosing a probe that has a high molar absorptivity and whose mobility is comparable to the mobilities of the analytes optimizes both sensitivity and efficiency.

Control of the EOF is essential for optimizing the analysis time for inorganic anions. This is because in bare silica fused capillaries, the electrophoretic mobilities of small inorganic anions are of the same magnitude but in the opposite direction to the EOF (Section 1.4). Such counter-EOF separations can enhance resolution, and have even been demonstrated to resolve the isotopes of chloride [13]. However, it also results in excessively long migration times. To establish co-EOF conditions for anions in fused-silica capillaries, dynamic coatings with positively charged additives or permanent coatings with positively charged functional groups have been used to reverse the direction of the EOF [14-16]. Only limited studies have been performed on EOF reversal in the presence of organic solvents [17-19]. In Chapter 2, we showed how cationic surfactant, cetyltrimethylammonium bromide (CTAB) can be used to manipulate the magnitude and direction of the EOF in buffers containing zero up to 60% methanol solution.

This Chapter will focus on the development of CE methods for the rapid separation of inorganic anions using indirect detection, wherein the selectivity is modified using organic solvents. Consideration is given to the choice of the absorbing probe used for indirect detection, based on the relative mobilities of the probe and the

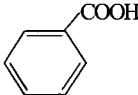
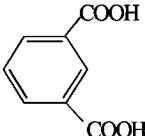
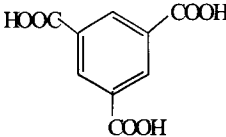
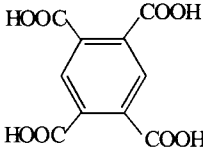
analytes and the desired limits of detection. A number of indirect probes are explored. The effect of the electrolyte buffer system, including the pH, buffer concentration and organic modifier on the probes and analytes mobilities are investigated. To our knowledge, this is the first report focusing on the effect of the organic solvent on the probes for indirect detection. Adjustment of the methanol content improves the selectivity and resolution of the inorganic anions under the co-EOF mode. Limits of detection, reproducibility and application of the method for quantification of anions in water samples will also be discussed.

## **3.2 Experimental**

### **3.2.1 Apparatus**

All experiments were performed on a HP-3D CE instrument (Agilent Technologies, Palo Alto, CA, USA) equipped with an on-column diode array UV absorbance detector. Data acquisition and control were performed using ChemStation software (HP-3D, Agilent Technologies) on an HP personal computer. Untreated fused silica capillaries (Polymicro Technologies, Phoenix, AZ, USA) with an inner diameter of 50  $\mu\text{m}$ , an outer diameter of 365  $\mu\text{m}$ , and a total length of 37 cm (28.5 cm to the detector) were used unless otherwise specified. In all the experiments, the capillary was thermostatted at  $25.0 \pm 0.1^\circ\text{C}$ .

**Table 3.1** Structure and pKa values of commonly used visualization agents (probes) for indirect detection of small anions.

Common names	Structure	pKa values*
Chromic acid	$H_2CrO_4$	$pK_{a1} = -0.98$ $pK_{a2} = 6.51$
Benzoic acid		$pK_{a1} = 4.21$
Phthalic acid (1,2-benzenedicarboxylic acid)		$pK_{a1} = 2.95$ $pK_{a2} = 5.41$
Trimellitic acid (1,2,4-benzenetricarboxylic acid)		$pK_{a1} = 2.52$ $pK_{a2} = 3.84$ $pK_{a3} = 5.20$
Pyromellitic acid (1,2,4,5-benzenetetracarboxylic acid)		$pK_{a1} = 1.92$ $pK_{a2} = 2.87$ $pK_{a3} = 4.49$ $pK_{a4} = 5.63$

\* The pKa values are in aqueous solution and were taken from reference [20].

### 3.2.2 Chemicals

All solutions were prepared with ultrapure (18-M $\Omega$ ) water (Barnstead, Chicago, IL). The chemicals were all reagent grade or better, and were used without further purification. Buffers were prepared from sodium salts of orthophosphate (BDH), potassium chromate (BDH), and HPLC-grade methanol (MeOH; Fisher, Fair Lawn, USA). The surfactants; cetyltrimethylammonium bromide and chloride (C<sub>16</sub>TA<sup>+X</sup> where X=Br<sup>-</sup> or Cl<sup>-</sup>; Sigma, St. Louis, MO, USA) and the carboxylic acids (benzoic acid (BDH), phthalic acid (1,2-benzenedicarboxylic acid; BDH), trimellitic acid (1,2,4-benzenetricarboxylic acid; BDH), and pyromellitic acid (1,2,4,5-benzenetetracarboxylic acid; BDH) were used as received. The pH was measured using a Model 445 digital pH meter (Corning, Acton, USA) calibrated with aqueous standards immediately prior to use. The pH was adjusted using 0.1 M NaOH (BDH) before the required amount of methanol and/or surfactant (0.0–2.5 mM) was added. Stock anion samples (5.0 mM) were prepared from reagent grade sodium nitrite (BDH), potassium nitrate (BDH), potassium bromide (Fisher Scientific, Fair Lawn, NJ, USA), potassium iodide (BDH), sodium chloride (BDH), sodium sulfate (Fisher), potassium thiocyanate (BDH), sodium fluoride (Fisher), potassium perchlorate (Sigma), and potassium iodate (BDH) without further purification. River sample was collected from the North Saskatchewan River (Edmonton, Alberta) in two new polyethylene bottles (at a single site) and was analyzed within a week after filtration with a 0.45  $\mu$ m pore size membranes.



### 3.2.3 EOF Measurements

Each new capillary was pretreated at high pressure (93.8 kPa) with 1.0 M NaOH for 10 min, and H<sub>2</sub>O for 8 minutes. Prior to each run, the capillary was conditioned by rinsing at high pressure (93.8 kPa) with 0.1 M NaOH for 2 min, H<sub>2</sub>O for 2 min, and with the running buffer for 3 min. A 0.5 s hydrodynamic injection (5.0 kPa) was used for aqueous buffers, while a 2.0 s injection (5.0 kPa) was used for all methanol/water buffers. EOF measurements were performed under an applied voltage of -15 kV unless otherwise indicated. All voltages used herein were experimentally verified to be within the linear region of the Ohm's plot. Direct and indirect UV detection methods were applied at wavelengths of 214 nm and 254 nm respectively with a data acquisition rate of 20 Hz. A 1 mM solution of mesityl oxide (Aldrich, Milwaukee, WI, USA) for detection at 254 nm and 1 mM solution of benzyl alcohol (Aldrich) for detection at 214 nm were used as the neutral EOF markers. The EOF was calculated using the relations given in eqn 2.1. When the EOF is slow, less than  $2 \times 10^{-4}$  cm<sup>2</sup>/Vs) the pressure-mediated three injections technique developed by Williams and Vigh [21] was applied, as described in Section 2.2.3.

### 3.2.4 Separation and Quantification of Anions

Anion samples containing 0.2 mM of each anion (NO<sub>2</sub><sup>-</sup>, NO<sub>3</sub><sup>-</sup>, Br<sup>-</sup>, I<sup>-</sup>, Cl<sup>-</sup>, SO<sub>4</sub><sup>2-</sup>, F<sup>-</sup>, ClO<sub>4</sub><sup>-</sup>, and SCN<sup>-</sup>) were prepared from the standard stock solutions. Sample was injected hydrodynamically for 2.0 s at 5.0 kPa. The direction of the EOF was reversed in the presence of the cationic surfactant CTAB or CTAC (i.e., from the cathode to the anode), so the anions were separated in the co-EOF mode. An applied potential of -15 kV was used in all separations unless otherwise specified. Standard addition of each

anion in each buffer was used to confirm the identity of each peak. All mobility measurements were performed in triplicate. The effective mobilities of the anions were determined from the migration times under constant voltage conditions as described in Section 2.2.5. The efficiency ( $N$ ) was computed using the peak width at half-maximum height method:

$$N = 5.54 \left( \frac{t_m}{W_{1/2}} \right)^2 \quad (3.1)$$

where  $N$  is the theoretical plate number,  $t_m$  is the migration time and  $W_{1/2}$  is the peak width at half-maximum height in minutes.

Limits of detection of the anions were determined using a procedure based on the US Environmental Protection Agency (EPA) methodology [22]. Using the experimental conditions described above, a calibration curve was generated using 0.25 mM CTAC, 30% MeOH and 5.0 mM chromate (pH 8.0) over the concentration range 0.5–10  $\mu\text{g/mL}$  by diluting the stock standard solution of the anions. Then, a 2.5  $\mu\text{g/mL}$  sample of anions (about 5–10 times the estimated detection limit) was analyzed eight times. The standard deviation for these replicate injections was determined. The limit of detection (LOD) is then determined as:

$$C_{LOD} = s \cdot t_{n-1} \quad (3.2)$$

where  $s$  is the standard deviation of the determined concentrations,  $t_{n-1}$  is the Student  $t$  value at the 99% confidence (one-sided) interval with  $n-1$  degree of freedom.

### 3.3 Results and Discussion

The choice of the background electrolyte is an important factor in indirect detection in CE. As shown in Section 1.2.3.2, the theoretical limit of detection in indirect detection ( $C_{LOD}$ ) is given by:

$$C_{LOD} = \frac{C_P}{T_R \times D_r} = \frac{N_{BL}}{T_R \times \varepsilon \times b} \quad (1.13)$$

where  $C_P$  is the concentration of the visualization probe,  $T_R$  is the transfer ratio (the number of probe molecules displaced by one analyte molecule), and  $D_r$  is the dynamic reserve (ratio of the background absorbance to the noise).  $N_{BL}$  is the baseline noise,  $\varepsilon$  is the molar absorptivity of the probe, and  $b$  is pathlength of the detection window. Thus, a low-concentration background electrolyte with a high molar absorptivity at the wavelength of detection is required to obtain the best possible detection sensitivity.

#### 3.3.1 Mobility Match in Hydro-Organic Buffers

A key objective in developing an indirect CE method is that the probe used as the visualizing chromophore should have an electrophoretic mobility that closely matches the mobilities of the analytes. This is important for two reasons. Firstly, the transfer ratio ( $T_R$ ) depends not only on the charges of the probe and analyte, but also on their electrophoretic mobility through Kohlrausch's regulating function [23, 24].  $T_R$  is a measure of the ability of the analyte ion to displace the probe. For strong ionic species, an expression for  $T_R$  can be derived from Kohlrausch function as [23]:

$$T_R = \frac{\Delta C_P}{C_B} = \frac{z_B \mu_P}{z_P \mu_B} \left[ \frac{\mu_B + \mu_C}{\mu_P + \mu_C} \right] \quad (3.3)$$

where  $z_B$  and  $z_P$  are the charges on the analyte and probe ion respectively, and  $\mu_B$ ,  $\mu_P$  and  $\mu_C$  are the effective electrophoretic mobilities of the analyte, probe and counter ions respectively.  $C_P$  and  $C_B$  refer respectively, to the concentrations of the probe and analyte ions. Hence, the value of  $T_R$  depends on the mobilities of all ions involved and the transfer ratio is maximized when the probe and analyte have similar mobilities. As can be seen from eqn 3.3 a one-to-one displacement occurs only if the mobilities of the analytes are equal to that of the co-ions ( $T_R=1$ ). In that case, the electrodispersion is minimal resulting in a minimal peak distortion.

Secondly, with the dilute background electrolytes used in indirect detection, the analyte ions contribute significantly to the total solution conductance within the sample zone. Consequently, if the mobility of the analyte differs from that of the background electrolyte, there will be differences in the conductivity, and hence the electric field strength, across the sample zone as discussed in Section 1.2.3.2. The resultant electrodispersion results in peak fronting if the mobility of the analyte is greater than that of the probe, and tailing if the analyte mobility is less than the probe [12, 25]. Thus, electrodispersion could severely degrade peak shape, and consequently lower both the resolution and sensitivity of the method.

Addition of organic solvents to the background electrolyte will affect the mobility of both the analytes and probe. Thus, it is important to assess the mobility of the probes relative to the mobility of the analytes in the mixed aqueous/organic solvent systems to ensure optimal efficiency and sensitivity. Five commonly used probes (Table 3.1) were selected for study on the basis of their relative mobilities and their high molar absorptivity [12, 26]. Figure 3.1 shows the effect of the addition of methanol on the

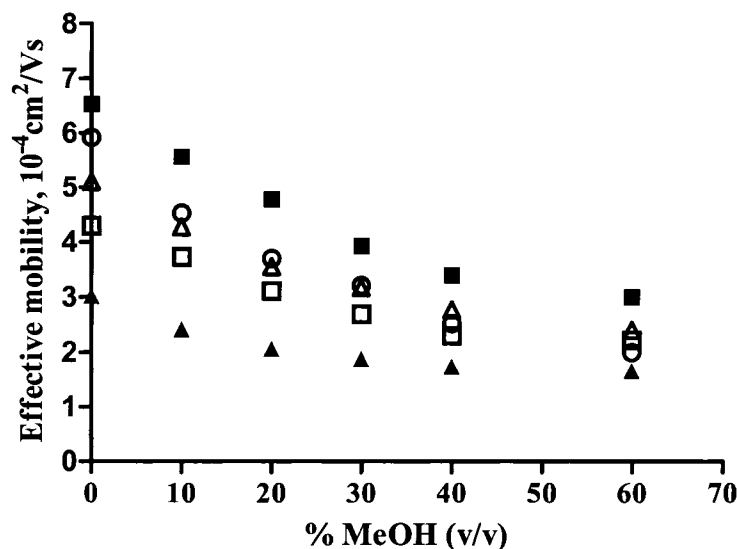


**Figure 3.1** Electrophoretic mobility of common indirect detection probes for anions detection in mixed methanol/water buffers. Chromate (■), pyromellitate (○), trimellitate (△), phthalate (□), benzoate (▲). Experimental conditions: 15 mM phosphate, pH 8.0; detection at 214 nm.

electrophoretic mobility of these probes. The buffer concentrations are maintained the same in each buffer system.

As shown in Figure 3.1, the electrophoretic mobilities of chromate and all the aromatic carboxylic acids decrease substantially as the amount of methanol increases from 0% to 50%. This is not surprising as the viscosity of methanol-water mixtures change from 0.89 cP in pure aqueous solution to 0.55 cP in 100% MeOH reaching a maximum value of 1.60 cP at about 45% MeOH (Section 2.3.3). The dielectric constant decreases almost linearly as the amount of the organic solvent increases [27]. However, some more subtle relative changes in mobility are also evident in Figure 3.1. The

mobility of pyromellitate decreased 55% in 40% MeOH relative to pure aqueous buffer, while the mobility of benzoate decreased only 42%. The mobility changes for all others probes are within this range. In 60% MeOH buffer, the mobilities of all of the probes except benzoate and phthalate are reduced by more than 50%.

In addition to viscosity and dielectric constant, the mobilities of the probes could be affected by solvent-induced pH or pKa changes (Section 1.4.1). Sarmini and Kenndler have shown that the pKa of benzoic acids change by one or two units upon switching

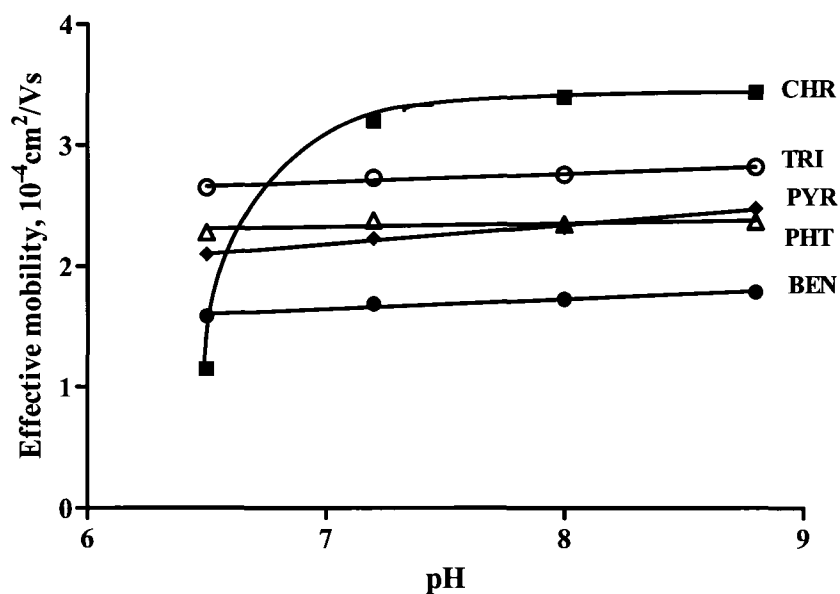


**Figure 3.2** Effect of pH on the effective mobilities of the probes at constant ionic strength. Conditions: I = 28 mM sodium phosphate buffer, 40% (v/v) MeOH, [CTAB] = 0.25 mM; neutral marker: 1.0 mM benzyl alcohol, detection at 214 nm, sample concentrations: 0.5 mM each of chromate (CHR), phthalate (PHT), trimellate (TRI), pyromellitate (PYR) and benzoate (BEN).

from an aqueous solution to 80% MeOH buffer [19]. Roses et al. also reported similar behavior of pKa changes of weak acids in buffers containing a variety of organic solvents [28-30]. Herein the influence of the degree of dissociation on mobilities of the probes was studied in MeOH/water buffer systems by measuring the effective mobility of the probes over pH values ranging from 6.5 to 9.0. The mobilities of these probes at various pH values in phosphate buffer containing 40% MeOH is given in Figure 3.2. To avoid buffer ionic strength changes with pH, the effective mobilities were determined at fixed ionic strength of 28 mM phosphate buffer. The effective mobility of chromate increases from  $1.0 \times 10^{-4} \text{ cm}^2/\text{Vs}$  to  $3.4 \times 10^{-4} \text{ cm}^2/\text{Vs}$  as the pH rises from 6.5 to 7.2 and then remains unchanged at higher pH. As shown in Figure 3.2, all the other acids show no significant changes over the pH range studied (6.5 to 9.0). The variations observed for these probes over the pH range 6.5 to 9.0 are less than 8%. Consequently, in the presence of up to 60% MeOH and at pH 8.0 where the measurements are made, all the probes are completely dissociated/ionized. Thus, the reduction in the effective mobilities of the probes upon methanol addition observed in Figure 3.1 is not caused by protonation of the probes.

Overall trimellitate and pyromellitate show the largest decrease in mobility with addition of methanol (Figure 3.1). This is consistent with the expectation that these highly charged probes (-3 and -4 charges respectively) would experience stronger dielectric friction and ionic strength effects than the lower charged ions [31]. From these results, chromate is the best choice as an indirect detection probe in mixed methanol-aqueous media, as it displays the highest mobility in all the buffers systems studied. Use of chromate ion also offers another advantage. It has high molar absorptivity at the

wavelengths of detection used ( $\epsilon \sim 3,900 \text{ L}\cdot\text{mol}^{-1}\cdot\text{cm}^{-1}$  at 214 nm and  $\epsilon \sim 2,640 \text{ L}\cdot\text{mol}^{-1}\cdot\text{cm}^{-1}$  at 254 nm) that gives rise to better detection sensitivity (eqn 1.14).

The next question is how good is chromate as a visualizing agent for small inorganic anions in mixed organic-water media? Figure 3.3 shows the electrophoretic mobility of a few representative inorganic anions relative to that of chromate. In aqueous solution, the mobility of chromate is comparable to that of the anions. This is why it has been the preferred probe for indirect detection of these ions in CE [7, 26]. Upon addition of methanol, however, the mobility of chromate is affected more dramatically than the mobilities of the anions. Hence, the relative mobilities of the anions increase as more methanol is added. At 50% MeOH, the mobilities of chloride and bromide are about 1.5 times that of chromate. Thus, even though chromate is the fastest migrating probe in

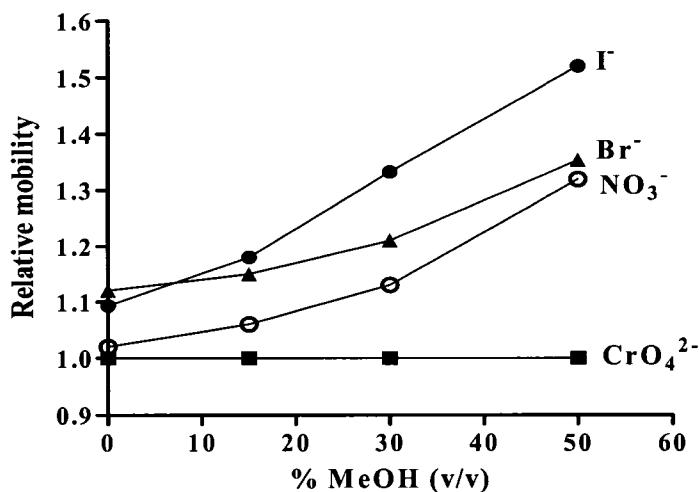


**Figure 3.3** Comparison of mobility of selected anions with chromate at different percent methanol. Experimental conditions:  $V = -15 \text{ kV}$ , 15 mM phosphate buffer at pH 8.0; detection at 214 nm.



methanol/water media (Figure 3.1) compared to the carboxylate ions, its low mobility relative to the inorganic anions (and the resultant electrodispersion) may limit indirect CE to buffers containing less than 40% MeOH.

### 3.3.2 Selectivity Changes in Mixed Organic-Water Buffers

The effect of methanol on mobility of small inorganic anions was examined under indirect detection conditions using a 5.0 mM chromate buffer at pH 8.0. Separations were performed in the co-EOF mode by addition of 0.25 mM CTAC to the run buffer. The migration time of the water peak was used to calculate the effective electrophoretic mobility of the anions by applying eqn 1.11. Figure 3.4 shows the electrophoretic mobilities of the anions studied at different concentrations of methanol in the run buffer. In the presence of organic solvents, all the ions exhibit lower mobility than in aqueous solutions. The ratio of the dielectric constant to the viscosity ( $\epsilon/\eta$ ) is one of the important parameters determining the mobility of an ion in different solvent systems, as indicated in Sections 2.3.2 and 3.3.1. For methanol/water mixture this value first decreases and reaches a minimum at about 45% MeOH and there after increases slightly. This  $\epsilon/\eta$  change would partly explain why the mobilities of all the anions decrease up to 60% MeOH.

However, as shown in Figure 3.4a, the sulfate ion displays a more significant decrease in mobility when the buffer is changed from pure aqueous to 40% MeOH buffer. Sulfate is the fastest migrating anion in aqueous solution but the slowest migrating in 40% MeOH methanol. Rapid separations (< 2.5 min) with good resolution are also achieved. Chloride and sulfate ions have the highest mobility and co-migrate in aqueous solution but are well separated in 40% MeOH. Iodide and chloride are resolved

in aqueous solutions but their separation is compromised in 40% MeOH. An optimum condition for the separation of these four anions is 5 mM chromate with 30% MeOH and 0.25 mM CTAB. Figure 3.4b shows the changes in mobility of a second set of anions versus changes in percent methanol. Here also significant selectivity changes are observed. The migration order in 10% MeOH buffer is  $\text{Cl}^- > \text{Br}^- > \text{I}^- > \text{F}^- > \text{ClO}_4^-$ , while in 30% MeOH the order is  $\text{Cl}^- \sim \text{I}^- > \text{Br}^- > \text{ClO}_4^- > \text{F}^-$ . The electropherograms in Figure 3.5 show the separation of six different anions using 5 mM chromate in the presence of 0.25 mM CTAC surfactant. Significant changes in mobilities among the anions are observed for small changes in the amounts of under these conditions. The efficiency of the peaks was calculated using the technique described in Section 3.2.4. Theoretical plate number ( $N$ ), ranging from 112,000 to 250,000 plates/m are achieved for the separations shown in Figure 3.5. The occurrence and position of system peaks is of major concern in indirect detection because this peak will interfere with the detection of surrounding peaks. In 10% MeOH the system peak (SP) is close to the fluoride peak, and interferes with the detection of fluoride. However, the system peak is well removed from the analyte peaks in 30% MeOH, and thus does not affect detection of the analyte ions.

In CE the electrolyte is buffered to provide pH stability and separation reproducibility [32]. This can be accomplished by the addition of a co-anion buffer such as borate and phosphate [33] to the BGE. However, with indirect CE detection any additional co-ion present will compete with the probe and cause both the occurrence of additional system peaks and a reduction in detection sensitivity [34]. Based on experimental and simulation results, Doble and Haddad suggested that when  $n$  UV absorbing co-anions are present in the BGE,  $n - 1$  system peaks would be generated [35].

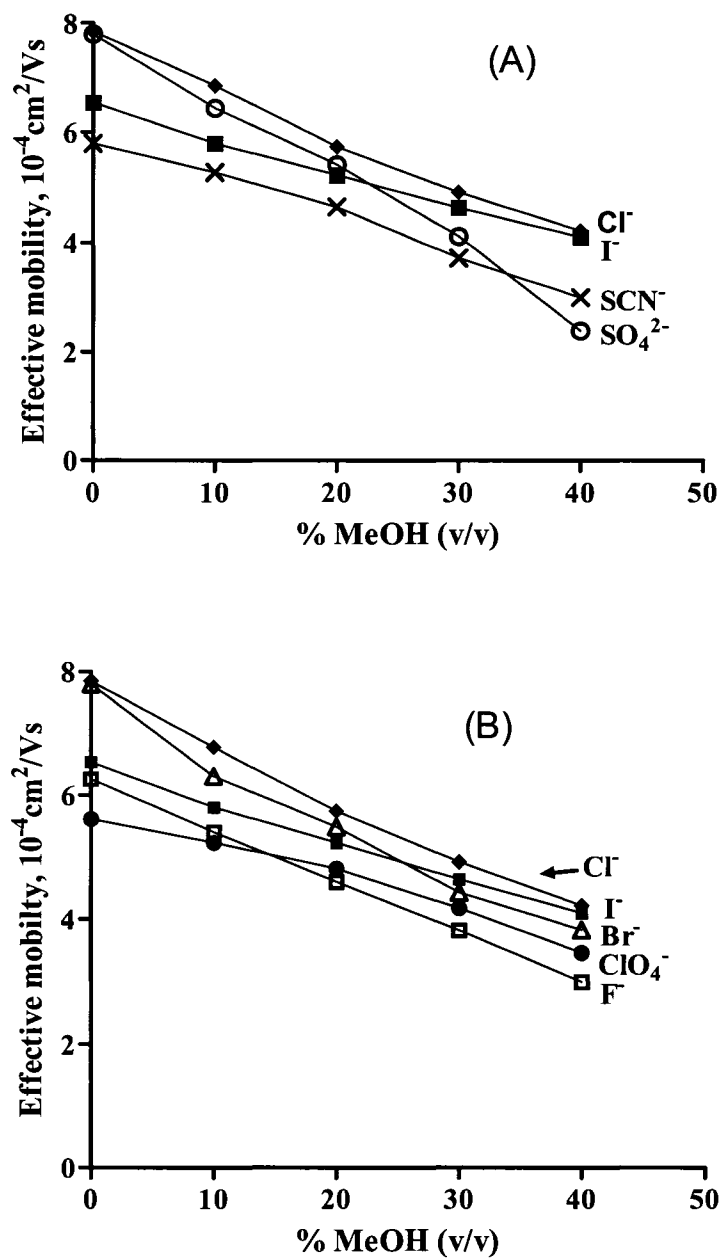


**Figure 3.4** Selectivity changes of anions with percent methanol. Conditions: 5 mM chromate, 0.25 mM CTAC; pH = 8.0 and indirect detection at 254 nm.  $\text{Cl}^-$  ( $\blacklozenge$ ),  $\text{SO}_4^{2-}$  ( $\circ$ ),  $\text{I}^-$  ( $\blacksquare$ ),  $\text{SCN}^-$  ( $\times$ ),  $\text{Br}^-$  ( $\Delta$ ),  $\text{F}^-$  ( $\square$ ),  $\text{ClO}_4^-$  ( $\bullet$ ).

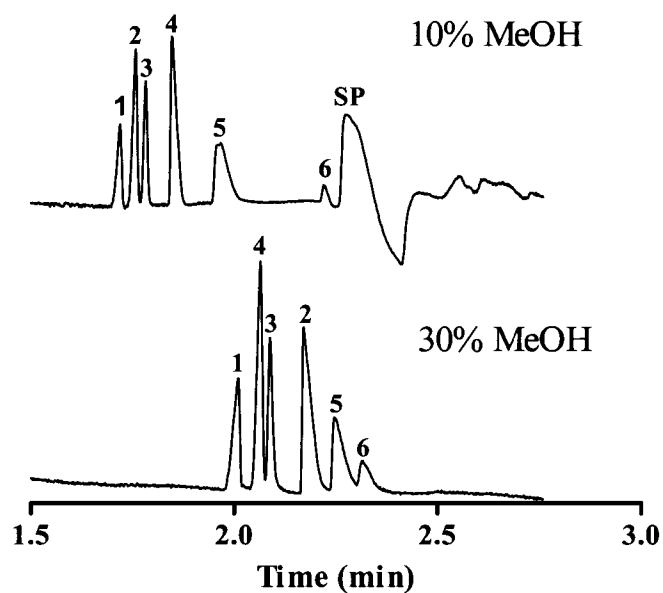


**Figure 3.5** Co-electroosmotic separation of six anions with buffer containing 0.25 mM CTAC , 5.0 mM chromate;  $V = -15$  kV and indirect UV detection at 254 nm. Peaks: 1)  $\text{Cl}^-$  2)  $\text{SO}_4^{2-}$  3)  $\text{NO}_3^-$  4)  $\text{I}^-$  5)  $\text{ClO}_4^-$  6)  $\text{F}^-$  . SP: systematic peak

Hence, to avoid complications associated with system peaks for the separations performed herein, we used only one co-ion in the electrolyte, namely the probe itself. However, this does leave the background electrolyte with limited buffering capacity. As a result, the background disturbances increased over a number of runs and the buffers were observed to become cloudy after four runs. Therefore, in all further studies the inlet and outlet buffer reservoirs were replaced after four runs.

As shown in Figure 3.4, the inorganic anions show significantly different mobility behaviors in mixed methanol/water buffer than in aqueous solutions. In addition to the changes in the viscosity and dielectric constant, the solvated radius of ions will be affected by the presence of organic solvents due to changes in the solvation behavior of the medium. There are two limiting theoretical views of the influence of solvation on ion mobility: the solvent-berg model and dielectric friction. In the solvent-berg approach, addition of organic solvents is viewed to change the selectivity by altering the solvated radii of the ions. However, this parameter is difficult to measure and there are hardly any reports on the solvated radii of small inorganic anions in these solvent systems. Recently, Descroix et al. used Density Functional Theory (DFT) coupled with a polarizable continuum model to predict solvated radii of a few inorganic anions in water and methanol [36]. In water, the predicted values agree with the experimental behavior but the model failed to predict the correct mobility order in pure methanol.

In a different but related model, the solvation phenomena have been explained in terms of changes in the frictional forces acting on the ions [37]. Roy and Lucy have shown that dielectric friction can be an important factor affecting the mobility of ions particularly in nonaqueous solvents in addition to the hydrodynamic friction [31, 38]. They found that the Hubbard-Onsager (HO) dielectric friction model is successful at predicting solvent-induced selectivity changes in alcohol–water and acetonitrile–water media [39, 40]. The HO model treats ion-solvent interactions as a dynamic perturbation of the solvent orientation caused by the ion's charge and size. Thus, dielectric friction can be considered as a charge-induced friction resulting from the finite relaxation time of the solvent dipoles surrounding the ion. The viscosity, dielectric constant, and relaxation

time for methanol are 0.55 cP, 32.7, and 53 ps [31, 38]. For water, these values are 0.89 cP, 78.4, and 10 ps respectively. Hence, the dielectric friction in solvent systems with lower dielectric constant and higher relaxation time becomes more important as the charge density on the ion increases. This indicates that the contribution of the dielectric friction would be much stronger in methanol than in water.

As shown from the results in Figure 3.4 the mobility of doubly charged sulfate decreased more significantly than the singly charged anions as the amount of MeOH increased from 0 to 40% v/v. This is consistent with the predictions that the contribution of dielectric friction for the halide ions would be smaller, as these ions possess only a single charge [37]. For similarly charged ions, the HO model predicts a direct dependence of dielectric friction on ion size and solvent composition. Smaller ions will experience higher frictional forces. Ibuki and Nakaraha [41] observed an increase in the residual frictional coefficient in the order  $I^- < Br^- < Cl^-$  in methanol. This is similar to the changes observed in Figures 3.4 and 3.5, where the mobility of iodide increases relative to chloride and bromide as the methanol concentration is increased. However, the selectivity changes amongst the other singly charged ions are modest since these ions do not display large differences in size.

### **3.3.3 Effect of Type of the Background Carrier Electrolyte**

Based on the mobility match results obtained in Figure 3.2, we were interested to explore further if iodide could be used as a probe rather than chromate. Iodide's mobility remains comparable to that of the other inorganic anions in the presence of methanol, and has the strongest molar absorptivity at 214 nm [42, 43]. Hence, concentrations of KI

**Table 3.2** Comparison of theoretical plate numbers obtained in 5 mM chromate and 3 mM iodide carrier electrolytes in the presence of 30% MeOH at 214 nm.

Anion	5 mM Chromate	3 mM Iodide
Cl <sup>-</sup>	200,000	280,000
Br <sup>-</sup>	150,000	176,000
NO <sub>3</sub> <sup>-</sup>	250,000	166,000
SO <sub>4</sub> <sup>2-</sup>	210,000	167,000
ClO <sub>4</sub> <sup>-</sup>	112,000	78,000

ranging from 2 to 7 mM were investigated as carrier electrolyte for indirect detection of the other anions (Cl<sup>-</sup>, NO<sub>3</sub><sup>-</sup>, SO<sub>4</sub><sup>2-</sup>, Br<sup>-</sup>, ClO<sub>4</sub><sup>-</sup>) at 214 nm. At higher concentrations (> 7 mM), the iodide forms a precipitate with the EOF modifier (CTAC). Separation efficiencies of 176,000 and 280,000 plates/m respectively are obtained for Br<sup>-</sup> and Cl<sup>-</sup> in buffer containing 30% MeOH and 3 mM KI. These efficiencies are better than those obtained using chromate buffer in Figure 3.5 (112,000 to 250,000 plates/m). A comparison of efficiencies obtained in chromate and iodide background electrolytes is presented in Table 3.2. The better efficiency for the fast moving anions in the iodide electrolyte emanates from the better mobility match between the probe and the analyte ions. Unfortunately, iodide yields poor detection sensitivity at 214 nm. This is mainly due to two reasons. First, some of the anions exhibit strong UV absorbance at 214 nm, which offsets the decrease in absorbance caused by displacement of the iodide probe. As a result, non-UV absorbing anions such as Cl<sup>-</sup> and SO<sub>4</sub><sup>2-</sup> display good detection sensitivities, whereas the UV absorbing anions such as Br<sup>-</sup> and NO<sub>3</sub><sup>-</sup> show poor

sensitivities. Secondly, the poor detection sensitivity is also due to high background absorbance at 214 nm caused by the presence of high methanol concentration.

### 3.3.4 Influence of Concentration of Background Electrolyte

The effect of increasing the concentration of chromate on the separation selectivity of anions was also investigated. Chromate concentrations ranging from 2–12 mM were used as BGE and effective mobilities of each anion were determined at each buffer concentration. Increasing the ionic strength of the BGE to more than 12 mM resulted in Joule heating, as evidenced by a noisier baseline and a reduction in separation efficiency.

Li et al. [6] have shown that Pitts equation can be used to describe the influence of ionic strength on mobility of singly and multiply charged organic anions as discussed in Section 1.4.2. For 1:1 electrolyte system the mobility dependence in the Pitts treatment is expressed in a general form as [44]:

$$\mu_{eff} = \mu_0 - Az \frac{\sqrt{I}}{1 + Ba\sqrt{I}} \quad (1.19)$$

where  $z$  is the charge on the analyte ion,  $A$  and  $Ba$  are constants.  $A$  encompasses terms including the electrophoretic effect and relaxation effect. The assumptions used to derive the Pitts equation are analogous to those in the Debye-Huckel extended law for ionic activity (eqn 1.19). Both equations predict that the impact of changes in the ionic strength of the buffer is directly related to the charge on the ion. As a result, anions of same charge are affected similarly by ionic strength, while the mobility of multiply charged ions are more significantly affected by the ionic strength than singly charged ions [6]. The behavior of the univalent anions would be expected to follow the Pitts equation, and so changes in ionic strength would not be expected to significantly alter the



relative mobility of these anions [6]. Theoretically, a decrease in mobility of about 13% is expected for singly charged anions over the buffer concentration range 2 to 12 mM. The influence of chromate concentration on selectivity in a BGE containing 0.25 mM CTAC at pH 8.0 is shown in Figure 3.6. The results show that the mobilities of the anions decrease with increasing chromate concentration. However, the extent of mobility changes varies among the anions. The mobilities of bromide and nitrates change by about 11%, in agreement with the theoretical predictions given in eqn 1.20. The mobility of fluoride, however, decreases most dramatically, from  $6.23 \times 10^{-4} \text{ cm}^2/\text{Vs}$  to  $4.90 \times 10^{-4} \text{ cm}^2/\text{Vs}$  over the same buffer concentration range used. This change is more than expected and we have no explanation for the cause of such strong ionic strength effect on fluoride.

In contrast, thiocyanate, perchlorate and iodide exhibit only minor changes in mobility (less than predicted) as a function of the chromate concentration. The changes in mobility observed for these anions are less than 7%. This shows that there are factors other than ionic strength that contribute to the observed mobility changes. Since the mobilities are determined in the presence of 0.25 mM CTAC, interactions of the anions with CTAC could be an additional factor for the observed mobilities. It has been shown that large and polarizable anions such as thiocyanate and iodide have a greater tendency to interact with cationic surfactants in aqueous solution through ion pairing [17, 18, 45]. The chromate anion used as the background electrolyte also competes with analytes for the positive sites on the surfactants. Introduction of more chromate ions displaces the iodide and thiocyanate from their ion-pair form with CTAC. This yields ionic species of increased effective charge, which will migrate faster, resulting in the mobility behavior

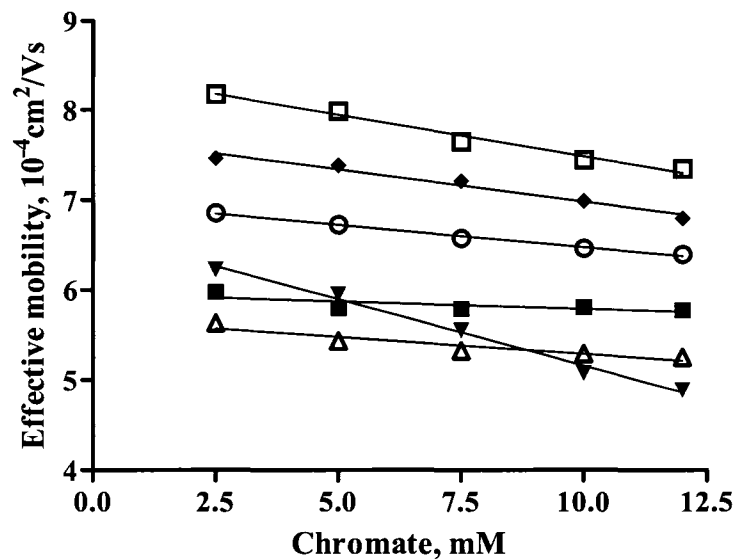


**Figure 3.6** Effect of concentration of chromate on mobility of inorganic anions in aqueous solutions. All other experimental conditions as shown in Figure 5. Br<sup>-</sup> (□), NO<sub>3</sub><sup>-</sup> (◆), I<sup>-</sup> (○), SCN<sup>-</sup> (■), ClO<sub>4</sub><sup>-</sup> (Δ), F<sup>-</sup> (▼).

observed in Figure 3.6. To see the contribution of such electrostatic interaction on the observed mobility of the anions, we have also examined ion-association of selected anions with the surfactant, as will be discussed in Section 3.3.5. Regardless, the behavior of the univalent anions would be expected to follow the Pitts equation, and so changes in ionic strength alone would not significantly alter relative mobility of these anions except fluoride.

### 3.3.5 Ion Association with the Surfactant in MeOH/Water Buffers

In addition to reversing the EOF, the cationic surfactant might also influence the anion mobility through ion pairing or ion association [18, 45, 46]. This would lead to a decrease in the effective mobility of the anion. In this study, ion association of the anions with the surfactant molecules or micelles is examined by analyzing the change in the electrophoretic mobility of the anions as the surfactant concentration is varied. Assuming a 1:1 combination of the anion,  $X^-$ , with the surfactant,  $CTA^+$ , the association equilibrium can be described as:



where  $K_{ass}$  is the ion association or ion-pairing constant. Since the ion-pair is neutral, it would migrate with the EOF. Hence the net migration of the anion only comes from the fraction of the anion that is not associated or has not formed ion pairs with the surfactants. This fraction ( $\alpha$ ) is derived from the equilibrium expression in eqn 3.4 as:

$$\alpha_{X^-} = \frac{[X^-]}{[X^-] + [CTA^+X^-]} = \frac{1}{1 + K_{ass}[CTA^+]} \quad (3.5)$$

where  $\alpha_{X^-}$  is the fraction of free anion unbound or unpaired with the surfactant, and  $[CTA^+]$  is the concentration of surfactant which is equal to the total surfactant concentration in the buffer. The electrophoretic mobility of the analyte anion ( $\mu_e$ ) is then given by:

$$\mu_e = \alpha_{X^-} \mu_{X^-} = \frac{\mu_{X^-}}{1 + K_{ass}[CTA^+]} \quad (3.6)$$

where  $\mu_{X^-}$  is the electrophoretic mobility of the free anion (i.e. in the absence of surfactant), and  $\mu_e$  is the electrophoretic mobility of the anion in the presence of the surfactant. Eqn 3.6 can be rewritten as:

$$\frac{\mu_{X^-}}{\mu_e} = 1 + K_{ass}[CTA^+] \quad (3.7)$$

A plot of the term on the left side of eqn 3.7 (measured experimentally) versus the total concentration of surfactant yields a straight line with slope equal to the ion-association constant ( $K_{ass}$ ). With such technique, association constants for bromide and iodide were determined in pure aqueous and 40% MeOH buffer solutions. A plot of  $1/\mu_{eff}$  versus the CTAC concentration for bromide and iodide ions in 5 mM chromate solutions (pH 8.0) is shown in Figure 3.7.

In aqueous solutions, both ions show binding, with iodide displaying slightly stronger interactions with the surfactant. Ion association constants calculated for bromide and iodide in aqueous solutions are  $73 \pm 3$  and  $301 \pm 4 \text{ Lmol}^{-1}$  respectively. This behavior is consistent with the selectivity trends observed with ion-exchange chromatography [47]. This retention phenomenon is associated with the interactions between the anions and the aqueous media. The disruption of the local water by the anions structure results in tight binding of surrounding water molecules with one another and in a decrease in entropy; this unfavorable situation enhances the formation of ion pairs [48]. However, large polarizable ions such as iodide orient water molecules with difficulty because of their low charge density. Hence, because of the strong interaction with the  $CTA^+$ , the iodide peak in the electropherogram is also tailed particularly when high concentrations of surfactant are used. Similar tailed peaks have been reported in the literature [45, 49]. This is because interactions with the dynamically coated surfactant

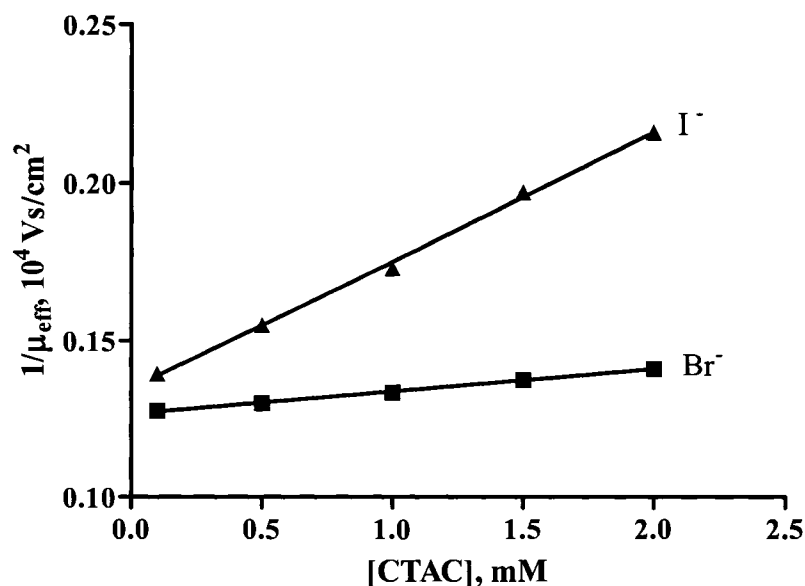


**Figure 3.7** Dependence of the reciprocal of the effective mobility bromide and iodide on the concentration of CTAC. Experimental conditions: 1.0 mM of each ion sample and 5.0 mM chromate aqueous buffer at pH 8.0. All other conditions as shown in Figure 3.5.

layers on the capillary wall would cause tailed peaks due to resistance to mass transfer of the anions to and from the surface to the bulk solution. Thus, in aqueous solutions interaction of the anions with the surfactant could contribute for the reduction in the mobility of the anion and sometimes could lead to the loss of efficiency. Use of 0.25 mM CTAC in aqueous solutions causes the mobility of iodide to decrease by about 7% through ion association.

In contrast, in 40% MeOH, the ion association constants for bromide and iodide are  $196 \pm 4 \text{ Lmol}^{-1}$  and  $125 \pm 3 \text{ Lmol}^{-1}$ , respectively. Iodide shows weaker binding with the surfactant in MeOH/water buffer than in the aqueous solution. This suppressed ion-exchange interaction of iodide with the surfactant in 40% MeOH leads to faster relative

mobility and the peak is more symmetrical. The efficiency of iodide peak increases from 112,000 plates/m in aqueous solution to more than 240,000 plates/m in 40% MeOH.

While the ion association for iodide decreases, bromide shows stronger binding with the surfactant in MeOH/water buffer than the aqueous solution. This stronger ion interaction is displayed by a slight decrease in efficiency of the bromide peak from 187,000 to 160,000 plates/m. This is consistent with the fact that electrostatic ion pairing requires small, highly charged ions and occurs more readily in solvents of low dielectric constant [48]. Similar behaviors of enhanced ion-pairing of bromide with increase in methanol content have been observed in ion chromatography [50]. Hadded et al. also reported increase in retention times of inorganic and organic anions at higher concentrations of acetonitrile in water [51].

### **3.3.6 Quantification and Applications**

Quantification of the anions was examined using the optimal conditions of 0.25 mM CTAC, 30% v/v MeOH and 5 mM chromate (pH 8.0). Limits of detection were determined using a procedure based on the US Environmental Protection Agency (EPA) methodology [22], as described in Section 3.2.4. This approach determines the minimum amount of sample that can be reported to be greater than the background noise (blank run) with 99% confidence. Using the experimental conditions detailed in Section 3.2.4, all the quantitative analyses were performed using calibration curves generated for each anion. Then, replicate separations of a 2.50  $\mu\text{g}/\text{mL}$  sample of each anion (about 5–10 times the estimated detection limit) were performed. The standard deviation for these

**Table 3.3** Limits of detection and migration time and peak area reproducibilities <sup>a</sup>.

Anion	% RSD (n=8)		Linearity correlation ( $r^2$ )	LOD, $\mu\text{g/mL}$
	Migration time	Peak area		
Cl <sup>-</sup>	0.2	1.3	0.997	0.12
NO <sub>3</sub> <sup>-</sup>	0.5	1.5	0.984	0.20
SO <sub>4</sub> <sup>2-</sup>	0.5	1.8	0.993	0.14
ClO <sub>4</sub> <sup>-</sup>	0.6	2.1	0.996	0.23
F <sup>-</sup>	0.3	2.0	0.998	0.09

<sup>a</sup> Experimental conditions: 0.25 mM CTAC, 5.0 mM chromate, 30% MeOH, V= -15 kV and indirect UV detection at 254 nm.

replicate injections was determined and the detection limit is the standard deviation multiplied by the Student *t* value for one-sided 99% confidence interval.

Calibration curves of the anions show linear dynamic ranges from 0.1 – 10  $\mu\text{g/mL}$  with correlation coefficients equal to or greater than 0.984. Detection limits (Table 3.3) range from 0.09 to 0.23  $\mu\text{g/mL}$ , which are better or comparable to literature values in aqueous buffers [4, 51, 52]. To examine the run-to-run reproducibility, eight replicate measurements of a standard solution of 2.50  $\mu\text{g/mL}$  of each anion were performed. The percent relative standard deviations (%RSD) for peak areas are presented in Table 3.3 and range from 1.3 to 2.0%. Good reproducibility of migration times is also obtained (0.2 to 0.8 %). Another important advantage of this methanolic method is that it offers fast separation. The method is at least two times faster than standard IC method and other reported CE methods [52-54].

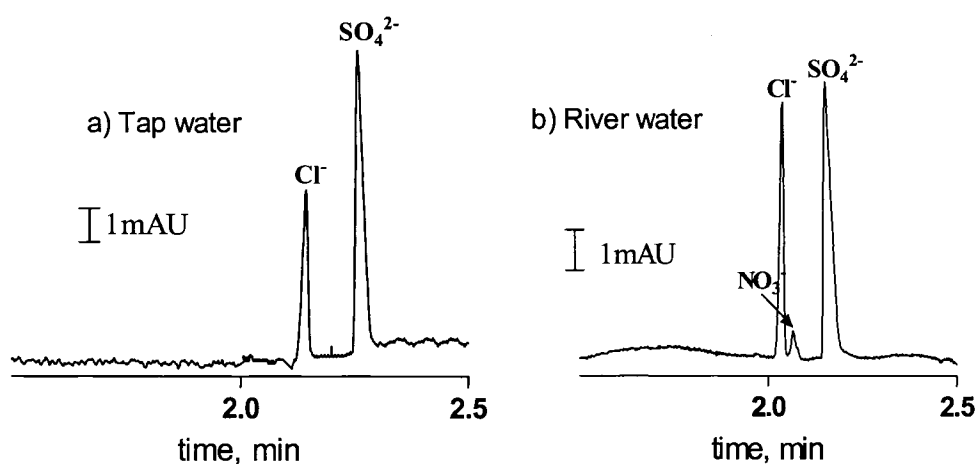


**Figure 3.8** Analysis of common inorganic anions in tap and river waters. All other experimental condition as indicated in Figure 3.5.

To evaluate the applicability of the separation technique for real samples, the method was applied to the analysis of anions in tap water from our lab and river water samples from the North Saskatchewan River (Edmonton, AB). The samples were diluted five times with de-mineralized water to bring the concentrations within the calibration range and filtered through 0.45  $\mu\text{m}$  membrane before injection. The peaks are identified by standard addition. An efficient separation and good detection sensitivity of the anions (chloride, nitrate, and sulfate) are obtained. Figure 3.8 shows the typical electropherograms for the river water (a) and tap water (b) sample solutions. The determination does not require any preliminary treatment of the samples and each sample was run in triplicates. The migration time reproducibility for each analyte ion was <1% RSD. Chloride and sulfate ion concentrations in the river water are found to be 28 and 35



mg/L. In tap water, the concentrations of these ions are 32 and 22 mg/L respectively. The ability to move peaks selectively using different percent of methanol demonstrates the flexibility of this technique. This method could also offer the ability to determine small quantities of nitrite, bromide, nitrate, chlorate, or iodide in samples containing high levels of sulfate and/or chloride ions. The proposed system is simple, rapid and reproducible to be useful for the analysis of natural water samples.

### **3.4 Concluding Remarks**

In CE analysis of small inorganic anions, the ability to control the EOF and to alter the electrophoretic mobility of the ions is essential to improve resolution and separation speed. This work demonstrates that indirect detection of small anions can be achieved using CTAC as EOF modifier in the presence of organic solvent. The organic solvent alters the electrophoretic mobility of the probes and the analytes differently and hence choosing of the appropriate probe is essential to achieve high degree of resolution and detection sensitivity. Chromate has the best mobility match with small inorganic anions under mixed MeOH/ water buffers. In addition, chromate also allows detection at a wavelength much greater than the absorption of most anions and methanol. Significant changes in selectivity among anions are observed by using up to 40% methanol in the running buffer. Good resolutions as well as separation speeds two times faster than standard ion chromatography techniques are achieved. The ability to move peaks selectively using different percent of methanol demonstrates the flexibility of this technique.

### 3.5 References

- [1] Benz, N. J., Fritz, J. S., *J. Chromatogr. A* 1994, 671, 437-443.
- [2] Harakuwe, A. H., Haddad, P. R., *J. Chromatogr. A* 1999, 834, 213-232.
- [3] Jandik, P., Bonn, G. *Capillary Electrophoresis of Small Molecules and Ions*; VCH: New York, 1993.
- [4] Buchberger, W., Haddad, P. R., *J. Chromatogr. A* 1992, 608, 59-64.
- [5] Harrold, M. P., Wojtusik, M. J., Riviello, J., Henson, P., *J. Chromatogr. A* 1993, 640, 463-471.
- [6] Li, D. M., Fu, S. L., Lucy, C. A., *Anal. Chem.* 1999, 71, 687-699.
- [7] Jones, W. R., Jandik, P., *J. Chromatogr.* 1991, 546, 445-458.
- [8] Melanson, J. E., Lucy, C. A., *J. Chromatogr. A* 2000, 884, 311-316.
- [9] Lucy, C. A., *J. Chromatogr. A* 1999, 850, 319-337.
- [10] Salimi-Moosavi, H., Cassidy, R. M., *Anal. Chem.* 1995, 67, 1067-1073.
- [11] Yeung, K. K.-C., Lucy, C. A., *Electrophoresis* 1999, 20, 2554-2559.
- [12] Johns, C., Macka, M., Haddad, P. R., *Electrophoresis* 2003, 24, 2150-2167.
- [13] Lucy, C. A., McDonald, T. L., *Anal. Chem.* 1995, 67, 1074-1078.
- [14] Masselter, S. M., Zemann, A. J., *Anal. Chem.* 1995, 67, 1047-1053.
- [15] Lucy, C. A., Underhill, R. S., *Anal. Chem.* 1996, 68, 300-305.
- [16] Preisler, J., Yeung, E. S., *Anal. Chem.* 1996, 68, 2885-2889.
- [17] Diress, A. G., Lucy, C. A., *J. Chromatogr. A* 2004, 1027, 185-191.
- [18] Zemann, A., Volgger, D., *Anal. Chem.* 1997, 69, 3243-3250.
- [19] Sarmini, K., Kenndler, E., *J. Chromatogr. A* 1998, 806, 325-335.
- [20] Soga, T., Ross, G. A., *J. Chromatogr. A* 1997, 767, 223-230.

- [21] Williams, B. A., Vigh, G., *Anal. Chem.* 1996, 68, 1174-1180.
- [22] Grant, C. L., Hewitt, A. D., Jenkins, T. F., *Am. Lab.* 1991, 23, 15-23.
- [23] Nielen, M. W. F., *J. Chromatogr.* 1991, 588, 321-326.
- [24] Poppe, H., *Anal. Chem.* 1992, 64, 1908-1919.
- [25] Kaniansky, D., Masar, M., Marak, J., Bodor, R., *J. Chromatogr. A* 1999, 834, 133-178.
- [26] Buchberger, W., Cousins, S. M., Haddad, P. R., *Trends Anal. Chem.* 1994, 13, 313-319.
- [27] Schwer, C., Kenndler, E., *Anal. Chem.* 1991, 63, 1801-1807.
- [28] Espinosa, S., Bosch, E., Roses, M., *Anal. Chem.* 2000, 72, 5193-5200.
- [29] Roses, M., *J. Chromatogr. A* 2004, 1037, 283-298.
- [30] Canals, I., Portal, J. A., Bosch, E., Roses, M., *Anal. Chem.* 2000, 72, 1802-1809.
- [31] Roy, K. I., Lucy, C. A., *Anal. Chem.* 2001, 73, 3854-3861.
- [32] Harakuwe, A. H., Haddad, P. R., *J. Chromatogr. A* 1996, 734, 416-421.
- [33] Shamsi, S. A., Danielson, N. D., *Anal. Chem.* 1995, 67, 1845-.
- [34] Gebauer, P., Borecka, P., Bocek, P., *Anal. Chem.* 1998, 70, 3397-3406.
- [35] Doble, P., Haddad, P. R., *Anal. Chem.* 1999, 71, 15-22.
- [36] Descroix, S., Varenne, A., Adamo, C., Gareil, P., *J. Chromatogr. A* 2004, 1032, 149-158.
- [37] Hubbard, J., Onsager, L., *J. Chem. Physics* 1977, 67, 4850-4857.
- [38] Roy, K. I., Lucy, C. A., *Electrophoresis* 2002, 23, 383-392.
- [39] Roy, K. I., Lucy, C. A., *Electrophoresis* 2003, 24, 370-379.
- [40] Roy, K. I., Lucy, C. A., *J. Chromatogr. A* 2002, 964, 213-225.

- [41] Ibuki, K., Nakahara, M., *J. Phys. Chem.* 1987, *91*, 1864-1867.
- [42] Guenther, E. A., Johnson, K. S., Coale, K. H., *Anal. Chem.* 2001, *73*, 3481-3487.
- [43] Gennaro, M. C., Bertolo, P. L., Cordero, A., *Anal. Chim. Acta* 1990, *239*, 203-209.
- [44] Pitts, E., Tabor, B. E., Daly, J., *Trans. Faraday Soc.* 1970, *66*, 693-707.
- [45] Woodland, M. A., Lucy, C. A., *Analyst* 2001, *126*, 28-32.
- [46] Kaneta, T., Tanaka, S., Taga, M., Yoshida, H., *Anal. Chem.* 1992, *64*, 798-801.
- [47] Haddad, P. R., Jackson, P. E. *Ion Chromatography: Principles and Applications*;  
Elsevier: Amsterdam, 1990.
- [48] Okada, T., *Anal. Chem.* 1988, *60*, 1511-1516.
- [49] Breadmore, M. C., Boyce, M., Macka, M., Avdalovic, N., Haddad, P. R., *J. Chromatogr. A* 2000, *892*, 303-313.
- [50] Dean, T. H., Jezorek, J. R., *J. Chromatogr. A* 2004, *1028*, 239-245.
- [51] Boyce, M. C., Breadmore, M., Macka, M., Doble, P., Haddad, P. R.,  
*Electrophoresis* 2000, *21*, 3073-3080.
- [52] Soga, T., Inoue, Y., Ross, G. A., *J. Chromatogr. A* 1995, *718*, 421.
- [53] Carou, M. I. T., Mahia, P. L., Lorenzo, S. M., Fernandez, E. F., Rodriguez, D. P., *J. Chromatogr. A* 2001, *918*, 411-421.
- [54] Kuban, P., Kuban, P., Kuban, V., *J. Chromatogr. A* 1999, *848*, 545-551.

## **CHAPTER FOUR: Semi-Permanent Capillary Coatings in Organic-Water Solvents for Capillary Electrophoresis**

### **4.1 Introduction**

Control of the electroosmotic flow (EOF) has attracted growing attention because of its importance for the separation of analytes in capillary electrophoresis (CE). In bare fused silica capillaries, the repeatability of the EOF can be very poor from run-to-run and between different capillaries, decreasing the reliability of capillary electrophoretic analyses. As a result, various techniques have been devised to control the EOF (Section 1.4). The most common and the easiest means to control the EOF have been to change the composition of the background electrolyte (BGE). For instance, altering the pH, changing the ionic strength, or by applying different buffer additives all can be used to alter the EOF. However, changing the BGE composition alone does not necessarily improve the repeatability of the EOF [1, 2]. The EOF can also be affected by applying external radial electric fields [3]. This method is less frequently used, as it requires a special type of instrumental setup.

One of the most plausible and practical approaches to controlling the EOF has been to modify the charge on the capillary surface through capillary wall coatings. By the use of an appropriate capillary coating, the EOF can be enhanced, reduced or reversed for the optimization of analysis time, resolution and efficiency. In addition, EOF modification is generally associated with efforts to minimize or eliminate analyte adsorptions to the silica capillary. Both permanent and dynamic wall coatings are commonly used for EOF control in CE as discussed in Sections 1.4.2 and 1.4.3. Excellent reviews on the area are also available in the literature [1, 4, 5].

For analysis of anionic species in CE, the EOF is typically reversed by the addition of cationic additives such as polymers or surfactants in the run buffer. Using this approach anionic compounds migrate co-electroosmotically, and thus rapid analysis of anions can be achieved. However, in most applications, the EOF modifier has to be kept in the run buffer to maintain the stability of the coatings and hence the EOF [6-8]. The problem with this approach is the modifier adds an ion exchange mechanism to the CE separation (Sections 2.3.5 and 3.3.2) which increases the complexity and compromises the efficiency of the separation. Recently, it has been shown that two tailed cationic surfactants such as didodecyldimethylammonium bromide (DDAB) form semi-permanent bilayer coatings, which allow separations to be performed without the EOF modifier in the run buffer [9, 10]. The stability of these coatings is attributed to the formation of bilayer coatings.

However, most of the capillary modifications in CE have been developed for use in aqueous buffers. Although organic solvents are increasingly used in CE, only limited work has been done to develop stable capillary coatings in mixed organic-water buffers or pure organic solvents. As discussed in Section 1.4.4, organic solvents used as either additives or as pure solvents in BGE improve the analytes solubility, Joule heating, detection capability with MS and more importantly can offer completely new electrophoretic selectivity in CE. Furthermore, the addition of organic solvents to the BGE in aqueous co-electroosmotic CE is advantageous to reduce hydrophobic and electrostatic interactions of anionic analytes with the EOF modifiers and thus adsorption at the modified capillary wall [6]. Hence, coated capillaries can be advantageous in many

capillary electrophoretic applications where nonaqueous background electrolytes are employed.

Belder et al. [11, 12] have investigated capillaries coated with polyethylene glycol (PEG) and polyvinyl alcohol (PVA) in pure methanol and acetonitrile buffers with a special emphasis on the influence of pH. Hassel and Steiner [13] have reported the influence of covalent modifications on the EOF with hydrophobic polymers in various organic solvents including MeOH, acetonitrile, *N*-methylformamide, and dimethyl sulfoxide. Esaka et al. have also separated benzoic acids in polydimethylsiloxane-coated capillaries using PEG [14] and polyacrylamide [15] as additives in acetonitrile. All of these coating techniques are based on covalent bonding of the coating to the surface. As a result, these coatings are usually stable only in a restricted pH range and their preparations are often based on a multi-step process that causes a large degree of variation between capillaries. For instance, the polymeric coating procedure employed by Hassel and Steiner takes more than 30 hrs of preparations and the EOF fluctuations ranges from 15-20% RSD [13].

On the other hand, modifications by non-covalent bonding such as dynamic coating offers advantages in its simple procedure and good reproducibilities (Section 1.4.3.3). Thus, it would be ideal if a stable and reproducible coating could be achieved using a simple dynamic procedure for nonaqueous CE. Gallaher and Johnson [16] reported a combination of a dynamic and a permanent coating procedures for the separation of positively derivatized fatty acids in MeOH. Hexadimethrine bromide (HDB) has also been used as dynamic coating material in nonaqueous BGEs [17, 18]. Recently Porras et al. [19] used a dynamic polymer coating in nonaqueous medium

(methanolic buffers) and Vayaboury et al. [20] explored the utility of noncovalent coating using adsorption of polyethylene oxide (PEO) and cationic polyelectrolytes. However, the precondition and preparation times for these procedures were long (>8 hrs).

This chapter describes new bilayer capillary coating techniques based on long double-chain surfactants. The resultant coatings are compatible with various organic solvents mixed in water buffers. The coating procedure involves a simple hydrodynamic rinse (<5 min) of the capillary with the surfactant solution. The excess surfactant is then flushed from the capillary. The resultant bilayer coatings are stable for days in buffers that contain up to 60% nonaqueous solvents. Compared to other types of capillary modifications, these coatings are simple, versatile and inexpensive. Factors that affect the stability of the bilayer coatings such as buffer ionic strength, pH, type and amount of organic solvent will be discussed. The utility of this approach for separation of small anions and basic analytes will also be illustrated.

## **4.2 Experimental**

### **4.2.1 Apparatus**

All capillary electrophoresis experiments were performed on a HP-3D CE instrument (Agilent Technologies, Palo Alto, CA, USA) equipped with an on-column diode array UV absorbance detector. Data acquisition and control were performed using ChemStation software (HP<sup>3D</sup>, Agilent Technologies) on an HP personal computer. Untreated fused silica capillaries (Polymicro Technologies, Phoenix, AZ,) with an inner diameter of 50  $\mu\text{m}$ , an outer diameter of 365  $\mu\text{m}$ , and a total length of 37 cm (effective length of 28.5 cm to the detector) were used unless otherwise specified. The polyimide coating at the detection window was removed by burning with a loop of nichrome wire.



In addition, about 10 mm of polyimide was removed from both ends of the capillary. The latter was done to avoid capillary blockage due to swelling of the polyimide coating in organic solvents [21]. In all of the experiments, the capillary cassette was thermostatted at 25.0 °C with forced air-cooling.

#### 4.2.2 Chemical and Reagents

All solutions were prepared with ultrapure (18-M $\Omega$ ) water (Barnstead, Chicago, IL). The chemicals were all reagent grade or better, and were used without further purification. Buffers were prepared from sodium salts of orthophosphate (BDH, Darmstadt, Germany), and HPLC-grade methanol (MeOH; Fisher, Fair Lawn, USA), HPLC-grade acetonitrile (ACN; Fisher), anhydrous ethanol (EtOH; Fisher), ACS certified 2-propanol (2-PrOH; Fisher) or 1-butanol (1-BuOH; BDH). The cationic surfactants didodecyldimethylammonium bromide (abbr. as DDAB or 2C<sub>12</sub>DAB), dimethylditetradecylammonium bromide (2C<sub>14</sub>DAB), dihexadecyldimethylammonium bromide (DHDAB or 2C<sub>16</sub>DAB), and dimethyldioctadecylammonium bromide (DODAB or 2C<sub>18</sub>DAB) were used as received from Aldrich (Milwaukee, WI, USA). The 2C<sub>14</sub>DAB, 2C<sub>16</sub>DAB, and 2C<sub>18</sub>DAB are only slightly soluble in water. Thus, the surfactant solutions were prepared by sonication of the buffer-surfactant mixture at a temperature well above the chain melting temperature (see Table 4.1) for 30 min. Then the solution was allowed to cool at room temperature (23 °C) with stirring for 15 min. This sonication/stirring cycle was repeated until a clear solution was obtained. The pH of BGE was measured using a Model 445 digital pH meter (Corning, Acton, USA) calibrated with aqueous standards immediately prior to use. The pH was adjusted using sodium hydroxide (BDH) before the required amount of organic solvent was added.

Mesityl oxide (Aldrich) solution was used as the neutral EOF marker at a concentration of 1 mM. It has been shown in previous studies by our group that mesityl oxide is an appropriate EOF marker for buffers containing low concentrations of surfactants [22]. The drug samples, propranolol (1-[(1-methylethyl) amino]-3-(1-naphthalenyloxy)-2-propanol) and metoprolol (1-[4-(2-methoxyethyl)-phenoxy]-3-[(1-methylethyl)amino]-2-propanol) (Figure 4.1) were obtained as a gift from Pars Minoos Pharmaceutical Company (Tehran, Iran) and were with purity of >99.98%.

#### 4.2.3 Capillary Coating Protocol and EOF Measurements

Fresh capillaries were used with each new buffer system to avoid memory effects. Before the coating, the new capillaries were rinsed under high pressure (93.8 kPa) with 1 M NaOH for 10 min and then with distilled water for 5 min. After the preconditioning steps, the capillary was rinsed at high pressure for 5 min with surfactant solution (0.1 mM) to coat the capillary. Then the excess surfactant was flushed out from the capillary and the neutral marker, (1 mM mesityl oxide in water) was injected into the capillary using hydrodynamic injection for 2 s at 5.0 kPa. The electroosmotic flow ( $\mu_{eo}$ ) was calculated using the relation:

$$\mu_{eo} = \frac{L_t L_d}{t_{eo} V} \quad (4.1)$$

where  $L_t$  and  $L_d$  are the total length of the capillary (37.0 cm) and the capillary length to the detector (28.5 cm), respectively,  $t_{eo}$  is the migration time of the neutral EOF marker (in seconds), and  $V$  is the applied voltage (in volts). All voltages used herein were experimentally verified to be within the linear region of the Ohm's plot so that no Joule heating effect was present in any of the electrophoretic separations. In all experiments, the EOF values were the average of three measurements.

#### 4.2.4 Coating Stability Studies

The stability of the surfactant coatings was monitored by measuring the EOF as a function of successive hydrodynamic rinsing times [23]. In this method, the preconditioned capillary was first coated by rinsing (5 min at 93.8 kPa) with surfactant solution. Then the excess surfactant was removed by flushing the capillary with the electrophoretic buffer (in the absence of surfactant) for an initial period of 3 min. A neutral marker (mesityl oxide) was injected and the EOF was measured as described above. The coating was then regenerated first by flushing with 1 M NaOH (5 min at 93.8 kPa), followed by distilled H<sub>2</sub>O for 5 min at 93.8 kPa and then with 0.1 mM surfactant solution for 5 min at 93.8 kPa. Then, the capillary was subjected to a longer rinsing time with the electrophoretic buffer (e.g. 1 min) and the EOF was again determined as described above. This process was successively repeated for rinsing times up to 30 min. The stability of the coating was then evaluated by plotting the values of EOF obtained versus the high pressure rinsing times.

#### 4.2.5 Preparation and Separation of Inorganic Anions

Samples containing 0.2 mM of each of the inorganic anions (NO<sub>2</sub><sup>-</sup>, NO<sub>3</sub><sup>-</sup>, Br<sup>-</sup>, I<sup>-</sup>, Cl<sup>-</sup>, SO<sub>4</sub><sup>2-</sup>, F<sup>-</sup>, ClO<sub>4</sub><sup>-</sup>, and SCN<sup>-</sup>) were prepared from standard stock solutions. For anion separations a fresh capillary was first flushed under a high-pressure rinse (93.8 kPa) with 1 M NaOH for 10 min, followed by rinsing with water for 5 min at 93.8 kPa. The coating procedure for the capillary consisted of a 5 min rinse with 0.1 mM 2C<sub>18</sub>DAB solution, followed by a 3 min rinse (93.8 kPa) with the electrophoretic buffer to remove the excess surfactant from the capillary. Sample was injected hydrodynamically for 2.0 s at 5.0 kPa. An applied potential of -20 kV was used in all separations unless otherwise stated and

anions were detected using the direct UV mode at 214 nm. Standard addition of each anion was applied to confirm the identity of each peak. The effective mobilities of the anions were calculated from the migration times under constant voltage conditions as shown in eqn 1.11. The efficiency was evaluated using the peak width at half-maximum height method as shown in Section 3.2.4:

$$N = 5.54 \left( \frac{t_m}{W_{1/2}} \right)^2 \quad (4.2)$$

where  $N$  is the number of theoretical plates,  $t_m$  is analyte migration time and  $W_{1/2}$  is width of the peak at half-peak height.

#### 4.2.6 Separation of Basic Drugs

A 5.0 mM stock solution of the drug samples, propranolol and metoprolol, were prepared in Nanopure water and stored in the fridge at +6 °C. The final sample solutions were prepared from the stock solutions by diluting to a concentration of 0.2 mM with the run buffer. The sample solutions were manually filtered through a 0.2 µm polypropylene membrane filter (Whatman) prior to injection. For the drug separations, a fresh capillary was flushed first with 1 M NaOH for 15 min at 93.8 kPa, followed by water for 5 min at 93.8 kPa. Then the capillary was coated by rinsing with 0.1 mM 2C<sub>18</sub>DAB solution followed by 3 min rinse at 93.8 kPa with the electrophoretic buffer to remove the excess surfactant from the capillary. A mixture of the drug sample (0.2 mM) was injected for 1.0 s at 5.0 kPa and separated in a sodium phosphate buffer (20 mM) at pH 3.0 using applied voltage of -20 kV. Detection for the drugs was performed using the direct UV mode at 220 nm. The efficiencies were computed using the width at half height method (eqn. 4.2).

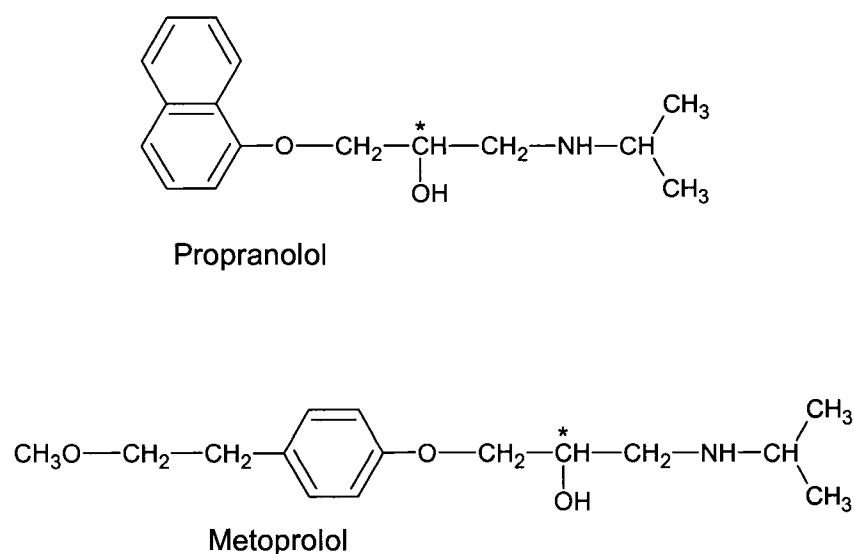


**Figure 4.1** Structure of basic drugs ( $\beta$ -blockers) analyzed.

### 4.3 Results and Discussion

#### 4.3.1 Stability of the Capillary Coatings

Bilayer structures have been characterized using a variety of techniques including Atomic Force Microscopy (AFM) [24, 25], ellipsometry [26], neutron scattering [27] and streaming potential [28]. However, none of these techniques is an easy or direct means to characterize the capillary coatings inside the small dimension capillaries used in CE. Instead, characterization of the properties of coated capillaries is commonly performed indirectly by measuring the EOF and investigating its dependence on different buffer conditions [8, 22, 29]. The value of the measured EOF is indicative of the zeta potential (i.e. the surface charge density) of the surface of the capillary, as described by the Smoluchowski equation (eqn 1.18). Determination of the EOF in the capillaries can be

obtained by photometric monitoring of the electrophoretic migration of a neutral marker [30] or by imaging the motion of a fluorescent neutral marker along the length of a capillary [31]. Such measurement of the EOF has been used to monitor the stability of various types of coatings in CE [5, 8, 24, 31]. In cases where the EOF is so low that migration times are excessively long, the pressure-mediated three peak injection technique developed by Williams and Vigh [32] can be applied (see Section 2.2.3 for details).

In this work, the change in EOF as a function of successive hydrodynamic rinsing times was used to infer the stability of bilayer cationic surfactant coatings [23]. In this approach, the capillary is first coated with the surfactant. Then the coating is subjected to increasingly long rinses with run buffer that does not have surfactant within it. The EOF is determined after each successive rinse. When possible, the measured EOF versus the rinsing time (in min) is fit to an exponential decay function with a nonzero asymptotic value (Prism Version 4.00, GraphPad Software Inc; San Diego, CA) as follows [23]:

$$\mu_{eo} = A_1 \exp(-k_d t) + A_\infty \quad (4.3)$$

where  $k_d$  is the observed decay rate of the EOF with rinsing time,  $A_\infty$  is the asymptotic value of the EOF, and  $A_1$  is a fitting parameter. The sum of  $A_\infty$  and  $A_1$  gives the value of the EOF at time zero (i.e. the EOF observed prior to rinsing the capillary with the run buffer). The slower the exponential decay (i.e., smaller  $k_d$ ), the more stable the coating. Alternately, the stability of the coating could also be assessed by the successive injection technique which is also known as the electrokinetic rinsing [8, 24, 31]. In this method, after the coating the capillary with surfactant as described for hydrodynamic rinsing, the

excess surfactant is removed by flushing the capillary with run buffer. Then consecutive EOF measurements are performed by injection of neutral marker (mesityl oxide) and application of the voltage for successively longer times. While the electrokinetic rinsing method is more common in the literature, the hydrodynamic technique is a more effective means of evaluating the stability of the capillary coatings [23]. Use of applied pressure than voltage generates much higher linear velocities, which shortens the overall experiment time. Thus, the hydrodynamic rinsing technique is used for the stability studies described below.

#### **4.3.2 DDAB Coating Stability in MeOH-Water Buffers**

In Chapter 3, I demonstrated that  $C_{16}TAB$  and  $2C_{12}DAB$  can be used as dynamic additives for control and manipulation of the EOF in phosphate buffers containing up to 60% MeOH [7, 33]. However, these EOF modifiers had to be kept in the run buffer to maintain the EOF. The presence of surfactants in the buffer is not desirable as the surfactant may interact with the analytes and interfere with detection modes such as electrospray ionization mass spectrometry (ESI-MS). A more desirable approach to the control of EOF in nonaqueous solvents would be to use semi-permanent coatings, which would allow the excess EOF modifier to be removed from the buffer prior to performing any separations. Interactions between the additive in the buffer and the analytes would thus be eliminated.

As a baseline study, the stability of the  $2C_{12}DAB$  (i.e. DDAB) coating in the presence of methanol in the run buffer was evaluated using the hydrodynamic rinse test (Section 4.2.4). Figure 4.2 shows the magnitude of the EOF generated by a capillary coated with 0.1 mM DDAB and then rinsed for various time periods with 20 mM sodium

phosphate buffer (pH 8.0) containing various amounts of MeOH. The results show that the EOF generated with DDAB decreases with rinsing time, i.e. the charge density on the capillary surface diminishes as the coating is subjected to more rinsing. The data points were fit to a first order nonlinear regression given in eqn 4.3. For both the pure aqueous and 20% MeOH, the EOF decays exponentially (correlation coefficient,  $R^2 \geq 0.998$ ) with rinsing time to asymptotic EOF values. This indicates that the degradation of the bilayer coating follows a first order process (eqn 4.3) in both buffer conditions. The rapid decrease in EOF is indicative of the steady loss of surfactant from the bilayer structure. Longer rinsing times at high pressure (93.8 kPa) introduces more fresh run buffer into the capillary. This may cause the dynamic aggregation/dissociation equilibrium inherent in surfactant aggregation to shift towards dissociation of more surfactant from the surface bilayer, which in turn leads to a lesser charge density on the surface bilayer. Hence, the degradation in the bilayer structure results in the reduction of the EOF. However, the asymptotic values i.e. the residual EOF are indicative of the presence of undisruptive surfactants on the surface even after long rinsing times. Mahmoud and Lucy also observed a similar nonzero residual EOF for cationic surfactant bilayers in purely aqueous buffers [23].

Further fitting the data in Figure 4.2 to eqn 4.3 reveals that the EOF decays more rapidly (i.e. the bilayer degrades faster) in 20% MeOH than in the aqueous buffer. In the aqueous solution, the EOF decays with a half-life of 8.1 min while in 20% MeOH the



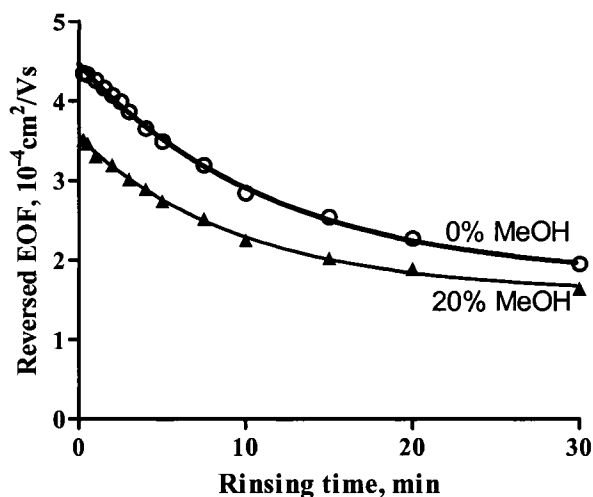


**Figure 4.2** Effect of hydrodynamic rinsing on the stability of  $2C_{12}DAB$  coating in MeOH-water buffers. (o) 0% MeOH, ( $\blacktriangle$ ) 20% MeOH. Experimental conditions: capillary was rinsed with 0.1 mM  $2C_{12}DAB$  for 5 min at 93.8 kPa; applied voltage, -20 kV; capillary, 37 cm x 50  $\mu\text{m}$  I.D. (28.5 cm to the detector); buffer, 20 mM phosphate at pH 8.0; neutral marker, 1.0 mM mesityl oxide at 254 nm. The data points were fit into eqn 4.3 and the  $k_d$  values for the aqueous and 20% MeOH were  $(86 \pm 4) \times 10^{-3}$  and  $(102 \pm 5) \times 10^{-3} \text{ min}^{-1}$  respectively.

decay half-life decreases to 6.8 min. The stability gets even poorer as the percentage methanol increases. In buffers containing more than 20% methanol, no reversed EOF was observed even for the shortest hydrodynamic rinse times (0.5 min). This indicates a complete lack of positively charged bilayer on the surface of the capillary wall in presence of higher percent (>20%) methanol.

One means to improve the stability of bilayer coatings is the use of high ionic strength buffers, which lower the critical micelle concentration (CMC) of the surfactants

(Section 1.4.3.3). However, such high concentration buffers lead to Joule heating, and would cause ion suppression when using detection such as ESI-MS. [23]. The use of high concentration buffer in the presence of organic solvents also results in precipitation. Thus, we decided to explore the use of longer chain surfactants as semi-permanent capillary coatings in various mixed organic-water buffers as described below in Section 4.3.3.

#### 4.3.3 $2C_n$ DAB Coating Stability in MeOH-Water Buffers

Increasing the length or number of the hydrocarbon chains of the surfactant can dramatically lower the CMC as discussed in Section 1.4.3.3 and shown in Table 4.1. For double-chained surfactants such as DDAB, the CMC can be estimated by [34]:

$$\log(\text{CMC in M}) = 3.495 - 0.6625 n \quad (4.4)$$

where  $n$  is the number of carbon atoms in each alkyl chain. Thus, for these types of surfactants, the CMC decreases by a factor of  $\sim 20$  for every two additional  $-CH_2-$  groups in each hydrocarbon chain. Hence,  $2C_{18}$ DAB is expected to aggregate to form a bilayer structure at a concentration  $10^4$  times lower than  $2C_{12}$ DAB (DDAB). Some physiochemical properties of the double chain surfactants employed for this study are shown in Table 4.1.

Figure 4.3 illustrates the stability of the  $2C_{18}$ DAB bilayer coating in the presence of 40% and 60% MeOH in 20 mM phosphate buffer at pH 8.0. No coating degradation (i.e., no drift in EOF) is observed in either buffer over 30 min of rinsing the coating at high pressure (93.8 kPa). This rinsing time corresponds to about 133 capillary

**Table 4.1** Physicochemical properties of some of the double chain surfactants

Surfactant	CMC, ( $\mu\text{M}$ ) <sup>a</sup>	Packing Parameter ( $P$ ) <sup>b</sup>	Chain Melting Temperature ( $^{\circ}\text{C}$ ) <sup>c</sup>
2C <sub>12</sub> DAB	35.0	0.62	16
2C <sub>14</sub> DAB	1.60	0.62	29
2C <sub>16</sub> DAB	0.078	0.62	28
2C <sub>18</sub> DAB	0.0037	0.62	45

<sup>a</sup>Determined based on eqn 4.4.; <sup>b</sup>Data taken from reference [35]; <sup>c</sup>Data taken from references [35] and [36].

volumes of run buffer introduced into the capillary. The stability of the EOF in 40% MeOH (% RSD = 1.5% over 30 min rinse) is slightly better than in the 60% MeOH buffer (% RSD = 4.2%) over same rinsing time. Also, the magnitude of the EOF observed in the 40% MeOH is higher than that in 60% MeOH, due in part to the lower dielectric constant and higher viscosity of the buffer mixture in the latter (Section 2.3.3). No stable reversed EOF was observed in buffers containing more than 60% MeOH. A small reversed EOF ( $0.86 \times 10^{-4} \text{ cm}^2/\text{Vs}$ ) was generated in 70% MeOH but the coating was not stable for two electrophoretic runs even in the absence of any hydrodynamic rinses. Thus, regeneration of the coating was necessary between the runs. This can be done by flushing the capillary with pure methanol (10 min) followed by rinsing with 1 M NaOH for 10 min, H<sub>2</sub>O for 5 min and 0.1 mM surfactant solution for 5 min successively, as had been done with CTAB in Chapter 2.

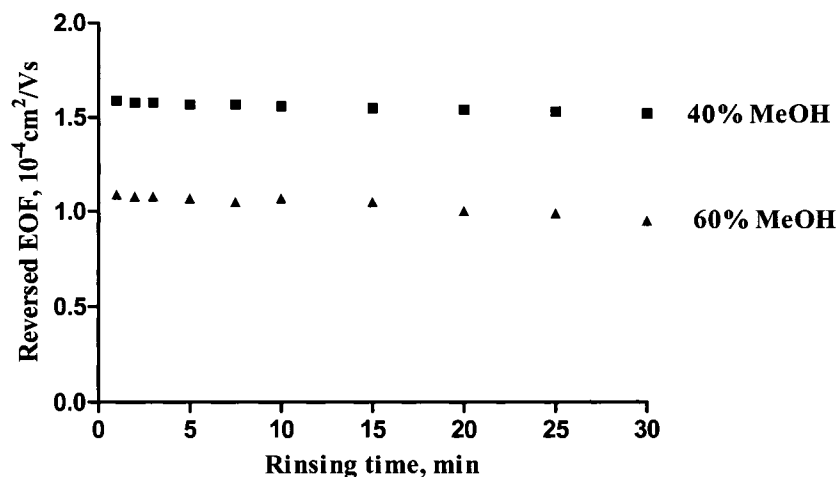


**Figure 4.3** EOF stability of  $2\text{C}_{18}\text{DAB}$  coatings in MeOH-water buffers. (■) 40% MeOH, (▲) 60% MeOH. Experimental conditions: capillary was rinsed with 0.1 mM  $2\text{C}_{18}\text{DAB}$  for 5 min at 93.8 kPa. All other experimental conditions as described in Figure 4.2.

Compared to the results obtained with  $2\text{C}_{12}\text{DAB}$  (Figure 4.2),  $2\text{C}_{18}\text{DAB}$  gives much better stability even with higher percent methanol buffers (up to 60% MeOH). Different concentrations of the surfactant were also examined (0.005 to 0.5 mM) using 5 min of coating times in MeOH containing buffers. Constant EOF values of  $1.64 \times 10^{-4}$  and  $1.13 \times 10^{-4} \text{ cm}^2/\text{Vs}$  were observed for 40% and 60% MeOH respectively. This observation indicated that the coating stabilities are independent of the surfactant concentration for the range examined. As a result, 0.1 mM of surfactant solution with 5 min of rinsing time was used as the coating protocol for all the experiments. Previously Yassine and Lucy observed that the bilayer coating stability depended on the buffer anion, with formate and acetate buffers yielding poor stability relative to phosphate buffers [23]. The studies

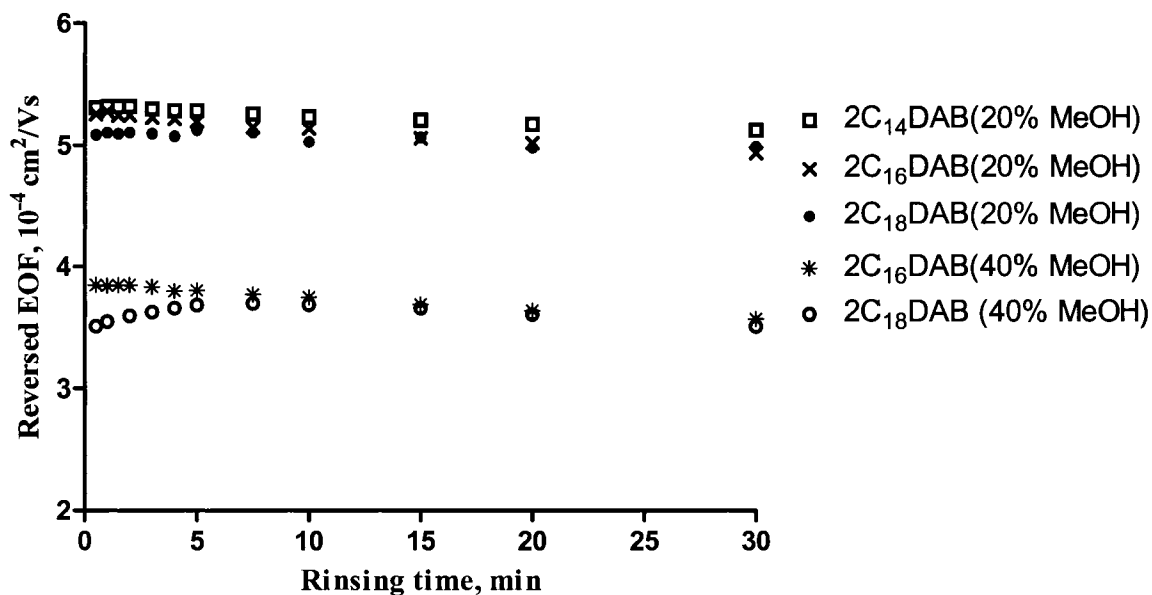


**Figure 4.4** Effects of surfactant chain length on stability of 2C<sub>n</sub>DAB surfactants.

Experimental condition: capillary rinsed with 0.1 mM 2C<sub>n</sub>DAB for 5 min at 93.8 kPa; applied voltage, -20 kV; capillary, 37 cm x 50 μm I.D.(28.5 cm to the detector); buffer, 20 mM ammonium formate at pH 4.7; neutral marker, 1.0 mM mesityl oxide at 254 nm.

herein (Figure 4.3) were performed in phosphate buffer, where greatest stability would be expected. Figure 4.4 shows the effect of methanol on the coating stability generated using 2C<sub>14</sub>DAB, 2C<sub>16</sub>DAB and 2C<sub>18</sub>DAB in 10 mM formate buffer at pH 4.7. In 20% MeOH, all the coatings show stable EOF (%RSD < 1.6%) over a 30 min rinse time. Interestingly, the magnitudes of the EOF generated are comparable (within 0.5 %) regardless of the hydrocarbon chain length. In 40% MeOH, however, the 2C<sub>14</sub>DAB

displays poor stability where the EOF decreases by about 25% over same length of rinse times ( $k_d = 75 \pm 4 \times 10^{-3} \text{ min}^{-1}$  and correlation coefficient,  $R^2 = 0.998$ ). In contrast, the longer chain surfactants, 2C<sub>16</sub>DAB and 2C<sub>18</sub>DAB generate stable bilayer coatings (% RSD of EOF < 2.0%) for 30 min of rinsing (equivalent to over 150 capillary volumes). This is consistent with the dramatic improvement in stability observed in aqueous phosphate buffers upon shifting from 2C<sub>12</sub>DAB to 2C<sub>18</sub>DAB surfactants [37].

#### 4.3.4 Effect of pH on the 2C<sub>18</sub>DAB Coating Stability

The effect of buffer pH on the magnitude and stability of the EOF generated with 2C<sub>18</sub>DAB coating was investigated in phosphate buffers containing various percent of methanol. The values of the EOF obtained as a function of rinsing time in buffers at pH 3.0, 5.0 and 8.0 is presented in Figure 4.5. The results show that in buffers containing up to 40% MeOH, the EOF (i.e., the bilayer coatings) are stable for long rinsing times (>30 min) regardless of the pH. In 60% MeOH, the EOF at pH 5.0 and 8.0 are also stable and a constant value of  $\sim 1.2 \times 10^{-4} \text{ cm}^2/\text{Vs}$  (with drift less than 2.1 %) are obtained even after subjected to over 30 minutes of high-pressure rinsing (about 128 capillary volumes). However, with 60% MeOH and at pH 3.0, the EOF decreases significantly for rinse times greater than 10 min.

The charge on the quaternary ammonium head groups would not be affected by changing the buffer pH as they are permanently charged in the pH ranges explored.

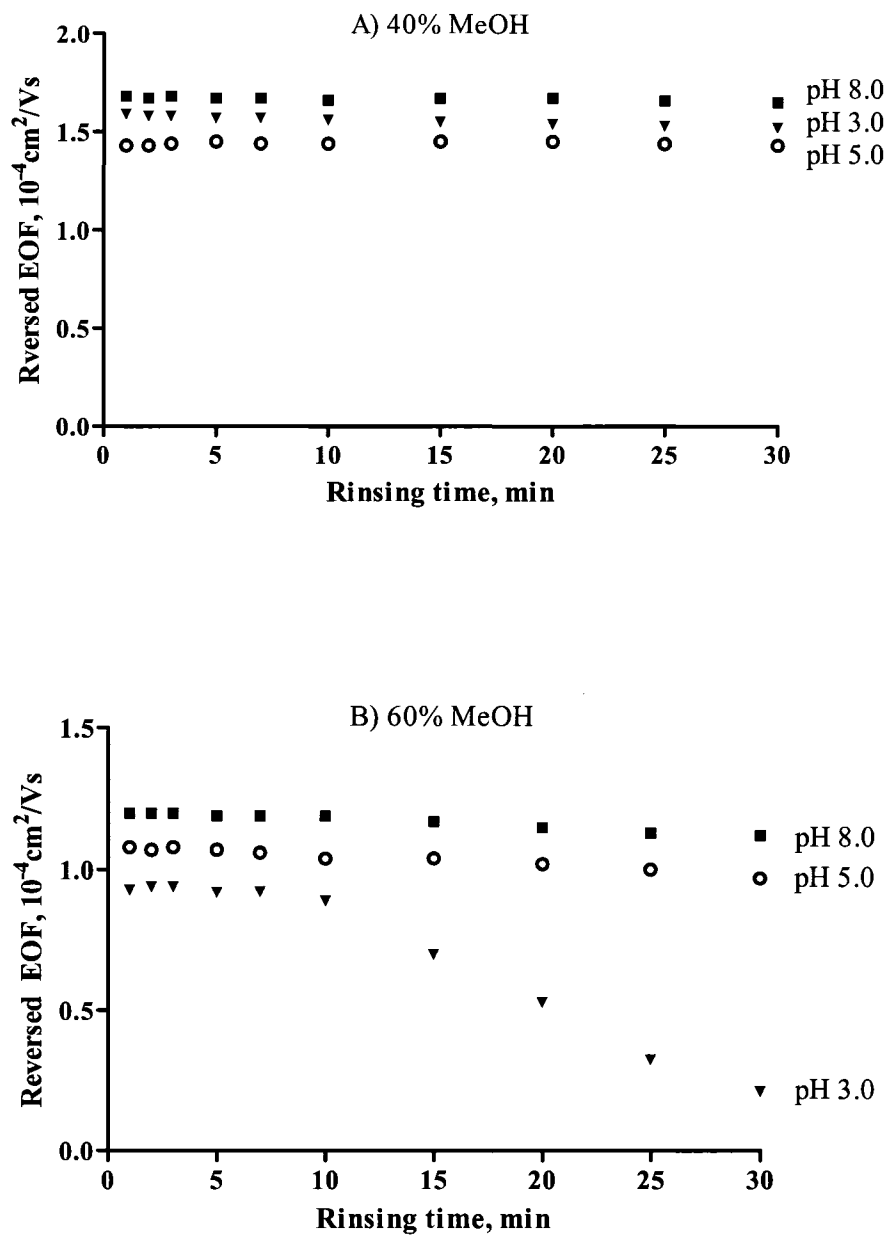


**Figure 4.5** Effect of pH on the stability of 2CDAB coatings in MeOH-water buffers. A) 40% MeOH, B) 60% MeOH at pH 3.0 (▼); pH 5.0 (○) and pH 8.0 (■). All other experimental conditions as described in Figure 4.2.

In addition, the change in CMC of the surfactants owing to increased concentration of the counterion (i.e.  $\text{HPO}_4^{2-}$  ion) is not a factor because the coatings at pH 5.0 and pH 8.0 in Figure 4.5 display similar behaviors. Nonetheless, the pH could affect the stability of the coatings in the presence of organic solvents in two ways. First as the pH increases the zeta potential on the capillary surface will also increase (Section 1.2.2.2), which would lead to stronger attraction of the cationic surfactants to the surface. Addition of methanol, however, lowers the zeta potential of the silica due to the intrinsic lower dielectric constant of the mixed organic-aqueous solvent resulting in a steeper drop in potential within the Stern layer (Section 2.3.3). Thus for a fully ionized silica capillary the zeta potential in 50% MeOH is about 40% lower than that in a purely aqueous buffer [7, 38]. Secondly, in buffers containing organic solvents, the zeta potential is further diminished by incomplete ionization of the silanols. Compared to pure aqueous solutions, the pKa of silanols increases with addition of methanol [38]. This lower degree of ionization of the silanols yields a lower silica surface charge that would result in weaker interaction of the surfactant with the capillary surface.

From the results shown in Figure 4.5, the independence of the coating stability on pH in buffers containing up to 40% MeOH indicates that the capillary surface still carries enough zeta potential such that the cationic surfactants could adsorb strongly to form the bilayer coating structure. However, in 60% MeOH the coatings are stable only at higher pH buffers, i.e., pH 5.0 and pH 8.0 where there is a greater charge density on the capillary surface. The strong hydrophobic interactions between the long tail groups also maintain the bilayer structure intact even when there is weak electrostatic attraction to the capillary wall.



### 4.3.5 Coating Stability in Different Solvents

In addition to MeOH, various other nonaqueous solvents are increasingly being used in CE as buffer additives to improve solubility and to alter the separation selectivity between analytes. To determine the compatibility of the coatings in such solvent systems, the stability of the surfactant coatings was also investigated in acetonitrile (ACN), ethanol (EtOH), 2-propanol (2-PrOH), and 1-butanol (1-BuOH). The physical and chemical properties of the solvents used are shown in Table 1.1, Section 1.4.4. For each EOF determination, the capillary was first coated with 0.1 mM  $2C_{18}DAB$  for 5 min and then the excess surfactant was removed by flushing the capillary with the run buffer for 3 min. Next mesityl oxide was injected and multiple EOF determinations ( $n = 5$ ) were made as described in Section 4.2.3 without regenerating the coating between runs. The magnitude and reproducibility of the EOF obtained in these solvent systems are given in Table 4.2. For the higher chain alcohols (ethanol, 2-propanol, 1-butanol) the concentrations were limited to less than 40% (v/v), because at higher alcohol contents the buffer solutions became turbid due to reduced solubility of the buffering electrolytes in the solvent, which possibly lead to precipitation inside the capillary during the measurements. Other more soluble electrolytes (e.g., acetate and formate) were not investigated because it was our intention to maintain the same experimental conditions in the entire series of investigations as consistent as possible.

The coating generated reversed EOF values ranging from  $0.85 \times 10^{-4} \text{ cm}^2/Vs$  to  $2.22 \times 10^{-4} \text{ cm}^2/Vs$  and EOF reproducibility less than 2.3% RSD. Rapid separations along with high resolutions are achieved under these buffer conditions. A typical electropherogram showing the separation of six anions using the surfactant coating in the

**Table 4.2** The value and reproducibility of EOF generated using 2C<sub>18</sub>DAB coating in different organic-aqueous solvent mixtures.

Buffer	EOF mobility, 10 <sup>-4</sup> cm <sup>2</sup> /Vs	$\varepsilon/\eta^*$ (cP <sup>-1</sup> )	Reproducibility (%RSD, n = 5)
20% ACN	2.22	74.1	1.6
40% ACN	1.95	57.7	1.4
60% ACN	1.91	61.4	2.8
20% EtOH	1.90	37.8	1.2
40% EtOH	1.01	32.4	1.9
20% 2-PrOH	1.75	31.5	1.5
40% 2-PrOH	0.85	26.4	1.6
10% 1-BuOH	1.55	23.6	1.1
20% 1-BuOH	1.25	17.3	1.6

Experimental conditions: 20 mM phosphate buffer (pH 8.0), neutral marker, mesityl oxide, detection at 254 nm. \* Values from references [39] and [40].

presence of 20% 1-BuOH in the BGE is given in Figure 4.6. The migration order migration of the anions is same as that observed in the presence of 20% MeOH (Section 4.3.7 below). In all buffers systems, however, addition of the organic solvents decreases the EOF and hence increases the migration time. For instance in 40% EtOH, the value of the EOF decreases to about one quarter of the mobility in aqueous solution. This is

mainly due to the changes in values of the dielectric constant and viscosity in the mixed organic-water buffers compared to pure aqueous buffers ( $\epsilon/\eta$  is 32.4 in 40% EtOH vs. 89.9 in pure aqueous solvent). As shown in Table 1.1, all the organic solvents used possess lower dielectric constants than water. However, the viscosity of ACN (0.37 cP) is lower than water (0.89 cP) while EtOH (1.08 cP), 2-PrOH (2.04 cP) and BuOH (2.57 cP) have higher viscosity than water. The viscosities of the mixtures also rise with increasing amount of the organic solvent. For instance, the viscosity values for EtOH-water mixtures are 1.62 cP, 2.25 cP, and 2.32 cP for 20%, 40%, and 60% EtOH respectively [41]. Consequently, the mixed organic-water systems display lower

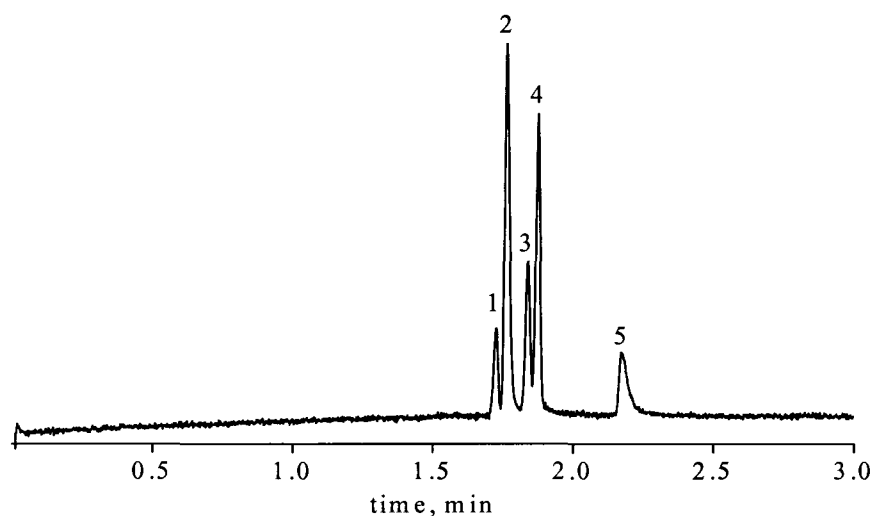


**Figure 4.6** Electropherograms of separation of five anions in the presence of 1-butanol. Experimental conditions: 20% 1-BuOH, 25 mM phosphate buffer (pH 8.0), 0.1 mM  $2C_{18}DAB$  (rinsed for 5 min), 0.25 mM anion sample. Peaks: 1)  $Br^-$  2)  $NO_2^-$  3)  $NO_3^-$  4)  $I^-$  5)  $SCN^-$ . All other conditions as described in Figure 4.2.

$\varepsilon/\eta$  values as the content of the organic solvent increases and hence slower EOF are observed, with the exception of acetonitrile. The mobility changes obtained in ACN-water buffers are modest and the values are higher than in the alcoholic solvents owing to the small viscosity variations for the ACN-water solvent systems. In addition, the EOF reductions are more pronounced with the higher chain alcohols (EtOH, 2-PrOH and 1-BuOH) than for MeOH (Section 4.3.3).

#### 4.3.6 Reproducibility and Regeneration of the Coatings

To test the stability and reproducibility of the 2C<sub>18</sub>DAB coating procedure in mixed MeOH-water buffers, a series of consecutive runs were performed with no hydrodynamic rinses between runs. The electropherograms in Figure 4.7 demonstrate the migration time reproducibility of the neutral marker (mesityl oxide) in 40% MeOH for 13 successive runs without regeneration or refreshing of the coating between the runs. A reasonably high EOF,  $2.31 \times 10^{-4} \text{ cm}^2/\text{Vs}$  with stable background is also obtained. The migration time reproducibility of the marker under this condition is 0.3 % RSD ( $n = 13$ ).

The performance and quality of the coatings were also investigated by performing multiple CE separations of analytes. We examined the electrophoretic mobilities of anions as a function of number of repetitive runs to determine the stability of the coatings and possible interactions of inorganic anions with the bilayer structure on the surface of the capillary wall. Separations of four anions using the 2C<sub>18</sub>DAB-coated capillary in 60% MeOH are shown in Figure 4.7. The migration time reproducibilities are less than 0.5 % RSD over the six runs. The peak height and peak area reproducibilities for all the anions are less than 2.4% and 2.1% RSD respectively. The high degree of repeatability and high efficiencies over a number of repetitive runs in mixed MeOH-water buffers

indicate the absence of significant interactions of the anions with the positively charged capillary surface.

The semi-permanent bilayer coatings used herein show stabilities over several capillary volumes (more than 130 capillary volumes) without significant degradation. If there is a need to change the coating for any practical reason (e.g. to work under new buffer conditions or if the coatings degrade over long time), the coatings can be removed and re-generated easily. Thus, another measure of reproducibility is the ability to recoat the capillary and generate the same EOF. The surfactant coating was removed by rinsing with 1.0 M NaOH for 10 minutes followed by distilled water for 5 min. Alternately, flushing the capillary with pure methanol (5-10 min) completely removed the surfactant coatings. We observed that regeneration of the coating through flushing with 100% methanol produces EOF within less than 0.5% of the original EOF value in the coated capillary. It is important to note that the viscosity of the solvent (or the electrophoretic medium) affects the time required to flush the capillary as well as the time for hydrodynamic injection of a certain volume into the capillary. The time required to flush the entire length of capillary at high pressure is determined by measuring the time required for an injection of neutral marker (mesityl oxide) to be pushed past the detector and then allowing for the extra 8.5 cm length of the capillary after the detector. In this case, a flushing time corresponding to 10 to 15 capillary volumes is used to ensure complete removal of the surfactants from the capillary before regeneration of the coating.

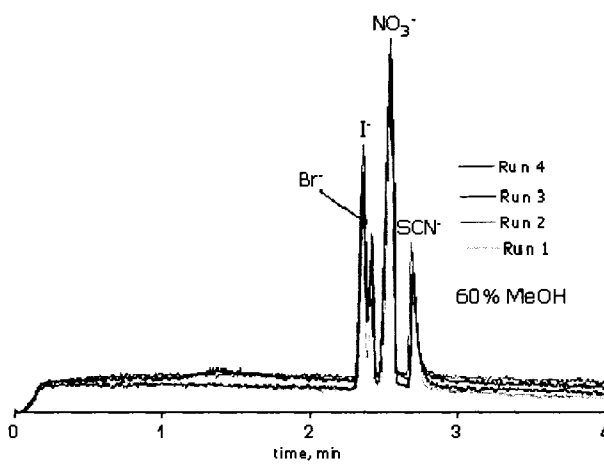
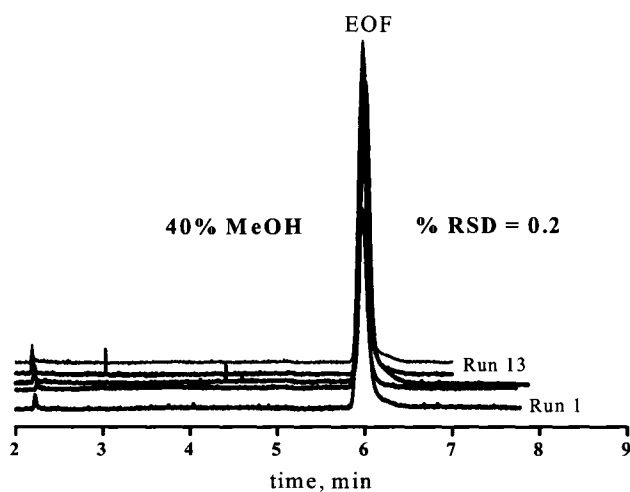


**Figure 4.7** Reproducibility of the EOF and anion separations. Experimental conditions: 0.1 mM  $2\text{C}_{18}\text{DAB}$ ; buffer, 20 mM sodium phosphate at pH 8.0; A) EOF measurement: neutral marker, 0.2 mM mesityl oxide at 254 nm; B) anion separation: sample, 0.25 mM each; detection at 209 nm; 20% MeOH. All other conditions as described in Figure 4.2.

For instance, 4 min rinse at 93.8 kPa for 60% MeOH or 2 min rinse at 93.8 kPa for pure water corresponds to about 10 capillary volumes for 40 cm long and 50  $\mu\text{m}$  I.D capillary.

#### 4.3.7 Separation of Anions and Basic Drugs

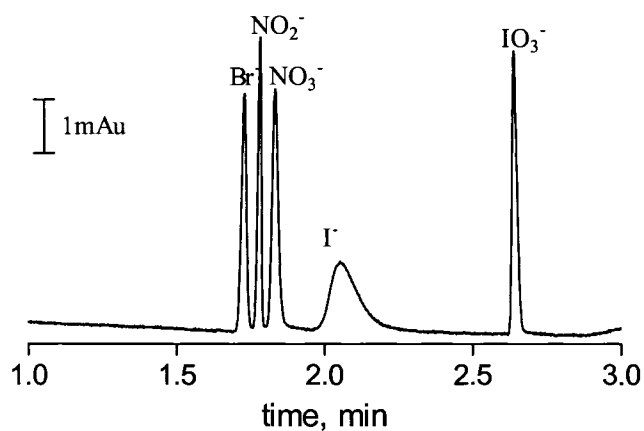
The use of normal EOF in CE for the analysis of small inorganic anions results in excessively long analysis times because the migration of the anions opposes the EOF, as discussed in detail in Section 2.1. As a result, modification of the capillary surface is essential to minimize or reverse the EOF so that analysis time is reduced while maintaining efficiency. Previously Baryla and Lucy showed the use of double-chained surfactants as semi-permanent coatings in aqueous solutions for anion separations. To explore the application of the  $2\text{C}_{18}\text{DAB}$  bilayer coatings for anion separations in mixed organic-aqueous BGE, a mixture of five common inorganic anions was examined. The capillary was coated with 0.1 mM  $2\text{C}_{18}\text{DAB}$  solution and then rinsed with run buffer (surfactant free) for 5 minutes at high pressure (93.8 kPa) to remove the excess surfactant. This removal of the surfactant eliminates interactions between surfactant aggregate in the buffer and analyte anion.

Figure 4.8 shows the separation of the five anions in 20 mM phosphate buffer at pH 8.0 containing 20% MeOH. The migration order is the same as that achieved in 20% MeOH with  $\text{C}_{16}\text{TAB}$  coating as described in Section 2.3.5. The separation efficiencies range from 0.5 to 0.7 million plates/m except iodide which shows an efficiency of 20,000 plates/m. The low efficiency for iodide may be due to its strong ion-exchange type of interaction with the positively charged bilayer on the surface. Similar poor efficiencies have been observed for iodide in aqueous separations in capillaries coated with  $2\text{C}_{12}\text{DAB}$  [42]. However, the efficiency of the iodide peak improved to over 260,000 plates/m

when 60% MeOH is used. Upon further addition of methanol selectivity changes similar to those in Chapter 2 were observed [7]. The strong EOF generated from the bilayer coatings enables separations to be performed in less than 2 minutes, as shown in the electropherogram (Figure 4.8). Even at higher percentage of methanol (60%), the separation speed was reasonable since the high EOF allows fast separation.

CE is gaining wider popularity in analytical laboratories and has become an important tool for routine analysis in the pharmaceutical and biotech industries [43]. Specific applications include drug analysis in biological matrices for pharmacokinetic and metabolism studies, *in vitro* drug metabolism studies as well as applications in forensic analysis and therapeutic drug monitoring [44, 45]. However, CE analysis of low concentrations of basic drugs often suffers from poor accuracy and precision [46]. A major cause is the inconsistencies in the EOF in bare silica capillaries between runs resulting in non-reproducible migration times. Because the peak area in CE is proportional to the migration time, variability in the latter parameter leads to low precision in peak area estimates and thus quantification. Another factor affecting precision is the adsorption of positively charged analytes to the capillary wall producing tailing and, therefore, affecting peak shape and consequently peak height and possibly area estimation. Improved migration time reproducibility and detection limits for basic drugs were reported using a polyamine-coated capillary, possibly through decreased analyte adsorption and peak tailing [47].





**Figure 4.8** Co-electroosmotic separation of five anions using 0.1 mM  $2C_{18}DAB$  surfactant. Experimental conditions: 20% MeOH phosphate buffer at pH 8.0 and detection 209 nm. All other conditions are as described in Figure 4.3.

The performance of the bilayer coating developed in this study was evaluated by analyzing basic analytes in buffers containing different percentages of methanol. The separation of two test drugs, propranolol and metoprolol using a  $2C_{18}DAB$ -coated capillary in 20 mM phosphate at pH 3.0 is presented in Figure 4.9. These drugs are commonly used as therapeutic agents ( $\beta$ -blockers). At pH 3.0, both drugs are fully charged (Figure 4.1) and they are completely soluble in both water and methanol. In aqueous buffers, the two peaks are well resolved with efficiencies of 450,000 and 570,000 plates/m for metoprolol and propranolol respectively. The migration time reproducibilities of the peaks are excellent (less than 0.3% RSD). Upon addition of 40% MeOH, the efficiencies of the two analytes remained in the same range but the migration times become longer (from 2 min to 2.5 min). This is due to the slower EOF caused by the lower dielectric-to-viscosity ratio in the mixed MeOH-water buffer. Nonetheless, the

separation speed and efficiencies achieved under both conditions are much better than previously reported results [13, 19]. This is partly because of the presence of strong EOF generated by the bilayer coating. For instance Riekkola and co-workers [19] reported separation of propranolol and other basic drugs in about 10 min (five times longer than the result herein) using a dynamic polymer coating in methanol.

Another important result obtained in going from aqueous to 40% MeOH is the reversal of the migration order of the analytes. Propranolol migrates faster in aqueous buffer but its mobility becomes lower than metoprolol in 40% MeOH buffer. Similar selectivity changes due to the influence of organic solvents on the effective electrophoretic mobilities of closely migrating ion have been reported. Geiser et al. [48] observed that peaks of oxprenolol, atenolol and metoprolol, which possess close molecular masses, were clearly separated in methanol and formamide but not in water nor in acetonitrile. Similarly, Masselter and Zemmann observed a markedly improved selectivity among methylated phenols up on addition of methanol to the aqueous buffer [6]. This result shows the potential of nonaqueous solvents to alter selectivity among analytes that is not possible in aqueous buffers. In 60% MeOH the migration order was similar to that in 40% MeOH, but poorer sensitivities were observed mainly because of increased absorbance of MeOH. Tailing was not observed in any of the electropherograms, suggesting that the charges on the bilayer coating helps to minimize interaction of the positively charged drugs with the negatively charged capillary wall. Both analytes were analyzed as racemic (enantiomeric) mixtures. Enantiomer separation

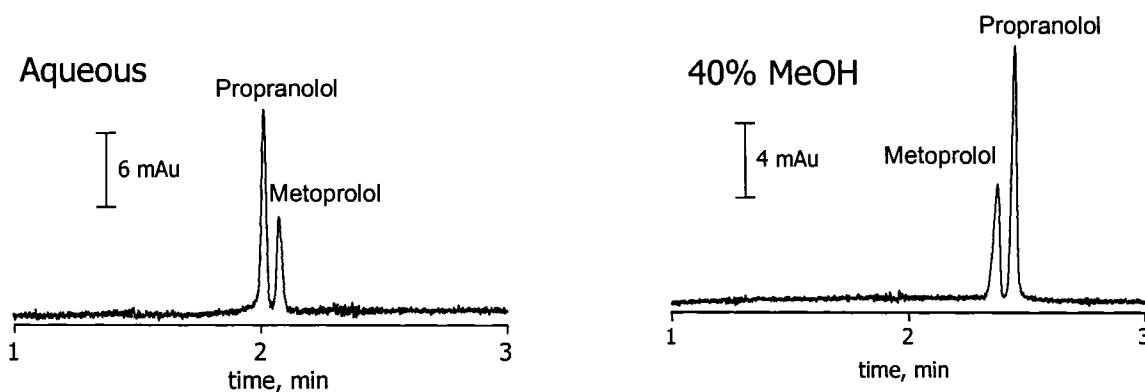


**Figure 4.9** Effect of methanol on the separation selectivity of two basic drugs. A) Aqueous buffer B) 40% MeOH; Experimental conditions: applied voltage, -20 kV; capillary, 40.5 cm x 50 $\mu$ m I.D. (32 cm to the detection window); 1.0 mM 2C<sub>18</sub>DAB; buffer, 20 mM phosphate at pH 3.0; Sample, 0.2 mM; detection at 220 nm; Peaks: 1) Metoprolol 2) Propranolol.

of these drugs in CE has been reported using chiral selective reagents such as cyclodextrin and its derivatives in the BGE [49]. Khaledi and coworkers have also utilized polycations and short chain surfactants to control the EOF and to enhance chiral separations of pharmaceutical drugs in NACE [46, 50]. Hence, further studies to investigate the application of different chiral selectors with these cationic coatings for enantiomeric separations of basic drugs in nonaqueous solvents would be important.

#### 4.4 Concluding Remarks

The results presented in this work show that long double-chain surfactants can be used as semi-permanent coatings in organic-water solvent systems. The coating procedure involves a simple hydrodynamic rinse of the capillary with the surfactant solution for less than five minutes. The resultant bilayer coatings show stability toward a large number of rinsing steps in buffers that contain up to 60% nonaqueous solvents. Compared to other types of capillary modifications, such surfactant-based coatings are simple, versatile and inexpensive. The absence of EOF modifier in the run buffer also allows greater flexibility in optimizing the separation conditions. This is particularly advantageous compared to the dynamic coatings we used in Chapters 2 and 3. The generation of pH-independent EOF also enables to perform separations under different pH conditions with mixed MeOH-water buffers. Rapid separations of small anions with migration time reproducibility of better than 2% RSD and efficiencies in the ranges of 0.4 – 0.6 million plates/m were achieved. The change in the order of migration of the basic drugs with addition of the organic solvent also shows that the use of the mixed nonaqueous-water solvent systems could be useful approaches for the optimization of separation of analytes that differ only slightly in electrophoretic mobility.

#### 4.5 References

- [1] Righetti, P. G., Gelfi, C., Verzola, B., Castelletti, L., *Electrophoresis* 2001, 22, 603-611.
- [2] Jandik, P., Bonn, G. *Capillary Electrophoresis of Small Molecules and Ions*; VCH: New York, 1993.
- [3] Hayes, M. A., Ewing, A. G., *Anal. Chem.* 1992, 64, 512-516.
- [4] Liu, C. Y., *Electrophoresis* 2001, 22, 612-628.
- [5] Horvath, J., Dolnik, V., *Electrophoresis* 2001, 22, 644-655.
- [6] Masselter, S. M., Zemann, A. J., *Anal. Chem.* 1995, 67, 1047-1053.
- [7] Diress, A. G., Lucy, C. A., *J. Chromatogr. A* 2004, 1027, 185-191.
- [8] Cordova, E., Gao, J., Whitesides, G. M., *Anal. Chem.* 1997, 69, 1370-1379.
- [9] Baryla, N. E., Lucy, C. A., *J. Chromatogr. A* 2002, 956, 271-277.
- [10] Melanson, J. E., Baryla, N., E., Lucy, C. A., *Trends Anal. Chem.* 2001, 20, 365-374.
- [11] Belder, D., Husmann, H., Warnke, J., *Electrophoresis* 2001, 22, 666-672.
- [12] Belder, D., Elke, K., Husmann, H., *J. Chromatogr. A* 2000, 868, 63-71.
- [13] Steiner, F., Hassel, M., *Electrophoresis* 2003, 24, 399-407.
- [14] Esaka, Y., Inagaki, S., Uchida, D., Goto, M., Kano, K., *J. Chromatogr. A* 2001, 905, 291-297.
- [15] Esaka, Y., Okumura, N., Uno, B., Goto, M., *Anal. Sci.* 2001, 17, 99-102.
- [16] Gallaher, D. L., Johnson, M. E., *Anal. Chem.* 2000, 72, 2080-2086.
- [17] Tjornelund, J., Bazzanella, A., Lochmann, H., Bachmann, K., *J. Chromatogr. A* 1998, 811, 211-217.

- [18] Ahrer, W., Buchberger, W., *Fresenius J. Anal. Chem.* 1999, *365*, 604-609.
- [19] Porras, S. P., Wiedmer, S. K., Strandman, S., Tenhu, H., Riekkola, M. L.,  
*Electrophoresis* 2001, *22*, 3805-3812.
- [20] Vayaboury, W., Kirby, D., Giani, O., Cottet, H., *Electrophoresis* 2005, *26*, 2187-2197.
- [21] Baeuml, F., Welsch, T., *J. Chromatogr. A* 2002, *961*, 35-44.
- [22] Lucy, C. A., Underhill, R. S., *Anal. Chem.* 1996, *68*, 300-305.
- [23] Yassine, M. M., Lucy, C. A., *Anal. Chem.* 2004, *76*, 2983-2990.
- [24] Baryla, N. E., Melanson, J. E., McDermott, M. T., Lucy, C. A., *Anal. Chem.* 2001, *73*, 4558-4565.
- [25] Liu, J. F., Min, G., Ducker, W. A., *Langmuir* 2001, *17*, 4895-4903.
- [26] Eskilsson, K., Yaminsky, V. V., *Langmuir* 1998, *14*, 2444-2450.
- [27] Schosseler, F., Anthony, O., Beinert, G., Zana, R., *Langmuir* 1995, *11*, 3347-3350.
- [28] Wang, T., Hartwich, R. A., *J. Chromatogr.* 1992, *594*, 325-334.
- [29] Kohr, J., Engelhardt, H., *J. Chromatogr.* 1993, *652*, 309-316.
- [30] Walbroehl, Y., Jorgenson, J. W., *Anal. Chem.* 1986, *58*, 479-481.
- [31] Preisler, J., Yeung, E. S., *Anal. Chem.* 1998, *68*, 2885-2889.
- [32] Williams, B. A., Vigh, G., *Anal. Chem.* 1996, *68*, 1174-1180.
- [33] Diress, A. G., Lucy, C. A., *J. Chromatogr. A* 2005, *1085*, 155-163.
- [34] Svitova, T. F., Smirnova, Y. P., Pisarev, S. A., Berezina, N. A., *Colloids Surf. A*  
1995, *98*, 107-115.
- [35] Warr, G. G., Sen, R., Evans, D. F., Trend, J. E., *J. Phys. Chem.* 1988, *92*, 774-783.

- [36] Blandamer, M. J., Briggs, B., Cullis, P. M., Kirby, S. D., Engberts, J., *J. Chem. Soc., Faraday Trans.* 1997, 93, 453-455.
- [37] Yassine, M. M., Lucy, C. A., *Anal. Chem.* 2005, 77, 620-625.
- [38] Schwer, C., Kenndler, E., *Anal. Chem.* 1991, 63, 1801-1807.
- [39] Akhadov, Y. Y. *Dielectric Properties of Binary Solutions. A Data Handbook*; Pergamon Press: New York, 1980.
- [40] Roy, K. I., Lucy, C. A., *J. Chromatogr. A* 2002, 964, 213-225.
- [41] Sarmini, K., Kenndler, E., *J. Chromatogr. A* 1998, 811, 201-209.
- [42] Baryla, N. E., Lucy, C. A., *J. Chromatogr. A* 2002, 956, 271-277.
- [43] Altria, K. D., Chen, A. B., Clohs, L., *LC•GC Eur.* 2001, 14, 736-744.
- [44] Hadley, M. R., Camilleri, P., Hutt, A. J., *Electrophoresis* 2000, 21, 1953-1976.
- [45] Shihabi, Z. K., *J. Chromatogr. A* 1998, 807, 27-36.
- [46] Quang, C., Khaledi, M. G., *Anal. Chem.* 1993, 65, 3354-3358.
- [47] Assi, K. H., Abushoffa, A. M., Altria, K. D., Clark, B. J., *J. Chromatogr. A* 1998, 817, 83-90.
- [48] Geiser, L., Cherkaoui, S., Veuthey, J. L., *J. Chromatogr. A* 2002, 979, 389-398.
- [49] Servais, A. C., Fillet, M., Abushoffa, A. M., Hubert, P., Crommen, J., *Electrophoresis* 2003, 24, 363-369.
- [50] Wang, F., Khaledi, M. G., *Anal. Chem.* 1996, 68, 3460-3467.

## **CHAPTER FIVE: Non-Covalent Coating for Modification of the Electroosmotic Flow in Nonaqueous Capillary Electrophoresis**

### **5.1 Introduction**

In Chapters 2 and 3, I demonstrated a number of potential advantages of using mixed hydro-organic media over a purely aqueous buffer system in CE. Purely nonaqueous media are particularly suitable for the analysis of analytes that are not readily soluble in water and for analytes that show very similar electrophoretic mobilities in aqueous media. A wide range of solvents have been used in nonaqueous CE including methanol, ethanol, butanol, acetonitrile, nitromethane, etc. or mixtures of two or more of these solvents. Good reviews of the recent CE studies in non-aqueous and mixed solvents are available in the literature [1-3].

However, in spite of the use of nonaqueous solvents since the mid 1980's [4], it was only a decade later that formamide (FA) was identified as a particularly promising organic solvent for CE. In 1994 Sahota and Khaledi [5] reported the first CE investigation of nonaqueous systems with formamide as a medium. Since that first report, formamide or formamide-aqueous buffers have been used for CE separations of enantiomers [6, 7], for control of EOF, as a solvent in MEKC [8-11], and for other applications [12-14]. What makes FA an interesting alternative solvent for CE are its physicochemical properties. For comparison some important physicochemical properties of FA, as well as those of the three most commonly used solvents in CE (water, methanol, and acetonitrile) are shown in Table 5.1. Liquid formamide is one of the few organic solvents that have a dielectric constant greater than that of water. This property makes ionic pairing often observed in low dielectric organic solvents such as acetonitrile



negligible [15]. Formamide also has a hydrogen-bonded 3-D structure that is even more pronounced than that of water. Consequently, FA has viscosity (3.3 cP), melting point (2.5 °C) and boiling point (210.5 °C) higher than that of water. Addition of formamide to the electrolytic buffers also could minimize evaporative loss during electrophoretic runs because of the lower vapor pressure of the solvent [16].

The use of higher electric fields reduces analysis time and enhances separation efficiency, but with aqueous media, high ionic strengths lead to appreciable Joule heating (Section 1.5.2). However, buffer ions exhibit much lower mobilities in formamide. Consequently the current and hence the resulting Joule heating generated is lower than that in the aqueous media. For instance, Sahota and Khaledi [5] found that the current produced in formamide was 3-4 times lower than that in the aqueous medium for the same concentration of 0.1 M phosphate buffer (pH 7.0). Therefore, the lower current in formamide allows the use of higher ionic strength and electric field strength to achieve better efficiencies and reduced analysis time. Another interesting characteristic of FA and some other organic solvents such as acetonitrile, is that acids are weaker in these solvents when compared to water. For instance, Porras and Kenndler [14] reported a  $pK_a$  shift of 1-3 units higher for weak acids in FA than in water. If two analytes of interest have very similar  $pK_a$  values in water (and similar electrophoretic mobilities as well), the respective  $pK_a$  values in FA would differ so their electrophoretic separation can be achieved by appropriate adjustment of the pH.

However, the potential of formamide as pure solvent or mixed with other solvents in CE has not been fully achieved yet. There are a number of challenges in performing CE with formamide. These include control and modification of the EOF for fast and

**Table 5.1** Physico-chemical properties of FA and some selected solvents at 25 °C.

Solvent	Boiling point (°C)	Dielectric constant ( $\epsilon$ )	Viscosity ( $\eta$ , cP)	Vapor pressure (kPa)	UV cutoff (nm)
FA	210.5	109.5	3.30	0.0088	245
Water	100.0	78.5	0.89	3.17	190
MeOH	64.5	32.7	0.55	16.9	205
ACN	81.6	35.9	0.34	12.2	195

efficient CE analysis of anionic species, and understanding the influence of the solvent on the actual and the effective mobilities of different analytes. Recently Porras and Kenndler [14] investigated a number of important aspects of FA as a solvent for CE. Khaledi and co-workers have also looked the utility of the solvent as nonaqueous solvent in CE for separation of basic analytes [5, 6].

This chapter focuses on the control and modification of EOF in BGE containing formamide. Double-chained cationic surfactants similar to those used in Chapter 4 are employed to reverse the EOF. Studies of the aggregation of single chain surfactants in formamide and similar solvent systems have been reported in the literature [17-19]. However, there have been no reports on the study of two tailed surfactants in mixed formamide-water or pure formamide solvent systems.

## 5.2 Experimental

### 5.2.1 Apparatus

The CE instrument, the bare fused silica capillaries, data acquisition and control employed were as described in Section 4.2.1. The polyimide coating at both ends of the capillary was removed by burning a small sections to avoid capillary blockage due to swelling of the polyimide coating in organic solvents [20]. In all experiments, the capillary was thermostatted at 25.0 °C with circulating air-cooling.

### 5.2.2 Chemical and Reagents

All chemicals were reagent grade or better, and were used without further purification. All solutions were prepared with Nanopure 18-M $\Omega$  water (Barnstead, Chicago, IL). Phosphate buffers were prepared from sodium salts of orthophosphate (BDH, Darmstadt, Germany) and adjusted to the desired pH with reagent grade sodium hydroxide (BDH). Ammonium formate and acetate buffers were prepared from ammonium formate salt (BDH) and ammonium acetate (BDH), respectively. Buffers concentrations were prepared by dilution of a 1.0 M stock buffer solutions. The pH was measured using a Model 445 digital pH meter (Corning, Acton, USA) calibrated with aqueous pH standards immediately prior to use. For 10%, 30%, 50% and 70% (v/v) formamide, the required amount of buffer and required volume of formamide (FA; Fisher, Fair Lawn, USA) were added before final dilutions with Nanopure water. For 100% FA, the calculated amounts of reagents to make the buffers at specified pH were dissolved in formamide and no pH adjustments were made. 1.0 mM Mesityl oxide (Aldrich, Milwaukee, WI, USA), dissolved in the solvent being studied, was used as the neutral EOF marker. The cationic surfactants dimethylditetradecylammonium bromide

(2C<sub>14</sub>DAB), dimethyldihexadecylammonium bromide (2C<sub>16</sub>DAB), and dimethyldioctadecylammonium bromide (2C<sub>18</sub>DAB) were used as received from Aldrich. The 2C<sub>14</sub>DAB, 2C<sub>16</sub>DAB, and 2C<sub>18</sub>DAB are only slightly soluble in water and formamide. Thus, the surfactant solutions dissolved in water or formamide were prepared by sonication of the buffer-surfactant mixture at a temperature well above the chain melting temperature (see Table 4.1) for 30 min. Then the solutions were allowed to cool at room temperature (24 °C) with stirring for 15 min. This sonication/stirring cycle was repeated until a clear solution was obtained. The drug samples, propranolol, metoprolol, chlorpheniramine, tramadol and chloroquine were gift from Pars Minoo Pharmaceutical Company (Tehran, Iran) and were of >99.98% purity.

### 5.2.3 EOF Measurements

To avoid hysteresis effects, fresh capillaries were used with each new buffer system. New capillaries were rinsed under high pressure (93.8 kPa) with 1 M NaOH for 10 min and then with distilled water for 5 min. For buffers prepared in pure formamide, the capillary was rinsed for 5 min with pure formamide instead of distilled water. After the preconditioning steps, the capillary was rinsed at high pressure for 10 min with surfactant solution to coat the capillary. Then the excess surfactant was flushed out from the capillary using a 3 min high pressure (93.8 kPa) rinse with buffer.

To measure the EOF, the neutral marker (1 mM mesityl oxide in water or formamide) was injected into the capillary using hydrodynamic injection for 2 s at 5.0 kPa. The electroosmotic flow ( $\mu_{eo}$ ) was calculated from the migration time using:

$$\mu_{eo} = \frac{L_t L_d}{t_{eo} V} \quad (5.1)$$

where  $L_t$  and  $L_d$  are the total length of the capillary (37.0 cm) and the capillary length to the detector (28.5 cm), respectively,  $t_{eo}$  is the migration time of the neutral EOF marker (in seconds), and  $V$  is the applied voltage (in volts). In all experiments, the EOF values were the average of three or more measurements. When the EOF is slow, (less than  $2 \times 10^{-4} \text{ cm}^2/\text{Vs}$ ) the three injections technique developed by Williams and Vigh [21] was used, as described in Section 2.2.3.

#### 5.2.4 Coating Stability Studies

The coating stabilities were examined using two techniques as described in Section 4.3.1. In the first method, *hydrodynamic rinsing*, the stability of the surfactant coatings was indirectly evaluated by monitoring the EOF as a function of high pressure rinsing time with the run (electrophoretic) buffer. In this procedure, the coated capillary was flushed with the electrophoretic buffer (in the absence of surfactant) at a constant pressure (93.4 kPa) for an initial period of 3 min. A neutral marker (1 mM mesityl oxide) was injected and the EOF was measured as described in Section 5.2.3 above. The coating was then regenerated first by rinsing with aqueous 1 M NaOH at high pressure (93.8 kPa) for 5 min, followed by distilled H<sub>2</sub>O for 5 min at 93.8 kPa and then with 1.0 mM aqueous surfactant solution for 10 min at 93.8 kPa. For buffers prepared in pure formamide, the capillary was rinsed for 5 min with pure formamide instead of distilled water and 1.0 mM surfactant dissolved in formamide was used for coating. Then, the capillary was subjected to a longer rinsing time with the electrophoretic buffer (e.g. 5 min) and the EOF was again determined as described above. This flushing/regeneration procedure was successively repeated for rinsing times up to 30 min at 93.8 kPa. The stability of the coating (i.e. the EOF) was then evaluated by plotting the values of EOF obtained versus

the high pressure rinsing times. Second, the stability of the coatings was also assessed based on separation of anions and basic drugs. These runs were carried out to test the long-term reproducibility and the capillary coating performance.

### 5.2.5 Separation of Basic Drugs

A 5.0 mM stock solution of the drug samples, propranolol, metoprolol, chloroquine, tramadol and chlorpheniramine were prepared in Nanopure water or pure formamide and stored in the fridge at +6 °C. The sample solutions were manually filtered through a 0.2 µm polypropylene membrane filter (Whatman) prior to injection. The final sample solutions were prepared from the stock solutions by diluting to concentrations of 0.25 and 1.0 mM with the run buffer. For the drug separations, a fresh capillary was flushed first with aqueous 1 M NaOH for 15 min at 93.8 kPa, followed by water or formamide for 5 min at 93.8 kPa. Then the capillary was coated by rinsing for 10 min with 1.0 mM 2C<sub>18</sub>DAB solution (prepared in water or formamide) followed by 3 min rinse at 93.8 kPa with the electrophoretic buffer to remove the excess surfactant from the capillary. A mixture of the drug samples was injected for 2.0 s at 5.0 kPa. Detection for the drugs was performed using the direct UV mode at 210 nm. The efficiencies were computed from the peak width at the base line as shown in eqn 1.25.

### 5.2.6 Determination of Relative Viscosity

The viscosities of the buffers containing formamide were measured relative to that of the pure aqueous buffer. For each of the buffers, mesityl oxide was injected into the capillary for 2.0 s at 5.0 kPa and then was pushed past the detector hydrodynamically using 5.0 kPa pressure. The relative viscosities were determined from the ratios of the mesityl oxide elution times in the FA-water buffers and aqueous buffers. The dielectric

constant and viscosity for the aqueous solutions are assumed to be equal to those of water.

### 5.3 Results and Discussion

In Chapter 4, I showed that long-chained two-tailed surfactants formed bilayer coatings that are stable for a number of runs in buffers containing various amounts of organic solvents such as methanol, acetonitrile, ethanol, propanol and butanol. As a continuation of that work, my interest in this study is to evaluate whether these long doubly chained surfactants could be used in buffers prepared in pure formamide. Molecular aggregation of amphiphiles in organic solvents has been the subject of increasing interest, particularly in comparison with aggregation patterns in water. The aggregation of amphiphilic substances in aqueous solutions to form micelles and similar structures has long been regarded as a manifestation of the solvophobic effect. In particular, Evans et al. [22, 23] identified the importance of a hydrogen bonding network in driving aggregation of the non-polar tails of the surfactants. As a result, most nonaqueous surfactant aggregation studies have focused on liquids such as formamide, ethyl glycol and hydrazine that also form a strong H-bond network [24-26]. Given these past studies, I hypothesized that our bilayer coatings might be stable in pure formamide.

Recently, Duval and Warr [27] observed using AFM imaging that tetradecyltrimethyl ammonium chloride (TTAC) formed similar micellar aggregates in formamide as those formed in pure water. The similarity in basic features of micelle formation in formamide are believed to be a combined effect of the high dielectric constant of the medium and the hydrogen bonding nature of the amide proton [22, 23, 28]. The high dielectric constant of formamide ( $\epsilon \sim 109.5$ ) facilitates better solvation of

the surfactant molecules resulting in a decrease in the electrostatic repulsion between the charged head groups. Formamide also has two potential hydrogen bonded network structures and therefore, formamide molecules would be more structured or ordered around the hydrocarbon parts of the surfactant molecules. Hence, removal of this hydrocarbon moiety from the solvent environment to the interior of the surfactant assembly would minimize the unfavorable interactions, and hence lead to micellar aggregation (Section 1.4.3).

Although there is conclusive experimental evidence for surfactant aggregation and micelle formations in formamide [18, 29, 30], there is some confusion as to whether the CMC values of the surfactants are lower or higher in formamide than those in water. Akhter et al. [31] reported approx 30 times lower CMC values in formamide than in water for series of anionic surfactants with different chain lengths based on conductivity and surface tension measurements at 22 °C. Almgren et al. [18] also observed a linear decrease in the CMC of sodium dodecyl sulfate (SDS) up to 60% (w/w) formamide in water, by which point the CMC had decreased about 20 fold from its aqueous value. Above 60% FA, the CMC increased slightly and in pure FA, the CMC was only 10 fold lower than that in pure aqueous solution. In contrast, Rico and Lattes [17] reported almost 100 fold higher CMC values for SDS and CTAB in formamide than in water based on surface tension measurements carried out at 60 °C. Olofsson [25] and Sjoberg et al. [32] also observed about thousand and hundred fold higher CMC for CTAB in formamide compared to water, respectively.



### 5.3.1 Bilayer Stability in Formamide-Water Media

Surfactant coatings were formed by rinsing the capillary with 1.0 mM aqueous surfactant solution for 10 min at 93.8 kPa, followed by a rinse for 3 min or more (depending on the viscosity of the buffer) with surfactant-free electrophoretic buffer at 93.8 kPa. The latter rinse was done to flush the excess (non-adsorbed) surfactant from the capillary. The time required to flush the entire length of capillary under a certain buffer condition was determined by measuring the time required for an injected neutral marker (mesityl oxide) to be pushed past the detector (Section 5.2.6) and then allowing for the extra 8.5 cm length of the capillary after the detector. A number of techniques were employed to characterize these surfactant coatings. First, I used the change in the electroosmotic flow mobility ( $\mu_{eo}$ ) to evaluate the stability of the surfactant coatings, as the value of  $\mu_{eo}$  is reflective of the zeta potential at the surface of the capillary [33, 34]. Hence, measurement of the  $\mu_{eo}$  value as function of high pressure rinsing time was used to infer the coating stabilities, as described in Section 5.2.4.

Figure 5.1 shows the coating stability of the double chain surfactant, 2C<sub>18</sub>DAB in the presence of 0-100% (v/v) FA in 25 mM phosphate buffer (pH 7.0). The time in the x-axis represents the duration for which the coating is subjected to a high-pressure (93.8 kPa) rinse. Both the initial value of the EOF and the coating stability depends on the volume fraction of FA in the run buffer. The magnitude of the initial EOF (at zero time) decreases as the amount of FA is increased. This is due in part to a decrease in the value of the dielectric constant to viscosity ratio (i.e. lower  $\epsilon/\eta$  value) according to eqn 1.8. The  $\epsilon$ ,  $\eta$  and  $\epsilon/\eta$  values along with the initial EOF for various FA-water mixtures at 25 °C are shown in Table 5.2. The  $\epsilon$  values are obtained by interpolation of data from the literature

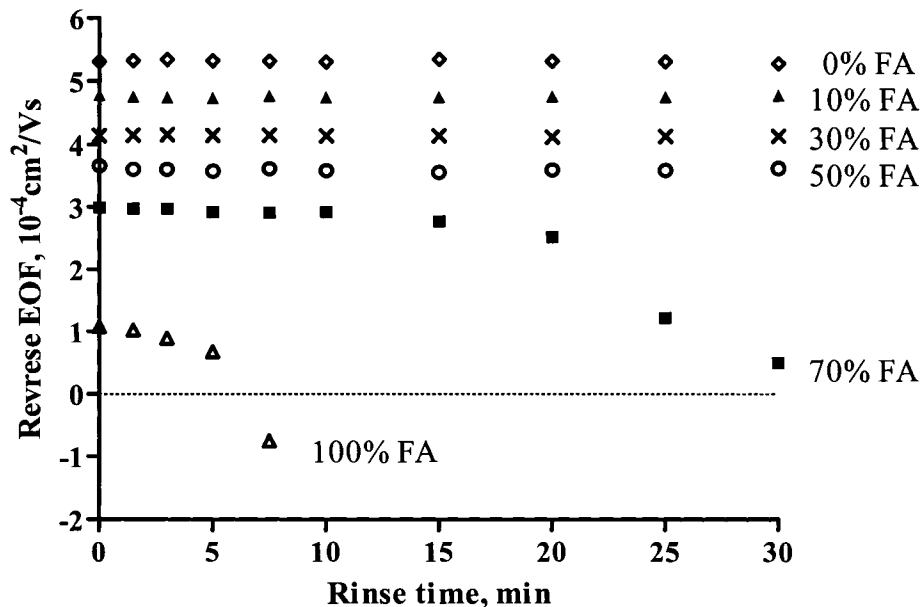


**Figure 5.1** Coating stability of 2C<sub>18</sub>DAB in formamide-aqueous phosphate buffers. 0% FA (◇), 10% FA (▲), 30% FA (×), 50% FA (△), 70% FA (■), 100% (○). Experimental conditions: 25 mM sodium phosphate buffer at pH 7.0; applied voltage, -20 kV; capillary, 37 cm x 50 μm I.D. (28.5 cm to the detector); neutral marker, 0.5 mM mesityl oxide at 254 nm; temperature, 25 °C. The capillary was rinsed with 1.0 mM 2C<sub>18</sub>DAB prepared in water for 10 min at 93.8 kPa and the capillary was regenerated between the runs by rinsing with 1 M NaOH and then recoated again with 2C<sub>18</sub>DAB solution.

[35]. The  $\eta$  of each solution containing 0% to 100% FA was calculated by multiplying the relative viscosity (see Section 5.2.6) and the viscosity of water. Both the  $\varepsilon$  and  $\eta$  increase but the  $\varepsilon/\eta$  ratio decreases with the content of FA, as the  $\eta$  increase is more dominant than the  $\varepsilon$  change. However, as shown in Table 5.2, the observed EOF

**Table 5.2** Effect of buffer organic solvent content on solvent parameters at 25 °C.

% FA (v/v)	$\varepsilon^a$	$\eta$ (cP) <sup>b</sup>	$\varepsilon/\eta$	Reverse EOF <sup>c</sup> ( $10^{-4}$ cm <sup>2</sup> /Vs)
0	78.5	0.89	88.2	5.31
10	82.8	1.01	81.9	4.78
30	93.5	1.27	73.6	4.14
50	101.8	1.62	62.8	3.67
70	111	2.13	52.1	2.99
100	110	3.26	32.9	1.08

<sup>a</sup> Values obtained from interpolation of literature data [35]. <sup>b</sup> Values calculated by multiplying the relative viscosity (see Section 5.2.6) and the viscosity of water. <sup>c</sup> Initial EOF values obtained without rinsing the coatings with the electrophoretic buffer. All other experimental conditions are as described in Figure 5.1.

decreases more than the  $\varepsilon/\eta$  ratio, which indicates that the zeta potential ( $\zeta$ ) also varies as the solvent shifts from water to formamide. Rearrangement of eqn 1.8 allows estimation of the  $\zeta$  in volts and the value decreases by about half in FA from its value in water. Similar pattern of changes in the zeta potential have been reported in the literature although there is inconsistency on the exact value [10, 36].

As shown in Figure 5.1, for buffers containing 0-50% FA the coating displays a constant EOF value (%RSD < 0.81%) with no noticeable drift over 30 min of continuous rinsing with the run buffer. In 70% FA (■ in Figure 5.1), the EOF remains constant for

15 min of rinsing ( $RSD_{0-15 \text{ min}} = 1.2\%$ ). However, rinsing the coating for more than 15 min (equivalent to  $\sim 53$  capillary volumes) with 70% FA containing buffer results in degradation of the  $2C_{18}DAB$  coating, as reflected by a rapid decrease in the magnitude of the EOF. In 100% FA, a small reversed EOF of  $1.22 \times 10^{-4} \text{ cm}^2/\text{Vs}$  is obtained with no rinsing ( $t = 0$ ) but the EOF decreases rapidly generating normal EOF beyond the five min rinse ( $\sim 6$  capillary volumes). The  $2C_{18}DAB$  degradation behaviors in 70% FA and 100% are different from what I observed for  $2C_{12}DAB$  in aqueous solutions (Section 4.3.2). In aqueous solution, the  $2C_{12}DAB$  coating degraded following a first order kinetics where it exponentially decays to residual EOF value. However, the EOF in Figure 5.1 decreases more dramatically after 15 min of rinse with 70% FA and even EOF reversal to the normal direction after 5 min rinse in pure FA. This might be due to collapse of the bilayer (or aggregate) structure because of the lower zeta potential with increasing rinsing or increasing amount of FA. Similar dramatic decrease in EOF has been observed in our group for double chain surfactants in aqueous solutions at higher ionic strength where the zeta potential is substantially lowered.

### 5.3.2 Effect of Surfactant Concentration on EOF

In CE, the concentration of the surfactant at which the EOF is reversed has been correlated with the CMC in the bulk solution [37, 38] and to the critical surfactant aggregation concentration (CSAC) at the capillary surface [39]. For the single chain cationic surfactant  $C_{16}TAB$ , the surfactant concentration required to reverse the EOF increased as the amount of methanol in the run buffer was increased (Section 2.3.2.2). This CSAC value for  $C_{16}TAB$  increased from  $\sim 0.5$  times the CMC in aqueous solution to 2 times the CMC in 60% MeOH. For the double chain surfactant,  $2C_{18}DAB$ , however,

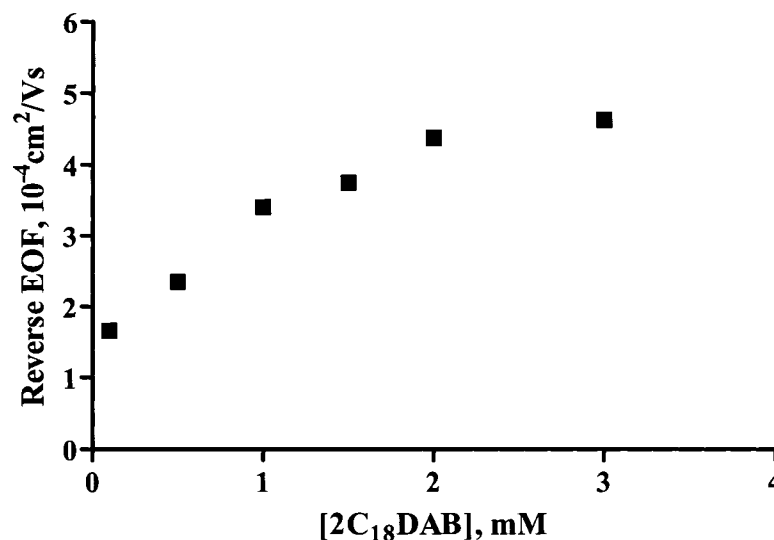


**Figure 5.2** Effect of 2C<sub>18</sub>DAB concentration on the value of the EOF mobility in formamide. Experimental conditions: buffer, 25 mM sodium phosphate buffer and pH 7.0 prepared in formamide; applied voltage, -20 kV; capillary, 37 cm x 50 μm I.D. (28.5 cm to the detector); neutral marker, 0.5 mM mesityl oxide at 254 nm; temperature, 25 °C; All the 2C<sub>18</sub>DAB solutions were prepared in formamide (see Section 5.2.2).

the CMC is too small to measure. Based on eqn 4.4, the CMC of 2C<sub>18</sub>DAB in water at 25 °C is predicted to be ~ 0.0037 μM. Hence a direct comparison of the CSAC with the CMC in the run buffer is not possible.

To determine whether the coating stability observed in Figure 5.1 depends on the surfactant concentration, I examined a series of coating solutions containing 0.1- 3 mM 2C<sub>18</sub>DAB in pure formamide. Figure 5.2 shows the effect of 2C<sub>18</sub>DAB concentration on the EOF mobility in 25 mM phosphate buffer prepared in formamide at pH 7.0. The same coating time of 10 min rinse at 93.8 kPa (corresponds to ~13 capillary volumes)

was used for all surfactant concentrations. The EOF mobility shows a gradual increase in magnitude in the reversed direction as the concentration of the surfactant rises from 0.005 to 1.5 mM. This increase becomes slower at concentrations above 2.0 mM. At concentrations greater than 2.0 mM, the surfactant does not dissolve well in formamide. Nonetheless, the EOF is reversed at all concentration ranges studied. This indicates that the  $2C_{18}DAB$  surfactant indeed forms aggregates on the capillary surface such that a positive charge is generated to reverse the EOF. For all other experiments, a concentration of 1.0 mM surfactant was used for coating, as it is a stable solution that is sufficient to generate a reasonably strong and reverse EOF.

In Chapters 2 and 4, I showed that the EOF is independent of surfactant concentration if the concentration is above the CMC or CSAC for aqueous and methanol containing buffers, respectively. In addition, the coating stability is inversely related to the CMC of the surfactant, i.e. the stability increases as the CMC decreases (Section 4.3.2). Comparison of the results obtained in FA with pure aqueous solution (Figure 5.1), reveals that the bilayer structures are less stable in formamide than in pure aqueous solution. This also implies that the minimum concentration for aggregation of  $2C_{18}DAB$  to occur is higher in formamide than in water. The results in Figure 5.2 also show an increase in the magnitude of the EOF even if concentrations well above the CMC are used as reflected by the reversed EOF. This behavior is some how similar to my previous observations of the single chain surfactant,  $C_{16}TAB$  in MeOH-water buffers (Section 4.3.3). In buffers containing 60% MeOH at pH 8.0 and 40% MeOH at pH 3.0, the EOF showed gradual increase as the concentration of  $C_{16}TAB$  increase. In both buffer conditions, the EOF was reversed at concentration higher than the CMC in the run buffer.

We attributed the effect to the decrease in zeta potential at the surface caused low pH or higher the amount of the MeOH. Similar factor might be responsible for the behavior observed in Figure 5.2. In fact Porras and Kenndler [14] determined that weak acids display a pKa shifts of 1-3 units in FA (i.e. less acidic) compared to water. Hence, because of the lower dissociation of weak silanol groups in FA (less charge density), the aggregation of the surfactant might happen over wider concentration range.

Alternatively, this phenomenon in formamide might be due to a progressive self-association of monomers into the bilayer that results in enhanced charge density on the capillary surface as the surfactant concentration rises. A similar effect has been reported for single chain surfactants in formamide. In study of the binding of formamide solvent molecules to C<sub>16</sub>TAB, Canet et al. observed that small aggregates are formed close to the CMC, growing in size up to ~ 0.3 M when aggregates with a size close to that in water are formed [40]. Ceglie et al. [41] and Porche et al. [28] also reported an increase in micellar size and aggregation number with SDS concentration in formamide, but a decrease in the amount of non-aggregated surfactant molecules (monomers). They suggested that aggregation is progressive due to the increased electrostatic screening in the system, which lowers the electrostatic potential on the micellar surface and, hence, enhances aggregation of the surfactant ion into the micellar phase.

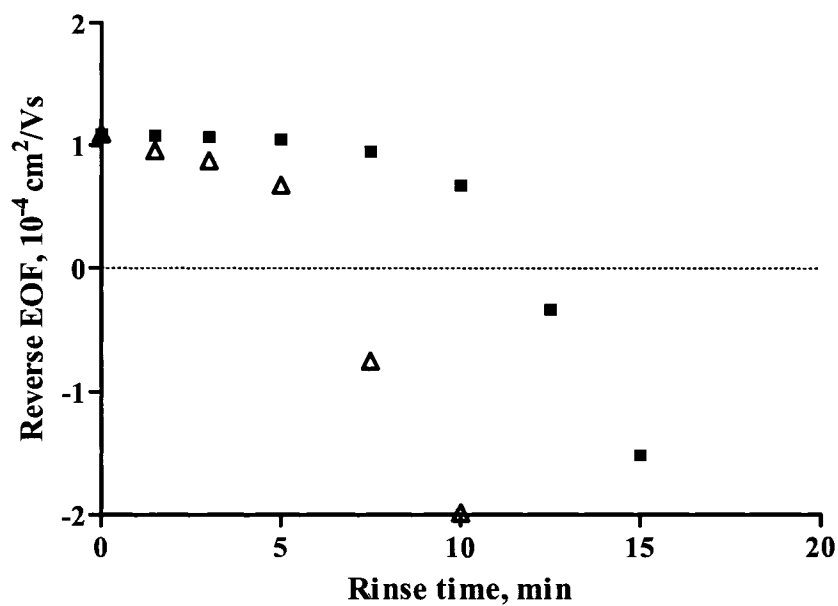
### 5.3.3 Effect of Capillary Diameter

Figure 5.3 shows the coating stability obtained for 2C<sub>18</sub>DAB coated 25- $\mu$ m and 50- $\mu$ m I.D. capillaries in formamide. The 25- $\mu$ m capillary was coated with 1.0 mM surfactant solution for 25 min (compared to 10 min rinse for the 50- $\mu$ m capillary) to

ensure that same volume of surfactant solution has passed through the narrow capillary. This was checked by measuring the initial EOF ( $t = 0$ ) for both capillary diameters. Similarly, the rinsing time shown in the x-axis for 25- $\mu\text{m}$  is converted to time scale that takes to flush same capillary volumes in the 50- $\mu\text{m}$  capillary.

As shown in Figure 5.3, as expected same initial EOF of  $\sim 1.12 \times 10^{-4} \text{ cm}^2/\text{Vs}$  is obtained for both capillaries, independent of capillary diameter. However, the coating shows better stability with the narrower capillary inner diameter. The  $2\text{C}_{18}\text{DAB}$  coatings are stable for 5 min of rinse ( $\sim 6$  capillary volumes) in pure formamide solution using the 50- $\mu\text{m}$  I.D. capillaries. In contrast, an EOF value of about  $1.03 \times 10^{-4} \text{ cm}^2/\text{Vs}$  with RSD = 1.4% is obtained after 10 min of rinsing ( $\sim 13$  capillary volumes) in the 25- $\mu\text{m}$  capillary. The coating then rapidly degrades as reflected by the quick reversal of the direction of the EOF to normal with longer 10 min of flushing time. Similar increase in the stability of bilayers coatings with a decrease in capillary diameter have been observed in aqueous buffers [42]. An increase in the capillary inner diameter results in larger volume-to-surface ratio. Thus, with increased capillary diameter, larger volumes of fresh run buffer are introduced into the capillary during rinsing. This may facilitate the dynamic adsorption/desorption equilibrium to shift towards desorption of more surfactant from the surface that leads to a lesser charge density on the surface bilayer. Hence, the degradation in the bilayer structure results in the reduction of the EOF. This is similar to the bilayer degradation observed when the coating is subjected to longer rinsing times (e.g. longer than 20 min flushing in 70% FA buffer).





**Figure 5.3** Effect of capillary inner diameter on stability of double chain surfactant in nonaqueous solvent. 25  $\mu\text{m}$  I.D. (■); 50  $\mu\text{m}$  I.D. (Δ). Experimental conditions: 25 mM sodium phosphate buffer (pH 7.0) and 1.0 mM  $\text{C}_{18}\text{DAB}$  surfactant both prepared in formamide. All other conditions as described in Figure 5.1.

#### 5.3.4 Effect of Buffer

Previous studies have shown that the nature and concentration of the buffer has an influence on the stability of surfactant coatings because it changes the CMC of the surfactants [42, 43]. Hence, the coating stability was also examined in another two common buffers: ammonium acetate ( $\text{NH}_4\text{Ac}$ ) and ammonium formate ( $\text{NH}_4\text{Fa}$ ) buffers prepared in FA at pH 4.0. Surfactant concentrations of 0.1 mM, 1.0 and 2.0 mM and

**Table 5.3** Effect of buffer type and surfactant concentration on the value of EOF in formamide.

Buffer system	C (mM)	EOF ( $10^{-4} \text{ cm}^2/\text{Vs}$ ) (n = 4)		
		0.1 mM C <sub>18</sub> DAB	1.0 mM 2C <sub>18</sub> DAB	2.0 mM 2C <sub>18</sub> DAB
NH <sub>4</sub> Ac	25	6.3 ± 0.4	6.7 ± 0.4	6.4 ± 0.4
NH <sub>4</sub> Ac	50	4.7 ± 0.2	5.0 ± 0.3	4.9 ± 0.1
NH <sub>4</sub> Fa	25	7.6 ± 0.1	7.3 ± 0.3	7.8 ± 0.3
NH <sub>4</sub> Fa	50	5.8 ± 0.2	6.1 ± 0.4	5.7 ± 0.2

Experimental conditions: applied voltage, -15 kV; capillary; 37 cm x 50  $\mu\text{m}$  (28.5 cm to the detector); 1.0 mM 2C<sub>18</sub>DAB was added to 25 mM or 50 mM ammonium acetate (or ammonium formate) buffer at pH 4.0; neutral marker, 1.0 mM mesityl oxide dissolved in formamide; each EOF determinations was done four times; temperature, 25.0 °C.

buffer concentrations of 25 and 50 mM dissolved in FA were employed for the EOF measurement in these buffers. For this study, after the capillary was coated with surfactants solutions for 10 min, the coating was subjected to a 3 min or longer rinse with surfactant free buffer. For both acetate and formate buffers in FA, no reversed EOF was observed for any of the surfactant or buffer concentrations. Instead, normal EOF values of about  $4.31 \times 10^{-4}$  and  $4.85 \times 10^{-4} \text{ cm}^2/\text{Vs}$  were obtained in 25 mM formate and acetate buffers, respectively. The magnitudes of the EOF, however, are less than that obtained in bare silica capillary ( $\sim 8.0 \times 10^{-4} \text{ cm}^2/\text{Vs}$ ) indicating that some surfactant molecules may

still be on the wall reducing the charge density on the capillary surface. Complete removal of the surfactant can be achieved by flushing the capillary with 1.0 mM NaOH for 10 min followed by 10-15 min with FA at high pressure (93.8 kPa).

Similar poor coating stabilities in acetate and formate buffers compared to phosphate have been observed in aqueous solutions [42, 43]. For instance, 2C<sub>12</sub>DAB coating degrades in acetate buffer at rate three times faster than that in phosphate for same ionic strength [42]. This is because the stronger adsorption of the phosphate counterions onto surfactant head groups leads to increased electrostatic screening between the charged head groups, which in turn allows tighter head group packing. However, when the surfactant was added into the run buffer as a dynamic additive, a strongly reversed EOF was obtained for both buffer conditions (Table 5.3). The magnitudes of the EOF generated in both 25 and 50 mM buffers are also independent of the surfactant concentrations maintained in the run buffer. The magnitude of the reversed EOF decreases as the buffer concentration is increased for both acetate and formate buffers, consistent with the expected inverse dependence on the ionic strength [14, 44].

### 5.3.5 Separations of Basic Drugs in Nonaqueous Buffers

The utility of the coating in the presence of nonaqueous solvent was investigated by analyzing cationic drugs. Figure 5.4 shows separation of the four drugs (propranolol, metoprolol, chloroquine, and chlorpheniramine) in sodium phosphate buffer (pH 3.0) prepared in pure formamide solvent. The electropherograms (a) and (b) were obtained using a bare silica capillary (with no coating) and 2C<sub>18</sub>DAB coated capillary, respectively. In bare silica, the peaks observed are severely tailed resulting from strong interactions of the positively charged analytes with the negatively charged wall. This

gives rise to poor separation efficiency ( $N < 150,000$  plates/m) and poor migration reproducibility (% RSD = 3.2- 4.4).

On the other hand, the use of a 2C<sub>18</sub>DAB coated capillary improved the separation as shown in Figure 5.4b. The migration order of analytes is reversed from that of Figure 5.4a because in the coated capillary the analytes migrate opposite to the EOF. Peak efficiencies ranging from 0.2 – 0.5 million plates/m are obtained. No peak tailing is observed as the interaction of the analytes with the capillary wall is eliminated with the capillary coating. This is particularly important for quantification (or recovery) studies for analytes in unknown samples. We carried out a number of consecutive separations and monitored migration times, and peak areas of the analytes in capillary coated with 1.0 mM surfactant (10 min at 93.8 kPa). The coating was regenerated after five runs in FA buffers. The migration time and peak area reproducibilities observed using the 2C<sub>18</sub>DAB coated capillary in FA without regeneration are < 0.8 and < 3.5 % RSD, respectively (Table 5.4). Peak efficiencies in the ranges of 0.2 million/m with reproducibilities less than 2.3% RSD are also observed. Relatively high concentration of sample was used in the FA buffer because of the background UV absorbance from FA. Other alternative detection techniques such as electrochemical, mass spectrometry could be employed to improve the detection sensitivity. Nonetheless, the 2C<sub>18</sub>DAB bilayer coating is promising for rapid separation of cationic drugs in buffers prepared in pure formamide.

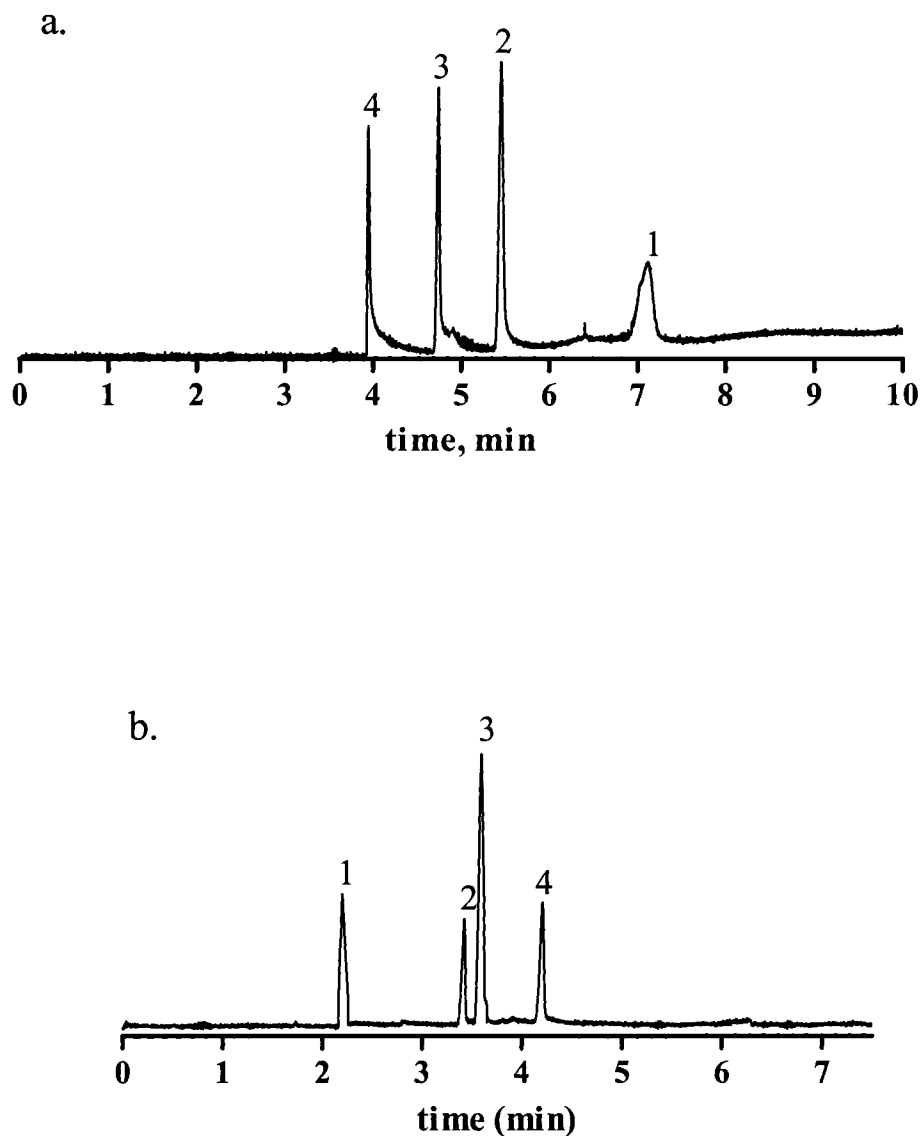


**Figure 5.4** Electropherogram of basic drugs in FA using bare silica capillary and coated capillary. Conditions: Buffer: 25 mM phosphate at pH 3.0 prepared in FA, Sample concentration, 0.5 mM; detection at 210 nm; a) bare silica capillary, 40.5 cm (32 cm to the detection window); applied voltage, 20 kV; b) 2C<sub>18</sub>DAB coated capillary, 33 cm (24.5 cm to the detection window); applied voltage, -25 kV; 1.0 mM 2C<sub>18</sub>DAB. Peaks: 1) Chlorpheniramine 2) Metoprolol 3) propranolol 4) Chloroquine.

**Table 5.4** Migration time and peak area reproducibilities of four basic drugs in a sodium phosphate buffer prepared with formamide.

Analyte	Reproducibility (%RSD, n = 5)	
	Migration time	Peak area
Metoprolol	0.83	1.5
Propranolol	0.67	1.9
Chloroquine	0.81	3.4
Chloropheniramine	0.79	2.5

#### 5.4 Concluding Remarks

One of the easiest ways to control the EOF is the use of coated capillaries. The results presented in this work showed that double chain surfactant, 2C<sub>18</sub>DAB forms a dynamic coating that reverse the EOF in pure formamide. The long-term stability of 2C<sub>18</sub>DAB coating in pure FA is poor compared to aqueous solutions. Nevertheless, these coatings can offer rapid separation for a number of runs without the need to regenerate the coating. This is the first report to show application of double chain surfactants in either mixed formamide-water or pure formamide solvent system. The coating stability is enhanced by decreasing the diameter of the capillary, using buffers that can reduce the aggregation concentration of the surfactant such as phosphate and by reducing the volumes of liquid flushed through the capillary. FA has some interesting properties and use of FA as a nonaqueous solvent for the BGE could offer many possibilities such as adjustment of selectivity and dissolution of some organic molecules.

## 5.5 References

- [1] Ward, V. L., Khaledi, M. G., *J. Chromatogra. A* 1999, 859, 203-219.
- [2] Porras, S. P., Riekkola, M. L., Kenndler, E., *Electrophoresis* 2003, 23, 1485-1498.
- [3] Steiner, F., Hassel, M., *Electrophoresis* 2000, 21, 3994-4016.
- [4] Walbroehl, Y., Jorgenson, J. W., *J. Chromatogr.* 1984, 315, 135-143.
- [5] Sahota, R. S., Khaledi, M. G., *Anal. Chem.* 1994, 66, 1141-1146.
- [6] Wang, F., Khaledi, M. G., *Anal. Chem.* 1996, 68, 3460-3467.
- [7] Mori, Y., Ueno, K., Umeda, T., *J. Chromatogr. A* 1997, 757, 328-332.
- [8] Lin, J. M., Nakagawa, M., Uchiyama, K., Hobo, T., *Electrophoresis* 2002, 23, 421-425.
- [9] Lin, J. M., Nakagawa, M., Uchiyama, K., Hobo, T., *Chromatographia* 1999, 50, 739-744.
- [10] Wright, P. B., Lister, A. S., Dorsey, J. G., *Anal. Chem.* 1997, 69, 3251-3259.
- [11] Steiner, F., Hassel, M., *Electrophoresis* 2003, 24, 399-407.
- [12] Bjornsdottir, I., Hansen, S. H., *J. Pharm. Biomed. Anal.* 1995, 13, 687-693.
- [13] Geiser, L., Cherkaoui, S., Veuthey, J. L., *J. Chromatogr. A* 2002, 979, 389-398.
- [14] Porras, S. P., Kenndler, E., *Electrophoresis* 2004, 25, 2946-2958.
- [15] Salimi-Moosavi, H., Cassidy, R. M., *Anal. Chem.* 1996, 68, 293-299.
- [16] Baur, L., Sanger-van, G. C., Watzig, H., *J. Chromatogr. A* 2002, 979, 97-103.
- [17] Rico, I., Lattes, A., *J. Phys. Chem.* 1986, 90, 5870-5872.
- [18] Almgren, M., Swarup, S., Lofroth, J. E., *J. Phys. Chem.* 1985, 89, 4621-4626.
- [19] Aguiar, J., Bolivar, J. M., Garcia, J. P., Ruiz, C. C., *J. Colloid and Interf. Sci.* 2002, 255, 382-390.

- [20] Baeuml, F., Welsch, T., *J. Chromatogr. A* 2002, *961*, 35-44.
- [21] Williams, B. A., Vigh, G., *Anal. Chem.* 1996, *68*, 1174-1180.
- [22] Warr, G. G., Sen, R., Evans, D. F., Trend, J. E., *J. Phys. Chem.* 1988, *92*, 774-783.
- [23] Evans, J. B., Evans, D. F., *J. Phys. Chem.* 1987, *91*, 3828-3829.
- [24] Ramadan, M. S., Evans, D. F., Lumry, R., Philsont, S., *J. Phys. Chem.* 1985, *89*, 3405-3408.
- [25] Olofsson, G., *J. Chem. Soc. Faraday Trans.* 1991, *87*, 3037-3042.
- [26] Akhter, M. S., Alawi, S. M., *Colloids and Surf. A* 2003, *219*, 281-290.
- [27] Duval, F. P., Warr, G. G., *Chem. Commun.* 2002, 2268-2269.
- [28] Perche, T., Auvray, X., Petipas, C., Anthore, R., Rico-Lattes, I., Lattes, A., *Langmuir* 1997, *13*, 1475-1480.
- [29] Thomason, M. A., Bloor, D. M., Wyn-Jones, E., *Langmuir* 1992, *8*, 2107-2109.
- [30] Gamboa, C., Rios, H., Sanchez, V., *Langmuir* 1994, *10*, 2025-2027.
- [31] Akhter, M. S., Alaw, S. M., *Colloids and Surf. A* 2000, *173*, 95-100.
- [32] Sjoberg, M., Henriksson, U., Warnheim, T., *Langmuir* 1990, *6*, 1206-1211.
- [33] Melanson, J. E., Baryla, N. E., Lucy, C. A., *Anal. Chem.* 2000, *72*, 4110-4114.
- [34] Cordova, E., Gao, J., Whitesides, G. M., *Anal. Chem.* 1997, *69*, 1370-1379.
- [35] Rohdewald, P., Moldner, M., *J. Phys. Chem.* 1973, *77*, 373-377.
- [36] Valko, I. E., Siren, H., Riekkola, M. L., *J. Microcol. Sep.* 1999, *11*, 199-.
- [37] Lucy, C. A., Underhill, R. S., *Anal. Chem.* 1996, *68*, 300-305.
- [38] Tavares, M. F. M., Colombara, R., Massaro, S., *J. Chromatogr. A* 1997, *772*, 171-178.
- [39] Liu, J. F., Ducker, W. A., *J. Phys. Chem. B* 1999, *103*, 8558-8567.



- [40] Belmajdoub, A., Boubel, J. C., Canet, D. J., *J. Phys. Chem.* 1989, *93*, 4844-.
- [41] Ceglie, A., Colafemmina, G., Monica, M. D., Olsson, U., Jonsson, B., *Langmuir* 1993, *9*, 1449-1455.
- [42] Yassine, M. M., Lucy, C. A., *Anal. Chem.* 2004, *76*, 2983-2990.
- [43] Bostrom, M., Williams, D. R. M., Ninham, B. W., *Langmuir* 2002, *18*, 6010-6014.
- [44] Li, D. M., Fu, S. L., Lucy, C. A., *Anal. Chem.* 1999, *71*, 687-699.

## CHAPTER SIX: Summary and Suggestions for Future Work

### 6.1 Summary

This thesis demonstrated optimization of the EOF with different coating agents in the presence of organic solvents. In Chapters 2 and 3, dynamic coatings based on single chain surfactants such as cetyltrimethylammonium bromide (CTAB) were successfully applied to the separation of small inorganic anions. Chapter 4 and 5 used the long double chain surfactants such as dihexadecyldimethylammonium bromide ( $2C_{16}DAB$ ) and dioctadecyldimethyl-ammonium bromide ( $2C_{18}DAB$ ) to develop semi-permanent coatings in mixed organic-water and pure organic solvents such as methanol, ethanol, 2-propanol, 1-butanol, acetonitrile and formamide. These semi-permanent coatings were applied for the rapid separation of anions and cationic drugs.

The reversed EOF generated by the cationic surfactants, CTAB and DDAB, was systematically altered by the addition of methanol (MeOH) to the background electrolyte. For both aqueous and low MeOH containing buffers surface aggregation of the surfactants at the capillary wall and EOF reversal occurs at a concentration below the surfactant's CMC in the bulk solution. In aqueous solution, the resultant critical surface aggregation concentration (CSAC) was about  $\frac{1}{2}$  of the CMC in the buffer solutions. Decreasing the zeta potential of the silica surface either by lowering the pH or adding MeOH resulted in an increase in the CSAC of the surfactant required to reverse the EOF. Consequently, in 60% (v/v) MeOH the CSAC was more than the CMC of the surfactant in the running buffer. The impact of MeOH on reversed EOF was found to be predominantly a function of the diminished zeta potential of the silica, and to a lesser extent on the CMC of the surfactant. Alteration of the EOF in this manner results in

more rapid separations, improved reproducibility and resolution of particularly difficult separation tasks for small inorganic anions.

The use of dynamic surfactant coating in the presence of organic solvents was also demonstrated for indirect detection of small anions in Chapter 3. The organic solvent alters the electrophoretic mobility of the UV absorbing probes and the analytes differently. Hence, choice of an appropriate probe – one that has mobility comparable to that of the analytes is essential to achieve high degree of resolution and detection sensitivity. A number of UV absorbing indirect probes including chromate, benzoate, phthalate, pyromellitate and trimellitate were examined to explore their suitability as indirect probes in buffers containing various percent of MeOH. Chromate showed the best mobility match with small inorganic anions in mixed MeOH-water buffers. In addition, chromate also enables detection at a wavelength much greater than the absorption of most anions and methanol. Resolutions as well as separation speeds two times faster than standard ion chromatography techniques were also achieved. The ability to move peaks selectively using different percent of methanol demonstrated the applicability of the technique for detection of small inorganic anions in tap and river waters.

The use of these cationic surfactants (CTAB and DDAB) allowed separation in the co-EOF mode where both the EOF and anions are migrating in the same direction. Variation of the EOF in such a manner increased the apparent mobility of the anions and shortened the migration times. Dramatic selectivity changes were also observed by adjustment of the MeOH content for the separation of small inorganic anions. In aqueous buffer in direct UV detection, the mobility of the ions followed the order:  $\text{Br}^- > \text{NO}_2^- \sim$

$\text{NO}_3^- > \text{I}^- > \text{SCN}^-$ . In 60% (v/v) MeOH the mobility of iodide and thiocyanate have been significantly altered, such that the mobility order changed to  $\text{I}^- > \text{Br}^- > \text{NO}_3^- > \text{NO}_2^- > \text{SCN}^-$ . Under the indirect UV detection similar migration orders and selectivity changes like that of the direct mode were observed among the singly charged ions. However, the impact of the organic solvent was more dramatic for the doubly charged ions. Changes in solvation of ions and ion-association interactions with the surfactant were the major factors responsible for the observed changes in selectivity.

This work also indicated that CE is useful for quantitative estimation of the degree of ion pairing (or ion-association). Ion-association constants ( $K_{ass}$ ) for iodide and bromide were determined from measurements of effective electrophoretic mobilities in aqueous and MeOH-water buffers in Chapter 3. The results indicated that anions form pairs with the cationic surfactant to different extents in both aqueous and nonaqueous buffers. The  $K_{ass}$  values obtained for the anions in aqueous solution were consistent to their retention factors observed in ion exchange chromatography. As the amount of MeOH was increased in the run buffer, the ion association constant for bromide increased but the value for iodide decreased. The effects were attributed to changes in solvation of the ions altering the charge to size ratio and extent of their interaction with the surfactant.

Chapter 4 showed that long double-chain surfactants could be used as semi-permanent coatings in organic-water solvent systems. The coating procedure involves a simple hydrodynamic rinse (<5 min) of the capillary with the surfactant solution. The excess surfactants can then be removed by flushing the capillary with run buffer. The resultant bilayer coatings show stability toward a large number of rinsing steps in buffers that contain up to 60% (v/v) of various nonaqueous solvents as MeOH and ACN.

Compared to other types of capillary modifications, such surfactant-based coatings are simple, versatile and inexpensive. The absence of EOF modifier in the run buffer also allowed greater flexibility in optimizing the separation conditions. This is particularly advantageous compared to the dynamic coatings achieved using single chain surfactants such as CTAB. The reversed EOF generated was also independent of pH, which allows fast separations to be performed under different pH conditions in various organic-water buffers.

Pure nonaqueous CE has shown to be an important choice as separation medium for many applications. However, modification of the capillary in nonaqueous solvents is essential to control the EOF and eliminate analyte adsorptions. The results presented in Chapter 5 showed that double chain surfactant, 2C<sub>18</sub>DAB forms semi-permanent coating that reversed the EOF in pure formamide. The long-term stability of 2C<sub>18</sub>DAB coating in pure FA was poor compared to aqueous solutions. Nevertheless, these coatings can be used for a number of runs without the need to regenerate the coating. This is the first report to show application of double chain surfactants in either mixed formamide-water or pure formamide solvent system. The coating stability was affected by the nature of buffer and capillary diameter. Use of buffer that interacts strongly with the quaternary amine such as phosphate and reducing the capillary diameter improved the coating stability. FA has some interesting properties including networks of hydrogen bonding like water that supports surfactants aggregation. Hence, the use of surfactants along with FA as a nonaqueous solvent for the BGE could offer many possibilities such as adjustment of selectivity and dissolution of some organic molecules.

In conclusion, CE is a separation technique based on differential migration of charged molecules in the presence of an electric field and selectivity is a key parameter in separation science. Modification of the charge on the capillary surface to control the EOF is essential because of its importance to improve resolution and separation speed. In bare fused silica capillaries, the repeatability of the EOF is poor from run-to-run and between different capillaries, decreasing the reliability of capillary electrophoretic analyses. With the introduction of high-throughput capillary array electrophoresis instruments, the importance of a reproducible coatings process has also increased dramatically. The coating procedures proposed in this work are simple, reproducible and yield stable coatings under nonaqueous-water and nonaqueous conditions. The use of organic solvents offers many advantages compared to pure aqueous solutions. Most importantly, replacing the aqueous solvent with nonaqueous solvents offers different solvation states for the analytes which result in different relative mobilities and hence unique separation selectivity.

## **6.2 Suggestions for Future Work**

### **6.2.1 Separation and Identification of Peptides**

The potential of capillary electrophoresis (CE) for bioactive peptides has been demonstrated [1, 2], and its role in proteome studies has also been indicated [3, 4]. Most commonly, CE separations of mixtures of peptides in aqueous and nonaqueous solvents are carried out at low pH to ensure that all analytes are charged. In some cases, however, the efficiencies are considerably compromised, because of interactions between peptides and the silanol groups [5]. Furthermore, changes in the surface of the capillary wall due to adsorption of analytes causes non-uniform liquid flow profiles leading to poor

migration time repeatability [1]. Using CE with bare fused-silica capillaries, peptide analysis at low pH can lead to extensively long analysis times (> 30 min) due to the very low EOF [2].

The most common means optimizing the EOF and minimizing peptide interaction/adsorption has been covalently binding materials such as polymers to the shield the silanol groups [5, 6]. However, this type of coating is usually stable only over a restricted pH range and its preparation is often based on a multi-step chemical reaction scheme that may cause a large variance between capillaries (Section 1.4.3.1). Besides, covalent coatings often present a limited lifetime and commercially available coated capillaries can be quite expensive. Only a few studies of peptide analysis in nonaqueous solvents have been described. Hansen and co-workers [7] separated Ala-Phe diastereomers using ammonium acetate-acetic acid in a 1:1 mixture of methanol and acetonitrile. Gramicidin S and bacitracin were analyzed by nonaqueous capillary electrophoresis-mass spectroscopy (NACE-MS) in a BGE consisting of ammonium acetates dissolved in mixtures of acetonitrile and methanol [8]. Czerwenka et al. [9] reported the enantiomer separation of *N*-protected alanine peptides containing up to six amino acid residues using *t*-butylcarbamoylquinine as chiral counterion in mixtures of methanol and ethanol. Psurek and Scriba also used alkaline methanolic BGE to separate neuropeptides and determined their pKa [10].

Therefore, studying the suitability of the non-covalent bilayer coatings for peptide analysis at various ranges in mixed nonaqueous-water or nonaqueous solvents would be quite attractive. These bilayer coatings have already been successfully applied to achieve efficient separation of cationic proteins in aqueous solutions [11]. First, the coatings

generate high and pH-independent EOF (Section 4.3.3). This allows rapid analysis time for peptides at various pH ranges or allows employing buffer pH change for optimization of selectivity. Secondly, selectivity is a key parameter in separation science and organic solvents offer the potential for separation mechanisms different from that observed in aqueous media. Hence, the use of nonaqueous solvents would yield selectivity adjustments for peptides in a variety of mixtures. Thirdly, some peptides have limited solubility in aqueous solution and analysis of such peptides in nonaqueous solvents such as formamide and methanol would be desirable. Nonaqueous solvents such as formamide, *N,N*-dimethylformamide, dimethylsulfoxide etc have high UV cut off wavelengths and detection of analytes in lower UV regions could compromise their sensitivity. Alternative detection means such as electrochemical detection, laser induced fluorescence [12], and mass spectrometry [13] would provide better sensitive detection.

### 6.2.2 Enantiomeric Separation of Pharmaceutical Drugs

CE has become an important tool for routine analysis in the pharmaceutical and biotech industries. The applications include drug analysis in biological matrices for *in vitro* drug metabolism studies as well as applications in forensic analysis and therapeutic drug monitoring [14-16]. In addition, enantiomeric separation of drugs in CE has been reported using chiral selective reagents such as cyclodextrin and its derivatives in the BGE [17]. Khaledi and coworkers have also utilized polycations and short chain surfactants to control the EOF and to enhance chiral separations of pharmaceutical drugs in NACE [18, 19]. Hence, further studies to investigate the application of these cationic coatings for quantification and monitoring of pharmaceutical drugs, for enantiomeric separations using different chiral selectors in nonaqueous solvents would be important.



As recent studies from our group showed the commonly used chiral selector, cyclodextrin (CD) interacts with hydrophobic part of surfactants such as DDAB in aqueous solutions [20]. Therefore, use of selectors that have no or weak interactions with the surfactants should be considered [21, 22].

### 6.3 References

- [1] Kasicka, V., *Electrophoresis* 1999, 20, 3084-3105.
- [2] Messana, I., Rossetti, D., Cassiano, L., Misiti, F., Giardina, B., Castagnola, M., *J. Chromatogr. B* 1997, 699, 149-171.
- [3] Shen, Y., Smith, R. D., *Electrophoresis* 2002, 23, 3106–3124.
- [4] Figeys, D., Aebersold, R., *J. Chromatogr. B* 1997, 695, 163-168.
- [5] Hutterer, K., Dolník, V., *Electrophoresis* 2003, 24, 3998-4012.
- [6] Horvath, J., Dolnik, V., *Electrophoresis* 2001, 22, 644-655.
- [7] Hansen, S. H., Bjørnsdottir, I., Tjørnelund, J., *J. Chromatogr. A* 1997, 792, 49-55.
- [8] Yang, Q., Benson, L. M., Kenneth, L. J., Naylor, S., *J. Biochem. Biophys. Methods* 1999, 38, 103-121.
- [9] Czerwenka, C., Lämmerhofer, M., Lindner, W., *Electrophoresis* 2002, 23, 1887–1899.
- [10] Psurek, A., Scriba, G. E., *Electrophoresis* 2003, 24, 765-773.
- [11] Yassine, M. M., Lucy, C. A., *Anal. Chem.* 2005, 77, 620-625.
- [12] Tjørnelund, J., Hansen, S. H., *J. Chromatogr. A* 1997, 779, 235–243.
- [13] Geiser, L., Cherkaoui, S., Veuthey, J. L., *J. Chromatogr. A* 2002, 979, 389-398.
- [14] Shihabi, Z. K., *J. Chromatogr. A* 1998, 807, 27-36.
- [15] Huie, W. R., Newman, R. A., Hutto, T., Madden, T., *J. Chromatogr. B* 1997, 693, 451–461.
- [16] Clohs, L., Winstanley, A. K., *LC.GC Europe* 2002, 15, 288-292.
- [17] Servais, A. C., Fillet, M., Abushoffa, A. M., Hubert, P., Crommen, J., *Electrophoresis* 2003, 24, 363-369.

- [18] Quang, C., Khaledi, M. G., *Anal. Chem.* 1993, *65*, 3354-3358.
- [19] Wang, F., Khaledi, M. G., *Anal. Chem.* 1996, *68*, 3460-3467.
- [20] Funasaki, N., Neya, S., *Langmuir* 2000, *16*, 5343-5346.
- [21] Hofstetter, O., Hofstetter, H., Schurig, V., Wilchek, M., Green, B. S., *J. Am. Chem. Soc* 1998, *120*, 3251-3252.
- [22] Hofstetter, H., Hofstetter, O., *Trends Anal. Chem.* 2005, *24*, 869-879.